



Scuola Dottorale in Scienze Matematiche e Fisiche

XXVII Ciclo di Dottorato

Transport phenomena in low dimensional systems in the presence of spin-orbit coupling

Juan Borge de Prada
Dottorando

_____ firma

Prof. Roberto Raimondi
Docente Guida

_____ firma

Prof. Roberto Raimondi
Coordinatore

_____ firma

*“If I have seen further it is by standing
on ye shoulders of Giants”.*

Isaac Newton

*“Physics is like sex: sure, it may give some practical
results, but that’s not why we do it”.*

Richard P. Feynman

“Oh! È importante però, che non dici cazzate”

Glauco, Boris, seconda Stagione

Contents

1	Introduction	1
1.1	Spintronics	1
1.2	Spin-orbit coupling	3
1.3	Outline	10
2	Spin-orbit interaction	13
2.1	The origin of the spin-orbit interaction	14
2.2	The $k \cdot p$ method and the Kane model	15
2.3	Intrinsic spin-orbit coupling in 2-D systems	21
3	The linear response theory and its application to Fermi systems	26
3.1	The Green function and the linear response theory	27
3.2	Disorder, impurities and the self-consistent Born approximation	35
3.3	The spin Hall and Edelstein conductivities in the 2DEG Rashba model	40
3.4	The spin-Hall conductivity and extrinsic SOC	46
4	Spin Hall and Edelstein effects in metallic films: From two	

to three dimensions	57
4.1 The model	58
4.2 The transport coefficients	65
4.3 Discussion of the results	75
4.4 Inter-band contributions	77
4.5 The connection between the spin Hall and Edelstein effects . .	80
5 Thermospin effects: the spin Nernst effect	84
5.1 The heat and spin dialogue	84
5.2 The spin equivalent of Mott's formula	87
5.3 Spin Nernst effect and spin thermopower in electron and hole gases	94
6 Conclusions	101
Appendix	104
A Effective Hamiltonians	105
A.1 The k.p method	105
A.2 Symmetries and the Kane model	107
B Integral of the Green functions	110
B.1 The intra-band integrals	110
B.2 The inter-band integrals	112
C Kinetic equations: a quasiclassical approach	113
C.1 The SU(2) formalism	113

Chapter 1

Introduction

1.1 Spintronics

The word “spintronics” refers to a multidisciplinary field of study centered on the manipulation of spin degrees of freedom in solid state systems [1–4]. One of the most important scopes is to understand what is the relation between the charge and the spin of the electrons. A good knowledge of this relation could allow us to realize devices capable of making use of both, the charge and the spin of the electrons. In contrast to *electronics* which is based only on semiconductors, in *spintronics* metals, both normal and ferromagnetic, are important too. The field is considered “new” due to this new point of view, but it is closely related to “old” subfields like magnetism, superconductivity, the physics of semiconductors, information theory, optics, mesoscopic physics or electrical engineering.

Typical spintronics issues are

- how to polarize a system, just a single electron or an ensemble (induce

magnetization in a material);

- how to keep it in a desired spin configuration longer than the time required by the device to make use of the information carried by this configuration;
- how to transport the information carried by this spin configurations across a device and, finally, accurately read it.

Generation of spin polarization usually means creating a nonequilibrium spin population. This can be achieved in different ways, optically, through electrical spin injection, through temperature gradients and through many other ways. Historically the optical injection using circularly polarized light which transfers its angular momentum to electrons has been the most used and studied technique. This is the principle that is behind the so-called spin light emitting diodes (spin LEDs). But for device applications electrical spin injection is much more desirable.

The electrical control of spin population could be exploited by two different physical mechanisms, ferromagnetism interactions and spin-orbit coupling (SOC). The idea of spintronics devices based on ferromagnetic properties is to inject spin currents in paramagnetic materials. One of the most studied effect due to this type of injections is the famous giant magnetoresistance effect also known as GMR effect [5,6]. The GMR effect occurs in hybrid systems made of magnetic and nonmagnetic parts, exploiting the different conductivity property of majority and minority spin populations. The effect consists on the appearance of a significant change of the electrical resistivity due to the change of the relative magnetization between the two different

ferromagnets. We will find a different value for the resistivity if both are magnetized parallel or antiparallel. The GMR effect led Albert Fert and Peter Grünberg to win the Nobel Prize in 2007. It is probably the most well known spintronic effect due to its huge applications on hard disk storage that were implemented by the first time by Stuart Parkin at the IBM [7].

This research field is extremely broad and we will focus ourselves on spin-orbit based effects. We refer the interested reader to the vast literature, especially to the reviews [2–4].

1.2 Spin-orbit coupling

Spin-orbit coupling appears in the non-relativistic limit of the Dirac equation in the following form

$$H_{so} = \frac{\lambda_0^2}{4} \boldsymbol{\sigma} \cdot \nabla V(\mathbf{r}) \times \mathbf{p}, \quad (1.2.1)$$

where $\lambda_0 = \frac{\hbar}{mc} \simeq 3.9 \times 10^{-3}$ is the Compton wavelength divided by 2π , $V(\mathbf{r})$ the atomic potential, \mathbf{p} the momentum, and $\boldsymbol{\sigma}$ the Pauli matrices. Effective Hamiltonian arising in solid-state theory have often a form similar to Eq.(1.2.1) but with a λ_{eff}^2 , that in systems like GaAs, can be 6 orders of magnitude bigger. This fact makes the spin-orbit interaction experimentally relevant for possible technological applications, in contrast to the vacuum value.

Spin-orbit coupling gives rise to several interesting transport phenomena arising from the induced correlation between charge and spin degrees of freedom [8–21]. It has been proposed as an efficient way to achieve the control of the electron spin through electrical and thermal external perturbations. One

of the biggest advantages of the devices based on this type of interaction is that we do not need external magnetic fields or ferromagnetic materials to achieve electrical control of the spin population. Among the many interesting effects that arise from spin-orbit coupling, two stand out for their potential technological importance: the spin Hall effect and the Edelstein effect.

The spin Hall effect (SHE) consists in the appearance of a spin current flowing perpendicular to an external electric field, spin polarized perpendicular to both, the electric field and the spin current, Fig.(1.1)(left) [22–27]. This effect was predicted theoretically by Dyakonov and Perel in 1971 [28]. It was not much noticed until 1999 when first Hirsch [8] and latter Zang [9] rediscovered the effect and brought it to the center of the discussions of the spintronics community. There are different types of spin-orbit mechanisms responsible for the SHE. We classify them in two different categories depending on the origin of the potential that causes the spin-orbit interaction. If it is due to scattering with impurities, magnetic or not, we talk about *extrinsic* spin-orbit interaction. If its due to the bands potential of the solid or due to an external potential, like the confining potential in a quantum well, we talk about *intrinsic* one.

An example of extrinsic mechanism is the so-called skew scattering. The idea goes back up to Mott [29], who pointed out that spin-orbit interaction polarizes in spin the diffused particles, assumed to be initially non polarized, due to a collision. We can see in Fig.(1.2)(left) a scheme of the skew scattering mechanism.

Bychkov and Rashba devised an extremely simple and yet powerful model [30] describing the intrinsic spin-orbit coupling of the electrons in a 2-dimensional

electron gas (2DEG) in a quantum well in the presence of an electric field perpendicular to the plane in which the electrons move. In 2004 Sinova et al. [11] calculated the spin Hall conductivity (SHC) of this model Fig.(1.2)(right). They found an universal result of $\sigma^{SHE} = e/8\pi$. It triggered a great explosion of activity in the study of the SHE. In contrast some numerical calculations showed a 0 value of the SHC when simulating these systems. There were several months of debate around this argument until the inclusion of vertex corrections, which we will explain through this work, closed the discussion and showed that the SHC vanishes in a 2DEG with Rashba coupling [31–33]. This vanishing SHC, which can be demonstrated rigorously using exact operatorial relations, does not occur if we include extrinsic mechanism in the model [19, 24, 34–42]. When both Rashba and extrinsic SOC are present the things get much more complicated, but really interesting too [38, 43, 44].

There is a huge number of experiments which have measured the SHE in electron/holes systems through different techniques. The first experimental proof of the SHE in semiconductors was obtained by Kato et. al. in 2004 [22]. They produced an external electric field in an *n*-type GaAs semiconductor. In this experiment the charge current generates a spin current due to spin-orbit coupling, but the spin current cannot flow due to the boundaries in the perpendicular direction. Then a spin accumulation appears at the edges (positive at one edge, negative at the other), so that this spin-gradient balances the spin Hall current. The above mentioned experiment measured this spin accumulation through Kerr rotation microscopy. It is important to notice that spin relaxation mechanisms decrease the spin accumulation. But the spin relaxation length in GaAs allows the spin accumulation to be visualized

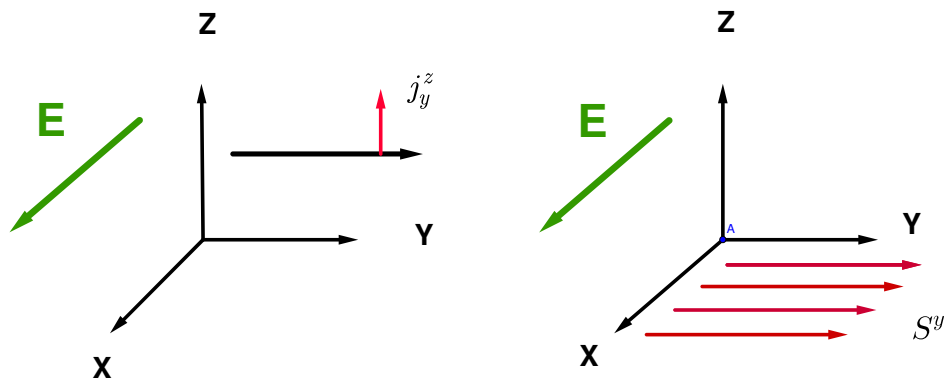


Figure 1.1: Left: Representation of the spin hall effect. The red line represents the direction of the spin polarization, the green one the external electric field and the black one the direction of the spin current. Right: Representation of the Edelstein effect. The red line represents the direction of the spin polarization, the green one the external electric field.

clearly enough by measuring the Faraday rotation of the radiation.

We know that in systems with spin-orbit coupling a charge current produces a spin current perpendicular to the first one. So a spin current will produce a charge current perpendicular to it because of Onsager relations. This is known as the inverse spin Hall effect (iSHE). This effect is easier to measure than the direct SHE because we know how to measure a charge voltage but it is not easy to measure a spin voltage. The iSHE has been measured in metals like Al [45] or Pt [36]. The geometry is the H-bar, one creates a charge current in one of the bars, because of spin-orbit coupling a spin current appears in the perpendicular bar and then we measure a voltage in the other vertical bar due to the iSHE.

This is only a very brief review of the experiments on the SHE. We refer the interested reader to literature [22–25, 36, 45–50].

The Edelstein effect, also known as current-induced spin polarization, [51, 52] consists in the appearance of a spin polarization perpendicular to an applied electric field, Fig.(1.1)(right). It has been proposed as a promising way of achieving all-electrical control of magnetic properties in electronic circuits. The effect has been measured experimentally following similar techniques as the ones used for measuring the SHE [22, 23, 53–58].

We can interpret the Edelstein effect as follows; the external electrical field induces a Zeeman effective field through the spin-orbit coupling. This effective magnetic field will be $b_{eff} \propto \Delta p \alpha$, where α depends on the spin-orbit interaction we are dealing with, for example in the 2DEG Rashba case $\alpha = eE\lambda_{eff}/4\hbar$, and Δp is the shift of the Fermi sphere due to the external electric field [59]. By looking to Eq.(1.2.1) the spin polarization will be

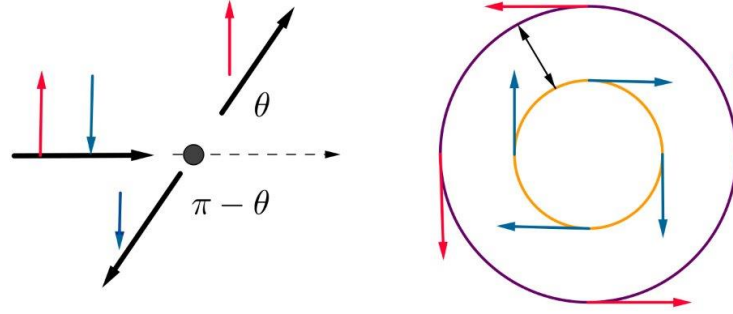


Figure 1.2: Left: Little representation of the extrinsic skew scattering mechanism predicted by Mott. Electrons with different spins get scattered in different directions due to spin-orbit coupling. Right: Fermi momentum in the case of 2DEG Rashba spin-orbit coupling.

perpendicular to the external electric field. In the concrete case of the Rashba SOC in a 2DEG which we mentioned before the Edelstein conductivity is

$$s^y = -eN_0\tau\alpha E_x, \quad (1.2.2)$$

where $N_0 = m/2\pi$ is the 2 dimensional density of states and τ the scattering time.

Both the Edelstein and the spin Hall effects are deeply connected as we will see through the following Chapters.

As we have seen these effects are at the center of spintronic research. As we pointed before the research of materials with intrinsic spin-orbit coupling and huge spin Hall conductivities is one of the biggest challenge for the physicists working in the field. Through this work we will calculate the spin Hall and the Edelstein conductivities following a new model proposed by

Wang et al. [60]. The model consists on a thin metal sandwiched by two different insulators. The inversion symmetry breaking and the interfaces generates giant spin-orbit coupling which is responsible for both effects. We will find really encouraging theoretical results which pushes ourselves to look after experimental data which confirm this predictions.

There is a deep connection between electrical and thermal effects. Thermoelectric studies are crucial if we are interested in describing all the transport properties of any physical system. In the case of metals most of the thermal effects are strongly correlated to the electrical ones. One example of this relation is the well known Wiedemann-Franz law, which states that, in the case of metals, the thermal conductivity is proportional to the electrical one.

The same thing happens in the field of spintronics. Knowing the coupling between the energy and the spin will be crucial if we want to describe the transport properties of any spintronic device. A new field has arisen, “spin caloritronics” which studies these spin thermoelectric effects.

One of the most important thermoelectric effect is the Seebeck effect, which consists in the generation of an electromotive force by applying an external temperature gradient. Analogously the spin Seebeck effect [61–67] consists in the generation of a spin voltage due to the application of an external temperature gradient. This spin voltage generates a spin current that has been experimentally detected due to the inverse spin Hall effect, in the same way that it was detected in the spin Hall experiments cited before [62].

Spin-orbit coupling plays an important role in “spin caloritronics” too.

	$H \neq 0$ $M = 0$	$H = 0$ $M \neq 0$	$H = 0$ $M = 0$
\vec{E}	Hall effect	AHE	SHE
∇T	Nernst effect	ANE	SNE

Table 1.1: Family of Hall- and Nernst-type effects [68].

By analogy with the spin Hall effect the spin Nernst effect (SNE) consists in the appearance of a pure spin current perpendicular to an applied temperature gradient [68–73]. This could be easily understood looking at Table 1.1 comparing both the electrical and thermal effects.

Through this work we will focus on the spin Nernst effect, and we will establish a relation between this and the spin Hall effect. We will see that metals are much more efficient devices as heat-to-spin than heat-to-charge converters.

1.3 Outline

This work is organized as follows.

Chapter 2 introduces spin-orbit coupling. We will firstly recall a little derivation of spin-orbit coupling in the non-relativistic limit of the Dirac equation. We will later explain how effective spin-orbit Hamiltonians terms arise in solid state systems. At the end of the Chapter we will pay some attention to two-dimensional systems which play an important role in spintronics. Supplementary material is given in Appendix A.

Chapter 3 is dedicated to the mathematical tools which are needed to

calculate all the transport properties on spin-orbit based systems. We will introduce the Green and the Matsubara Green functions We will recall the Kubo formula in the linear response regime. We will recall the impurity technique within the so-called self-consistent Born approximation. At the end of the Chapter we will use these techniques to calculate the spin Hall conductivity when Rashba and extrinsic spin-orbit coupling are present. Supplementary material is given in Appendix B.

In Chapter 4 we present original results regarding a model consisting on a thin metal sandwiched by two different insulators. After solving the model, we will calculate both the spin Hall and the Edelstein conductivities, taking into account the vertex corrections. We will discuss the relation that exist between both conductivities in this not strictly two-dimensional model. We will also present two interesting limit situations that can be described within this model, the insulator-metal-vacuum junction, and the insulator-metal-insulator junction with the same spin-orbit coupling constant at both interfaces. This last limit will provide encouraging results as we will see later on. At the end of the Chapter we will study the range of validity of the presented calculations. Supplementary material is given in Appendices B-C.

In Chapter 5 we present an original and general derivation of the spin Nernst effect. We will establish a total connection of the spin Nernst conductivity and the spin Hall conductivity with the same range of validity of the Wiedemann-Franz law. We will later calculate the spin Nernst conductivity in some specific cases showing that we are able to write a relation between the spin and the electric thermopowers. They are proportional one to the other by a factor which depends on the spin-orbit coupling. We will

show that in some cases metals present a better heat-to-spin efficiency than a heat-to-charge one.

The closing Chapter 6 is a brief summary and an overview of the current and future work.

Chapter 2

Spin-orbit interaction

Since spin-orbit interaction is crucial in spin-transport effects we will derive briefly how it appears in solid state systems. First we will recall its atomic derivation in the non-relativistic limit of the Dirac equation [74]. Then we will derive how it appears in different semiconductors following the so-called $\mathbf{k} \cdot \mathbf{p}$ method, within the Kane model [12, 75–77]. At the end of the Chapter we will apply these techniques to the special case of 2-D systems [78–80] and we will derive both the Rashba [30] and the Dresselhaus [81] spin-orbit coupling Hamiltonians.

This is only a brief recall of the effective spin-orbit coupling Hamiltonian terms in solid state systems. For a more extended treatment we refer the interested reader to the literature cited before.

2.1 The origin of the spin-orbit interaction

Spin-orbit interaction (SOI) arises in the non-relativistic limit of the Dirac equation. The Dirac equation reads

$$i\hbar\partial_t\psi = (\hat{\boldsymbol{\alpha}} \cdot \hat{\mathbf{P}} + \hat{\beta}mc^2 + \hat{V})\psi, \quad (2.1.1)$$

with

$$\hat{\boldsymbol{\alpha}} = \begin{pmatrix} 0 & \boldsymbol{\sigma} \\ \boldsymbol{\sigma} & 0 \end{pmatrix}, \hat{\beta} = \begin{pmatrix} 1 & 0 \\ 0 & -1 \end{pmatrix}, \hat{V} = V\hat{I}, \hat{\mathbf{P}} = \mathbf{p}\hat{I}, \psi = \begin{pmatrix} \psi_1 \\ \psi_2 \end{pmatrix},$$

where ψ_1, ψ_2 are the upper and lower components of the bispinor ψ and $V = e\phi$. Taking the zero energy as mc^2 , the Dirac equation can be written as

$$i\hbar\partial_t\psi_1 = e\phi\psi_1 + c\boldsymbol{\sigma} \cdot \mathbf{p}\psi_2 \quad (2.1.2)$$

$$i\hbar\partial_t\psi_2 = c\boldsymbol{\sigma} \cdot \mathbf{p}\psi_1 - (2mc^2 - e\phi)\psi_2. \quad (2.1.3)$$

We want to know the form of ψ when $e\phi$ and cp are small compared to the so-called Dirac gap $2mc^2$ (the non-relativistic limit). If we make an expansion in the parameter $1/(2mc^2)$, the second equation gives us the following relation

$$\psi_2 \simeq \frac{1}{2mc} \left(1 - \frac{i\hbar\partial_t}{2mc^2} + \frac{e\phi}{2mc^2} \right) \boldsymbol{\sigma} \cdot \mathbf{p}\psi_1. \quad (2.1.4)$$

The normalization condition for the original wave function $\langle\psi|\psi\rangle=1$ implies

$$\langle\psi|\psi\rangle = \langle\psi_1|\psi_1\rangle + \langle\psi_2|\psi_2\rangle, \quad (2.1.5)$$

then, if we define

$$\tilde{\psi} = \left(1 + \frac{(\boldsymbol{\sigma} \cdot \mathbf{p})^2}{8m^2c^2} \right) \psi_1, \quad (2.1.6)$$

$\tilde{\psi}$ satisfies $\langle \psi | \psi \rangle = 1$ at order $1/c^2$. The equation for $\tilde{\psi}$ reads

$$i\hbar\partial_t\tilde{\psi} = \left(1 - \frac{(\boldsymbol{\sigma} \cdot \mathbf{p})^2}{8m^2c^2}\right) \left[e\phi + \frac{1}{2m}\boldsymbol{\sigma} \cdot \mathbf{p} \left(1 + \frac{e\phi}{2mc^2}\right) \boldsymbol{\sigma} \cdot \mathbf{p} \right] \left(1 + \frac{(\boldsymbol{\sigma} \cdot \mathbf{p})^2}{8m^2c^2}\right) \tilde{\psi}. \quad (2.1.7)$$

By performing the products up to terms of order $1/c^2$, we get

$$H_{eff} = e\phi + \frac{p^2}{2m} - \frac{p^4}{8m^3c^2} + \frac{e\hbar\Delta\phi}{8m^2c^2} + \frac{e\hbar}{4m^2c^2}\boldsymbol{\sigma} \cdot \nabla\phi \times \mathbf{p}, \quad (2.1.8)$$

where the first two terms represents the "classical" non-relativistic Hamiltonian, the third term is the first relativistic correction to the kinetic energy, the fourth term is the so-called Darwin term, and finally the last one is the spin-orbit interaction. Let us rewrite this term

$$H_{so} = \frac{\lambda_0^2}{4}\boldsymbol{\sigma} \cdot \nabla\phi \times \mathbf{p}, \quad (2.1.9)$$

where $\lambda_0 = \hbar/(mc) \simeq 10^{-10}\text{cm}$ is the Compton wave length. In atoms, $e\phi$ is the central field due to the nucleus and to the screening of the electrons and the SOI term is the responsible of the fine structure of the atomic spectra. In solids the derivation is a little different, but we will find effective Hamiltonians that will include terms as the one of Eq.(2.1.9). In the next Section we will calculate this effective terms in semiconductors following the $k \cdot p$ method and the Kane model

2.2 The $k \cdot p$ method and the Kane model

We want to describe the motion of charge carriers in solid state systems. The goal is to describe this motion in terms of effective Hamiltonians that take into account external electric and magnetic, fields, impurities due to

disorder, and more importantly, spin-orbit interaction. These Hamiltonians will be derived through various approximations, but they will be able to describe all the relevant physics we are interested in. This is achieved via the Luttinger-Kohn method, also known as $k \cdot p$ method, and the so-called Kane model.

First of all we will treat the problem in the absence of external fields, and in the absence of impurities, and then we will see how to introduce them. The single-particle Schrödinger equation for an electron in a lattice described by the potential $U(\mathbf{x})$ and in the presence of spin-orbit coupling reads

$$\begin{aligned} H_0 \psi_{\nu\mathbf{k}}(\mathbf{x}) &= \left[\frac{(-i\hbar\nabla)^2}{2m_0} + U(\mathbf{x}) + \frac{\hbar}{4m_0^2 c^2} \nabla U(\mathbf{x}) \times (-i\hbar\nabla) \cdot \boldsymbol{\sigma} \right] \psi_{\nu\mathbf{k}}(\mathbf{x}) \\ &= \epsilon_{\nu\mathbf{k}} \psi_{\nu\mathbf{k}}(\mathbf{x}), \end{aligned} \quad (2.2.10)$$

where ν is the band index, m_0 the bare electron mass. From now on we will work in natural units, i.e. $\hbar = c = 1$. According to Bloch's theorem the translational symmetry of the lattice requires the wave function to be of the following form

$$\psi_{\nu\mathbf{k}}(\mathbf{x}) = e^{i\mathbf{k}\cdot\mathbf{x}} u_{\nu\mathbf{k}}(\mathbf{x}) \quad (2.2.11)$$

with $u_{\nu\mathbf{k}}(\mathbf{x})$ a function with the same periodicity of the lattice. In several solid state systems, like in GaAs, the bottom of the conduction band - and the maximum of the valence one - lies at the Γ point $\mathbf{k} = \mathbf{0}$. Then the eigenfunctions of Eq.(2.2.11) can be expanded in the following basis

$$u_{\nu\mathbf{k}}(\mathbf{x}) = \sum_{\nu'} c_{\nu\nu'\mathbf{k}} u_{\nu'0}(\mathbf{x}). \quad (2.2.12)$$

In such a basis, using ket notation, one obtain the matrix elements

$$\begin{aligned} H_{0,\nu\nu'} &= \langle u_{\nu 0} | H_0 | u_{\nu' 0} \rangle \\ &= \left(\epsilon_{\nu 0} + \frac{k^2}{2m} \right) \delta_{\nu\nu'} + \frac{1}{m_0} \mathbf{k} \cdot \boldsymbol{\pi}_{\nu\nu'}, \end{aligned} \quad (2.2.13)$$

where $\epsilon_{\nu 0}$ is the energy offset of the band at $\mathbf{k} = \mathbf{0}$

$$\left[\frac{(-i\nabla)^2}{2m_0} + U + \frac{1}{4m_0^2} \nabla U \times (-i\nabla) \cdot \boldsymbol{\sigma} \right] |u_{\nu 0}\rangle = \epsilon_{\nu 0} |u_{\nu 0}\rangle \quad (2.2.14)$$

and

$$\begin{aligned} \boldsymbol{\pi}_{\nu\nu'} &= \langle u_{\nu 0} | (-i\nabla) + \frac{1}{4m_0^2} \nabla U \times \boldsymbol{\sigma} | u_{\nu' 0} \rangle \\ &\approx \langle u_{\nu 0} | (-i\nabla) | u_{\nu' 0} \rangle. \end{aligned} \quad (2.2.15)$$

For more details about these approximations see Appendix A.

We can see from Eqs.(2.2.14,2.2.15) that the spin-orbit coupling enters only in the calculation of the diagonal terms $\epsilon_{\nu 0}$. For a real treatment of Eq.(2.2.12) we have to truncate the expansion of $u_{\nu 0}(\mathbf{x})$, and only the band closest to the gap will be considered (see Appendix A).

This leads to the so-called 8×8 Kane model, when we consider two spin degenerate s-wave conduction bands and six p-wave valence bands. The p-like bands are partially split by spin-orbit coupling into two groups. The first made of four degenerate levels, the light and heavy hole bands ($J = 3/2$), and the other two, also called split-off levels ($J = 1/2$). This is shown schematically in Fig.2.1. There are less-restrictive models, which take into account the effect of more conduction bands as the so-called Kane extended model, 14×14 . Obviously the more bands we take into account the more accurate the model is, but the normal Kane Hamiltonian explains quite well how spin-orbit coupling appears in solid state systems.

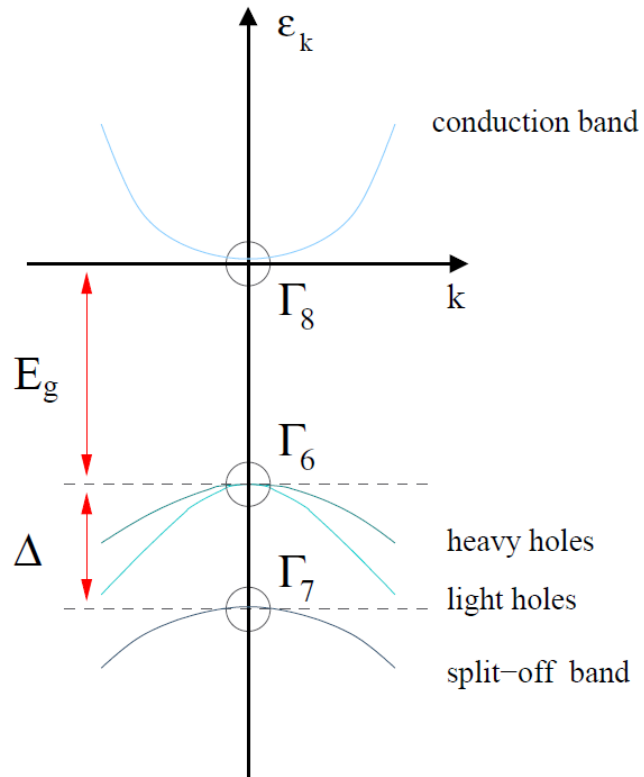


Figure 2.1: Schematic band structure at the Γ -point for 8×8 Kane model. Spin-orbit interaction, Δ , splits the six p-like valence levels into the light and heavy hole bands, with total angular momentum $J = 3/2$, and the split-off band, with $J = 1/2$.

The fully 8×8 Kane Hamiltonian can be written in the following way

$$\begin{aligned} H \begin{pmatrix} \phi_c \\ \phi_v \end{pmatrix} &= \begin{pmatrix} H_{c,2 \times 2} & H_{cv,2 \times 6} \\ H_{cv,6 \times 2}^\dagger & H_{v,6 \times 6} \end{pmatrix} \begin{pmatrix} \phi_c \\ \phi_v \end{pmatrix} \\ &= \epsilon \begin{pmatrix} \phi_c \\ \phi_v \end{pmatrix}, \end{aligned} \quad (2.2.16)$$

with ϕ_c and ϕ_v respectively a two-dimensional and six-dimensional spinor for the conduction and the valence bands. We will assume that the energy gap, E_g , is the biggest energy scale, in other words the two group of states are far away from each other and thus weakly coupled, $H_{cv}, H_{cv}^\dagger \ll E_g \sim H_v$. This pushes us to write a 2×2 equation for the electrons of the conduction band

$$\mathcal{H}(\epsilon) \bar{\phi} = \epsilon \bar{\phi}, \quad (2.2.17)$$

with

$$\mathcal{H}(\epsilon) = H_c + H_{cv}(\epsilon - H_v)^{-1} H_{cv}^\dagger \quad (2.2.18)$$

and $\bar{\phi}$ a renormalized conduction band spinor. When we expand Eq.(2.2.18) for energies close to the band minimum, and we insert this expansion in Eq.(2.2.17) the effective eigenvalue equation for $\bar{\phi}$ is obtained. The coupling with the valence band is translated into a renormalization of the effective mass, the g-factor, and the spin-orbit coupling constant. The eigenvalue equation in the presence of an external electromagnetic field and any possible potential V reads

$$\left[\frac{[(-i\nabla) + e\mathbf{A}]^2}{2m^*} + V - \frac{\mu_B g^*}{2} \boldsymbol{\sigma} \cdot \mathbf{B} + \frac{\lambda^2}{4} \nabla V \times [(-i\nabla) + e\mathbf{A}] \cdot \boldsymbol{\sigma} \right] \bar{\phi} = \epsilon \bar{\phi} \quad (2.2.19)$$

with μ_B the Bohr magneton, m^* and g^* the renormalized mass and g-factor, $\mathbf{B} = \nabla \times \mathbf{A}$ the external magnetic field and λ the new spin-orbit wavelength (the renormalized Compton wavelength). All these quantities are written in terms of parameters of the 8×8 Hamiltonian and their derivation is presented in Appendix A. The most important quantity is the new parameter $\lambda^2/4$ that, as we said before, has the same form as the spin-orbit term appearing in the expansion of the Dirac equation (Eq.(2.1.9)). In solids this parameter can be much bigger than the vacuum constant $\lambda_0^2/4$, it can be six orders of magnitude bigger. Here we present the value of these new parameters

$$\frac{1}{2m^*} = \left(\frac{1}{E_g + \Delta} + \frac{2}{E_g} \right), \quad (2.2.20)$$

$$g^* = \frac{2e}{\mu_B} \frac{P^2}{3} \left(\frac{1}{E_g} - \frac{1}{E_g + \Delta} \right), \quad (2.2.21)$$

$$\frac{\lambda^2}{4} = \frac{P^2}{3} \left(\frac{1}{E_g^2} - \frac{1}{(E_g + \Delta)^2} \right), \quad (2.2.22)$$

where P takes into account the correlation between the s and the p bands, and Δ the spin-orbit splitting between the $j = 1/2$ and the $j = 3/2$ valence bands (for details see Appendix A). Eq.(2.2.19) shows how the spin-orbit coupling in the bands arises in the presence of a non-crystalline potential V . We will distinguish between *intrinsic* and *extrinsic* effects depending on the origin of the potential V . If it is due to impurities we will talk about *extrinsic* mechanisms, whereas if it is due to confining potentials (or other type of geometry or interfacial effects) we will talk about *intrinsic* mechanisms.

It is important to remark that the 8×8 Kane model describes quite well the conduction band electrons in zincblende crystals, e.g. III-V (GaAs-based) and II-VI (CdTe based) semiconductors. If the symmetries of the crystal change, we should change the size and the symmetries of the Hamiltonian we

are treating. This derivation is not good if we want to describe, for example, spin-orbit coupling in Platinum. The materials with the crystal structure as the ones presented here (8×8 Kane Hamiltonian) have no inversion symmetry. Let us see how inversion symmetry is related to spin-orbit phenomena. Let's consider a state with vector \mathbf{k} and spin \uparrow . In the presence of time reversal symmetry, by Kramers theorem

$$E(\mathbf{k}, \uparrow) = E(-\mathbf{k}, \downarrow). \quad (2.2.23)$$

If the system has space inversion symmetry

$$E(\mathbf{k}, \downarrow) = E(-\mathbf{k}, \downarrow). \quad (2.2.24)$$

So if the system has space inversion symmetry there is a degeneracy of the spin states in the absence of external magnetic fields. But the materials with no inversion symmetry, as the ones treated here, have spin-split energies as we will see in the next Section.

2.3 Intrinsic spin-orbit coupling in 2-D systems

One of the most studied system in spin-orbit based transport phenomena, is the so-called two-dimensional electron gas (2DEG). Here we will derive how we model this type of devices and what are the spin-orbit coupling terms associated with this type of systems. The main idea is to grow different band structures, whose properties can be fine-tuned through strains, external potential gates or doping, with the goal of creating a potential well for the conduction electrons (holes). This is shown in Fig.2.2 for the typical example of GaAs/GaAlAs modulation-doped heterostructures. As shown in

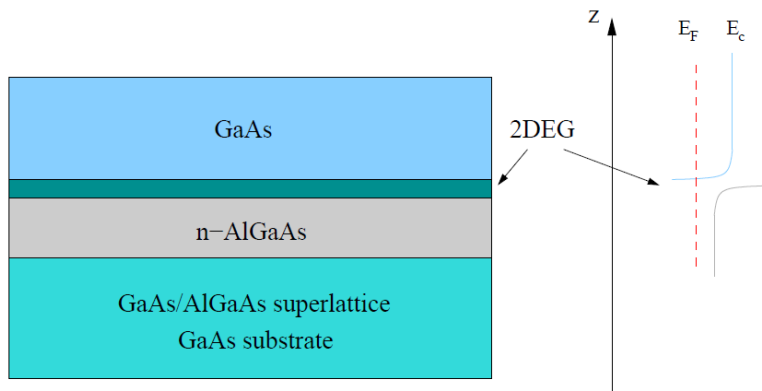


Figure 2.2: Scheme of a modulation-doped heterostructure based on the GaAs/n-AlGaAs, junction based on the experimental setup shown in [24].

Fig.2.3, electrons are trapped at the interface of this asymmetric quantum well, but they feel this external electric field $E_z = \nabla V$. This confining electric field is the responsible of the so-called Bychkov-Rashba (mostly referred as Rashba) spin-orbit interaction. In this case we can rewrite the Hamiltonian of Eq.(2.2.19) in the following way

$$H = \frac{k^2}{2m^*} + V - \mathbf{b}'(\mathbf{k}) \cdot \boldsymbol{\sigma}, \quad (2.3.25)$$

where $\mathbf{k} = -i\nabla + e\mathbf{A}$ and $\mathbf{b}'(\mathbf{k})$ contains two terms, one due to the external magnetic field, and the other due to the k-dependent spin-orbit coupling,

$$\mathbf{b}'(\mathbf{k}) = \mathbf{b}_{ext} + \mathbf{b}(\mathbf{k}) \quad (2.3.26)$$

In the 2DEG Rashba case we have $\nabla V = eE\hat{\mathbf{z}}$ and

$$\mathbf{b}(\mathbf{k}) \cdot \boldsymbol{\sigma} \rightarrow \mathbf{b}_R(\mathbf{k}) \cdot \boldsymbol{\sigma} = \alpha(k_x\sigma_y - k_y\sigma_x) = \alpha\hat{\mathbf{z}} \times \mathbf{k} \cdot \boldsymbol{\sigma} \quad (2.3.27)$$

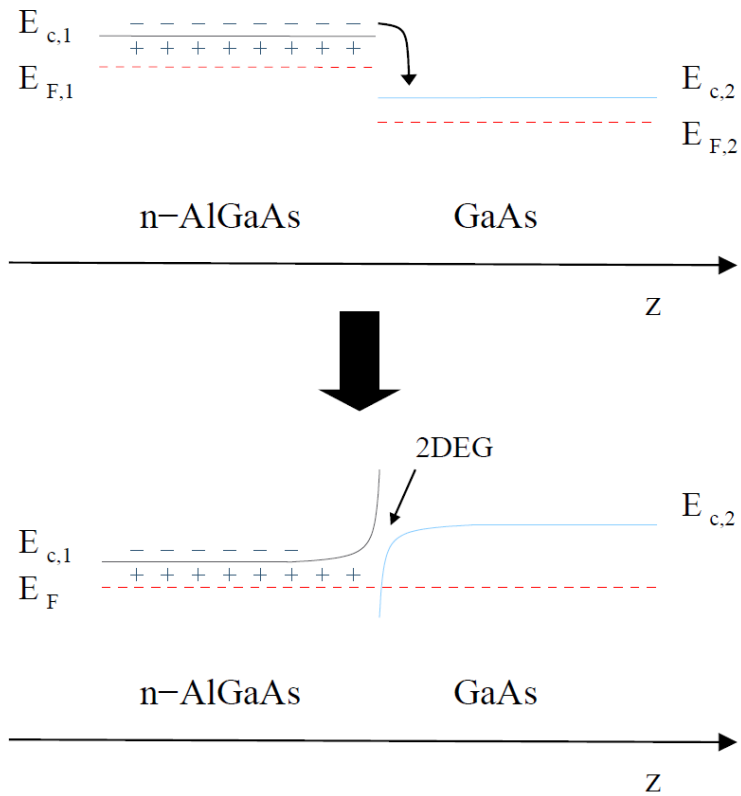


Figure 2.3: Schematic representation of the effect of modulating doping on the conduction band at the GaAs/n-AlGaAs interface. Matching the two sides means that the electrons released by the donor impurities move to the GaAs layer until equilibrium is reached (Fermi levels aligned). In this way electrons are trapped at the interface of an asymmetric quantum well

with the parameter $\alpha = eE\lambda^2/4$ tunable via the gates ($V = V(z)$).

Now we are able to calculate the eigenvalues and eigenfunctions of the Rashba 2DEG model. In the absence of disorder and external electromagnetic fields the Hamiltonian reads

$$H = \frac{k^2}{2m^*} + \alpha(k_y\sigma_x - k_x\sigma_y) \quad (2.3.28)$$

The solution of the Schrödinger equation is

$$E_{ks} = \frac{k^2}{2m^*} - \alpha ks \quad (2.3.29)$$

$$\psi_{\mathbf{k}s}(\mathbf{r}) = \frac{e^{i\mathbf{k}\cdot\mathbf{r}}}{\sqrt{\mathcal{A}}} \frac{1}{\sqrt{2}} \begin{pmatrix} 1 \\ ise^{i\theta_{\mathbf{k}}} \end{pmatrix}, \quad (2.3.30)$$

where $\theta_{\mathbf{k}}$ is the angle between \mathbf{k} and the x axis. As we can see momentum, \mathbf{k} , and the projection of the spin in the direction perpendicular to \mathbf{k} , i.e. the chirality, s , are good quantum numbers. We can also see, as predicted in the previous Section, that there is a spin splitting in the energy of the form $\Delta E_k = 2\alpha k$, because this type of 2-D systems have no inversion symmetry.

It is important to remember that other mechanisms give rise to similar spin-orbit interaction terms. For example considering the more elaborate 14×14 Kane model for zincblende crystals, where we calculate the effective spin-orbit interaction term for the electrons in the conduction band, the following cubic-in-momentum term, called the cubic Dresselhaus term, is obtained

$$\mathbf{b}_D(\mathbf{k}) \cdot \boldsymbol{\sigma} = Ck_x(k_z^2 - k_y^2)\sigma_x + \text{cyclic permutations}, \quad (2.3.31)$$

with C a crystal-dependent constant. If we are interested in the effects of the Dresselhaus SOI in a 2DEG, we have to average $\langle H_D \rangle$ along the growth

direction $\hat{\mathbf{z}}$, which we assume parallel to the [001] crystallographic direction. In this case k_z is quantized with $\langle k_z^2 \rangle \sim (\pi/d)^2$, d being the width of the well. The main bulk-inversion-asymmetry contribution is then

$$[\mathbf{b}_D(\mathbf{k})]_{2D} \cdot \boldsymbol{\sigma} = \beta(k_x \sigma_x - k_y \sigma_y), \quad (2.3.32)$$

with $\beta \simeq C(\pi/d)^2$. There is an important difference between the Rashba and the Dresselhaus terms. The first one has its origin in the non-crystalline potential and the second one depends on the crystal one. Both terms can be of comparable magnitudes, the predominance of one or the other depends on the specific characteristic of the system. In any case the spin-splitting caused by any of both SOI terms is usually much smaller than the Fermi energy, $|\mathbf{b}_R|, |\mathbf{b}_D| \ll \epsilon_F$.

In the following we will be more interested in the Rashba SOI, because it is one of the most studied system in literature [11, 13, 14, 18, 25, 30–33, 39, 52, 54, 60, 82–84]. We have focused our attention to *intrinsic* mechanisms. We will not show a complete description of *extrinsic* ones but as we will see later on they are also very important [19, 24, 34–42] in spin-transport effects in 2DEG systems.

Chapter 3

The linear response theory and its application to Fermi systems

We are interested in calculating the response of a physical system to an external perturbation. To this end we recall briefly some aspects of the Green function technique. Then we derive the Kubo formula for various spin transport coefficients. After that we recall the impurities technique for disordered electron systems.

In the last Sections of this Chapter we evaluate both the spin Hall conductivity in a 2DEG with Rashba and extrinsic SOC using the techniques shown through this Chapter.

We only refer to fermions all through the Chapter. Obviously these techniques are also extensible to bosons. We refer the interested reader to the literature [85–96]. We will work in natural units $\hbar = c = 1$.

3.1 The Green function and the linear response theory

The Green function is one of the most important tools in Quantum Field Theory. It is especially useful in dealing with perturbation theory solutions. It represents a great way to encode information and to calculate expectation values of different physical observables. The one-particle Green function, also known as propagator, is defined by

$$G_{\sigma\sigma'}(\mathbf{x}, t, \mathbf{x}', t') = -i\langle T_t \Phi_\sigma(\mathbf{x}, t) \Phi_{\sigma'}^\dagger(\mathbf{x}', t') \rangle, \quad (3.1.1)$$

where T_t is the time-ordering operator, $\langle \dots \rangle$ indicates the average over the ground state $\langle \Psi_0 | \dots | \Psi_0 \rangle$, and $\Phi_\sigma, \Phi_{\sigma'}^\dagger$ are the field operators. If we derive with respect to time Eq.(3.1.1) we obtain

$$i\partial_t G_{\sigma\sigma'}(\mathbf{x}, t, \mathbf{x}', t') = \delta(t - t')\delta(\mathbf{x} - \mathbf{x}')\delta_{\sigma\sigma'} - i\langle T_t i\partial_t \Phi_\sigma(\mathbf{x}, t) \Phi_{\sigma'}^\dagger(\mathbf{x}', t') \rangle. \quad (3.1.2)$$

Since we consider problems which can be described by single particle Hamiltonians, Eq.(3.1.2) can be written as

$$i\partial_t G_{\sigma\sigma'}(\mathbf{x}, t, \mathbf{x}', t') = \delta(t - t')\delta(\mathbf{x} - \mathbf{x}')\delta_{\sigma\sigma'} - i\langle T_t H \Phi_\sigma(\mathbf{x}, t) \Phi_{\sigma'}^\dagger(\mathbf{x}', t') \rangle, \quad (3.1.3)$$

so we are able to write the following equation

$$(i\partial_t - H)G_{\sigma\sigma'}(\mathbf{x}, t, \mathbf{x}', t') = \delta(t - t')\delta(\mathbf{x} - \mathbf{x}')\delta_{\sigma\sigma'}. \quad (3.1.4)$$

Let us see why the Green function is also called the propagator. Let us imagine that we know the wave function at a time t' . In this case we are able

to write the wave function at the time t as

$$\psi(\mathbf{x}, t) = \int d\mathbf{x}' G^R(\mathbf{x}, t, \mathbf{x}', t') \psi(\mathbf{x}', t'), \quad (3.1.5)$$

where G^R is the retarded Green function, which as we will see later is closely related with the Green function defined before. This equation is valid for $t > t'$. As we can see the Green function “propagates” the wave function from the position \mathbf{x}' at the time t' to the position \mathbf{x} at time t .

If the system is translational invariant we can define the Fourier transform of the Green function to respect $\mathbf{x} - \mathbf{x}'$ and to $t - t'$ as

$$G(\mathbf{x}, t, \mathbf{x}', t') = \frac{1}{V} \sum_{\mathbf{k}} e^{i\mathbf{k}\cdot(\mathbf{x}-\mathbf{x}')} \int_{-\infty}^{+\infty} \frac{d\omega}{2\pi} e^{i\omega(t-t')} G(\mathbf{k}, \omega). \quad (3.1.6)$$

In the limit of infinite volume, $V \rightarrow \infty$, the sum over momentum reduces to an integral, $1/V \sum_{\mathbf{k}} \rightarrow (2\pi)^{-d} \int d^d k$. From now on the sum over \mathbf{k} , $\sum_{\mathbf{k}}$, will be intended as an integral, $\int_{\mathbf{k}}$. When we calculate the Green function in the non-interacting Fermi sea case we obtain

$$G^0(\mathbf{k}, \omega) = \frac{1}{\omega - \xi(\mathbf{k}) + i\text{sgn}(|\mathbf{k}| - k_F)0^+}, \quad (3.1.7)$$

where $\xi(\mathbf{k}) = k^2/2m - \mu$, k_F is the fermi momentum and μ is the chemical potential. We have introduced an infinitesimal imaginary term in the denominator, $+i\text{sgn}(|\mathbf{k}| - k_F)0^+$, to make the integrals of Eq.(3.1.6) convergent [89].

Now, before we move on, we recall Wick’s theorem in its zero-temperature form for the case of the expectation value of four field operators.

$$\langle T_t \Phi_\sigma^\dagger(\mathbf{x}, t) \Phi_\sigma(\mathbf{x}, t) \Phi_{\sigma'}^\dagger(\mathbf{x}', t') \Phi_{\sigma'}(\mathbf{x}', t') \rangle = -\langle T_t \Phi_\sigma(\mathbf{x}, t) \Phi_{\sigma'}^\dagger(\mathbf{x}', t') \rangle \langle T_t \Phi_{\sigma'}(\mathbf{x}', t') \Phi_\sigma^\dagger(\mathbf{x}, t) \rangle, \quad (3.1.8)$$

which as we will see below it is crucial if we want to write the Kubo formula as a function of the Green functions.

In the zero-temperature limit, the Green function, which encodes information about the wave function, is sufficient to our purposes. This limit is allowed in all electrical-spin problems of our interest because we will describe systems in which room temperature will be smaller than the Fermi temperature. When we are dealing with spin thermoelectric situations, where temperature and statistical effects are important, the Green functions are no longer sufficient. We then define the Matsubara Green function as

$$\mathcal{G}_{\sigma\sigma'}(\mathbf{x}, \tau, \mathbf{x}', \tau') = -\langle T_\tau \Phi_\sigma(\mathbf{x}, \tau) \bar{\Phi}_{\sigma'}(\mathbf{x}', \tau') \rangle, \quad (3.1.9)$$

where the fictitious imaginary time is $i\tau$ with τ that varies in the interval $(0, \beta)$ with $\beta = 1/k_B T$ (from now on $k_B = 1$) and now $\langle \dots \rangle = Tr[e^{-\beta K + \beta \Omega} \dots]$, where $K = H - \mu N$ and Ω the grand canonical potential. These new Matsubara Green functions take into account the effects of finite temperature. The time dependence of the field operators are

$$\Phi_\sigma(\mathbf{x}, \tau) = e^{K\tau} \Phi_\sigma(\mathbf{x}) e^{-K\tau}, \quad \bar{\Phi}_\sigma(\mathbf{x}, \tau) = e^{K\tau} \Phi_\sigma^\dagger(\mathbf{x}) e^{-K\tau}. \quad (3.1.10)$$

It is important to notice that $\bar{\Phi}_\sigma(\mathbf{x}, \tau)$ is not the Hermitian conjugate of $\Phi_\sigma(\mathbf{x}, \tau)$ as it was in the standard Green functions definition, Eq.(3.1.1).

The Matsubara Green function has an important property

$$\mathcal{G}(\mathbf{x}, -\tau, \mathbf{x}', 0) = -\mathcal{G}(\mathbf{x}, -\tau + \beta, \mathbf{x}', 0), \quad 0 < \tau < \beta. \quad (3.1.11)$$

This is crucial for the definition of the Fourier series expansion of the Matsubara functions in the interval $(-\beta, \beta)$

$$\mathcal{G}(\tau) = \frac{1}{\beta} \sum_{n=-\infty}^{\infty} e^{-i\omega_n \tau} \mathcal{G}(\omega_n) \quad (3.1.12)$$

$$\mathcal{G}(\omega_n) = \frac{1}{2} \int_{-\infty}^{\infty} d\tau e^{i\omega_n \tau} \mathcal{G}(\tau), \quad (3.1.13)$$

with $\omega_n = (2n + 1)\pi/\beta$ and n running over the naturals.

All the techniques shown for the Green functions, including Wick's theorem, are analogous when we are dealing with the Matsubara Green functions, by analytical continuation by sending $i\omega_n \rightarrow \omega$. For an extended treatment of this formalism we refer the interested reader to the literature cited at the beginning of the Chapter.

The most important scope of this work is to calculate different transport coefficients in the presence of external perturbations. We will calculate them in the frame of the linear response theory. This theory is based on the idea that the external perturbation, for example an external electric field, is small enough so we can only take into account the linear perturbation term. We want to calculate the average of any operator $\langle O_A \rangle$. Let us divide the Hamiltonian into two terms

$$H = H_0 + H_{ext}, \quad (3.1.14)$$

where H_0 is the Hamiltonian in the absence of the external perturbation, and H_{ext} represents the external perturbation. We will be interested in describing the coupling of the electrons with an external field, so we will be able to write H_{ext} as

$$H_{ext}(t) = \int d\mathbf{x}' O_B(\mathbf{x}') U_B(\mathbf{x}', t), \quad (3.1.15)$$

where $U_B(\mathbf{x}', t)$ specifies the external field coupling with the observable $O_B(\mathbf{x}')$. We will use the interaction representation and we will introduce the interaction adiabatically, i.e. $H_{ext} \rightarrow 0$ when $t \rightarrow -\infty$, which is equivalent to $|\Psi_i(t_0 \rightarrow -\infty)\rangle = |\Psi_0\rangle$. This allows us to write

$$|\Psi_i(t)\rangle = |\Psi_0\rangle - i \int_{-\infty}^t dt' H_{ext}(t') |\Psi_0\rangle. \quad (3.1.16)$$

So $\langle O_A \rangle$ becomes

$$\begin{aligned}
\langle \Psi(t) | O_A | \Psi(t) \rangle &= \langle \Psi_i(t) | O_{i,A}(t) | \Psi_i(t) \rangle \\
&= \langle \Psi_0 | \left(1 + i \int_{-\infty}^t dt' H_{ext}(t') \right) O_{i,A}(t) \left(1 - i \int_{-\infty}^t dt' H_{ext}(t') \right) | \Psi_0 \rangle \\
&= \langle \Psi_0 | O_A(t) | \Psi_0 \rangle - i \int_{-\infty}^t dt' \langle \Psi_0 | [O_A(t), H_{ext}(t')] | \Psi_0 \rangle. \tag{3.1.17}
\end{aligned}$$

The first term is the average over the unperturbed system, which is not the one we are interested in, but the second gives us the information of the perturbation on the average of the operator.

$$\delta \langle O_A(\mathbf{x}, t) \rangle \equiv \langle O_A \rangle - \langle O_A \rangle_0 = \int_{-\infty}^{\infty} dt' \int d\mathbf{x}' R^{AB}(\mathbf{x}, \mathbf{x}', t - t') U_B(\mathbf{x}', t'), \tag{3.1.18}$$

where

$$R^{AB}(\mathbf{x}, \mathbf{x}', t) = -i\theta(t) \langle [O_A(\mathbf{x}, t), O_B(\mathbf{x}', 0)] \rangle_0. \tag{3.1.19}$$

This is the famous Kubo formula which expresses the linear response to an external perturbation H_{ext} in the zero-temperature limit. R^{AB} depends only on the properties of the unperturbed system. Since H_0 will be time independent, the response function depends on the time difference and not on both times separately. Then we introduce the Fourier transform respect time and space

$$R^{AB}(\mathbf{x}, \mathbf{x}', t - t') = \int_{-\infty}^{\infty} \frac{d\omega}{2\pi} \sum_{\mathbf{q}, \mathbf{q}'} R_{\mathbf{q}, \mathbf{q}'}^{AB}(\omega) e^{-i\omega(t-t')} e^{i\mathbf{q} \cdot \mathbf{x} + i\mathbf{q}' \cdot \mathbf{x}'}. \tag{3.1.20}$$

If the unperturbed system is also translational invariant then the response function will only depend on the difference of the space arguments which easily implies $R_{\mathbf{q}, \mathbf{q}'}^{AB}(\omega) = R_{\mathbf{q}}^{AB}(\omega) \delta_{\mathbf{q} + \mathbf{q}', 0}$ with

$$R_{\mathbf{q}}^{AB}(\omega) = - \int_{-\infty}^{\infty} dt e^{i\omega t} i\theta(t) \langle [O_A(\mathbf{q}, t), O_B(-\mathbf{q}, 0)] \rangle_0. \tag{3.1.21}$$

By Fourier transforming Eq.(3.1.18) we obtain

$$\delta\langle O_A(\mathbf{q}, \omega) \rangle = R_{\mathbf{q}}^{AB}(\omega) U_B(\mathbf{q}, \omega). \quad (3.1.22)$$

For uniform and static perturbations we will limit ourselves to calculate the limits $\mathbf{q} \rightarrow 0$ and $\omega \rightarrow 0$ of the response function.

Now we will define

$$P^{AB}(\mathbf{x}, \mathbf{x}', t) = -i\langle T_t O_A(\mathbf{x}, t), O_B(\mathbf{x}', 0) \rangle_0, \quad (3.1.23)$$

where T_t is the time-ordering operator. It is easy to show that

$$\begin{aligned} \text{Re}R_{\mathbf{q}}^{AB}(\omega) &= \text{Re}P_{\mathbf{q}}^{AB}(\omega) \\ \text{Im}R_{\mathbf{q}}^{AB}(\omega) &= \text{sgn}(\omega)\text{Im}P_{\mathbf{q}}^{AB}(\omega). \end{aligned} \quad (3.1.24)$$

So R^{AB} and P^{AB} contain the same information.

We will be interested in calculating different spin transport coefficients in the presence of different external perturbations. We will be specially interested in three different coefficients, the spin Hall (SHC), the Edelstein (EC) and the spin Nernst (SNC) conductivities, defined by

$$j_y^z = \sigma^{SHE} E_x \quad (3.1.25)$$

$$s^y = \sigma^{EE} E_x \quad (3.1.26)$$

$$j_y^z = N^{SHE} \nabla_x T. \quad (3.1.27)$$

One of the most interesting features of the Kubo formula is that we are able to associate each conductivity with a Feynmann diagram, Fig 3.1.

The spin Hall effect consists in the appearance of a spin current perpendicular to an external electric field. The operator to consider is the spin

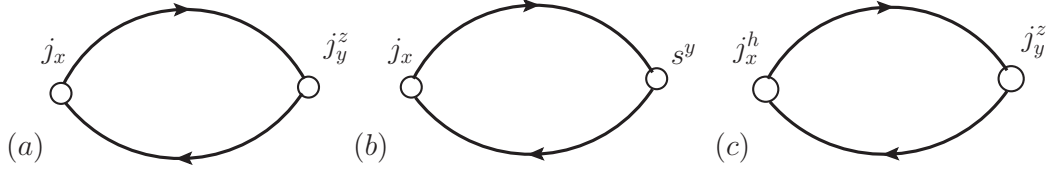


Figure 3.1: Feynman bubble diagrams for the SHC(a), EC (b) and SNC(c).

current $O_A \rightarrow j_k^a = j_y^z$, and the external perturbation will be an electric field $O_B \rightarrow j_i(r) = j_x(r)$, and $U_B \rightarrow A_i(\mathbf{x}, t)$, where we have chosen the Gauge with the external electric potential being zero, $\phi_{ext} = 0$. We know that $E_i = -\partial_t A_i$, which implies $U_B = 1/\omega E_x$. So the DC spin Hall conductivity reads

$$\sigma^{SHE} = \lim_{\omega \rightarrow 0} \lim_{\mathbf{q} \rightarrow 0} \frac{1}{\omega} R_{\mathbf{q}}^{AB}(\omega). \quad (3.1.28)$$

Since we know that the charge and spin current operators can be expressed as bilinear forms of the field operators

$$\begin{aligned} \mathbf{j}(\mathbf{x}, t) &= -i \frac{e}{2m} [\Phi_{\sigma}^{\dagger}(\mathbf{x}, t) \nabla \Phi_{\sigma}(\mathbf{x}, t) - (\nabla \Phi_{\sigma}^{\dagger}(\mathbf{x}, t)) \Phi_{\sigma}(\mathbf{x}, t)] - \frac{e^2}{m} \mathbf{A} \Phi_{\sigma}^{\dagger}(\mathbf{x}, t) \Phi_{\sigma}(\mathbf{x}, t) \\ \mathbf{j}^a(\mathbf{x}, t) &= -\frac{1}{4e} \{\mathbf{j}, \sigma^a\}, \end{aligned} \quad (3.1.29)$$

by using Wick's theorem, Eq.(3.1.8), we can write

$$\sigma^{SHE} = \lim_{\omega \rightarrow 0} \text{Im} \frac{1}{\omega} \int_{-\infty}^{\infty} \frac{d\epsilon}{2\pi} \text{Tr} [j_x G(\epsilon_+, \mathbf{k}) j_y^z G(\epsilon_-, \mathbf{k}')], \quad (3.1.30)$$

with $\epsilon_{\pm} = \epsilon \pm \omega/2$. Now the spin current operator reads $j_y^z = \sigma_z k_y / 2m$ and the charge current operator $j_x = -e \hat{v}_x$. This formula, Eq.(3.1.30) corresponds to calculate the diagram shown in Fig 3.1(a).

The Edelstein effect is the appearance of a spin polarization produced by the action of a perpendicular external electric field. The quantity we want

to average will obviously be the spin polarization $O_A \rightarrow s^a = s^y$, and the external perturbation is the same described before. The Kubo formula for the EC reads

$$\sigma^{EE} = \lim_{\omega \rightarrow 0} \text{Im} \frac{1}{\omega} \int_{-\infty}^{\infty} \frac{d\epsilon}{2\pi} \text{Tr} [j_x G(\epsilon_+, \mathbf{k}) s^y G(\epsilon_-, \mathbf{k}')], \quad (3.1.31)$$

which is represented by the diagram shown in Fig 3.1(b).

The spin Nernst effect is the spin current produced in a material with SOC when we apply a temperature gradient. As in the case of the SHE the quantity to consider is the spin current, $O_A \rightarrow j_k^a = j_y^z$, but now the external perturbation is the temperature gradient so $O_B \rightarrow j_l^h(r) = j_x^h(r)$, and $U_B \rightarrow \nabla T/T = \nabla_x T/T$.

Now if we want to write the Kubo formula for the spin Nernst conductivity in the same form of Eq.(3.1.30) we have to notice that the Green functions are defined in the zero-temperature limit. But this limit is not valid when we are dealing with heat problems, so we will use the so-called Matsubara Green functions defined before, which allows us to write

$$N^{SH} = \lim_{\Omega \rightarrow 0} \frac{1}{\Omega_\nu} \sum_{\epsilon_n} \text{Tr} [j_y^z \mathcal{G}_n j_x^h \mathcal{G}_{n+\nu}], \quad (3.1.32)$$

which is represented by the diagram shown in Fig 3.1(c).

3.2 Disorder, impurities and the self-consistent Born approximation

It is well known that at low temperatures the resistivity of a metal is dominated by the scattering of the electrons with impurities and defects. Impurities play a very important role in transport problems. In this Section we will study the impurities technique assuming that the impurity concentration is low.

We are not able to know the exact position of each impurity site. Since impurity atoms are distributed randomly we will model the disorder potential as a Gaussian distribution with only local correlations, also known as white noise, with elastic s-wave scattering

$$\overline{U(\mathbf{x})} = 0, \quad \overline{U(\mathbf{x})U(\mathbf{x}')} = \overline{u}^2 \delta(\mathbf{x} - \mathbf{x}') \equiv n_i v_0^2 \delta(\mathbf{x} - \mathbf{x}') = \frac{1}{2\pi N_0 \tau} \delta(\mathbf{x} - \mathbf{x}'), \quad (3.2.33)$$

where \overline{A} means the average of all possible configurations, \overline{u}^2 is the strength of the disorder potential due to the concentration of impurities, n_i the impurity concentration, v_0 the scattering amplitude, N_0 the density of states and τ the scattering time.

If we want to take into account the effect of impurities it is enough to average over all possible configurations of the disorder potential. We will use the important fact that the average distance between impurity atoms is much larger than the lattice spacing, because the impurity concentration is low, which assures us that the averaging can be carried out in volumes with dimensions much greater than the interatomic distances.

Let us see how to treat the Green function in the presence of an interaction term, H_i . The total Hamiltonian is now made of two parts, one H_0 , that we know how to solve, and the interaction one, $H = H_0 + H_i$. With this Hamiltonian Eq.(3.1.4) reads

$$(i\partial_t - H_0)G_{\sigma\sigma'}(\mathbf{x}, t, \mathbf{x}', t') = \delta(t-t')\delta(\mathbf{x}-\mathbf{x}')\delta_{\sigma\sigma'} + H_i G_{\sigma\sigma'}(\mathbf{x}, t, \mathbf{x}', t'). \quad (3.2.34)$$

We define G^0 as the Green function which solves Eq.(3.1.4) in the absence of the interaction term, i.e. $H_i = 0$. So Eq.(3.2.34) becomes

$$(G^0)^{-1}G = 1 + H_i G, \quad (3.2.35)$$

which explicitly is equal to

$$G_{\sigma\sigma'}(\mathbf{x}, t, \mathbf{x}', t') = G_{\sigma\sigma'}^0(\mathbf{x}, t, \mathbf{x}', t') + \int d\mathbf{x}'' dt'' G_{\sigma\sigma''}^0(\mathbf{x}, t, \mathbf{x}'', t'') H_i(\mathbf{x}'') G_{\sigma\sigma'}(\mathbf{x}'', t'', \mathbf{x}', t'). \quad (3.2.36)$$

This integral equation is the starting point for a perturbative expansion of the Green function.

$$\begin{aligned} G^0 &= G^0 \\ G^1 &= G^0 H_i G^0 \\ G^2 &= G^0 H_i G^0 H_i G^0. \end{aligned} \quad (3.2.37)$$

We are interested in calculate the Green function in the presence of impurities so $H_i = U(\mathbf{x})$. We will not know the exact form of $U(\mathbf{x})$ but it will be enough to average over all possible configurations (Fig.3.2(II)). We will use the so-called Born approximation which assumes that the Fermi energy

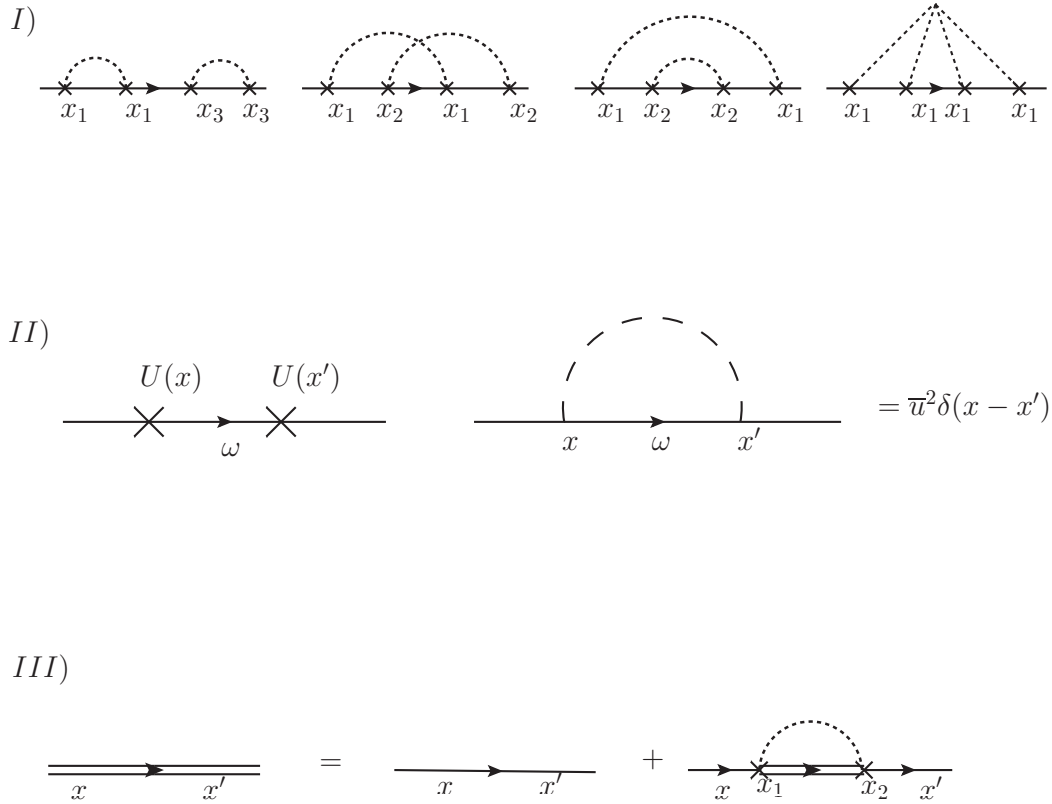


Figure 3.2: I: Fourth order diagrams for the Green function. II: Self-energy, before and after averaging over the impurity distribution. III: Dyson equation for the Green function in the Born approximation.

is large compared to the broadening caused by disorder. Mathematically this condition can be written as

$$\frac{1}{\tau} \ll \epsilon_F. \quad (3.2.38)$$

With this assumption it is easy to prove that the crossing diagrams, as in Fig.3.2(I-2), are negligible. The diagrams with the same form as the ones of Fig.3.2(I-4), which correspond to a scattering with only one site, are also negligible if we compare them with the one site second order ones (Fig.3.2(II)). From now on we should only take into account the I-1 and I-3 types of diagram. This allows us to write the following equation for Green function

$$G = G^0 + G^0 \Sigma(G) G, \quad (3.2.39)$$

defining the self energy as the diagram shown in Fig.3.2(II).

The Eq.(3.2.39) for the self-energy is self-consistent, G is determined by Σ , and Σ is determined by G . Now in our case we can calculate the self-energy in a perturbative way.

$$\Sigma^1(\omega, \mathbf{k}) = \frac{1}{2\pi N_0 \tau} \sum_{\mathbf{k}'} G^0(\omega, \mathbf{k}') = -\frac{i}{2\tau} \text{sgn}(\omega), \quad (3.2.40)$$

where for solving the integral we have make the following substitution $\sum_{\mathbf{k}}(\dots) \rightarrow N_0 \int_{-\infty}^{+\infty} d\xi(\dots)$. This approximation is allowed if the imaginary part of pole is much smaller than the chemical potential μ , as it is in this case (the imaginary part of the Green function is infinitesimal). It is important to notice that the real part of the integral over \mathbf{k}' in Eq.(3.2.40) diverges for large values of \mathbf{k}' . This is a consequence of the simple model taken for the scattering potential. A more realistic model, in which we introduce a cutoff for the scattering processes, cures this problem, and gives rise to a finite contribution to the

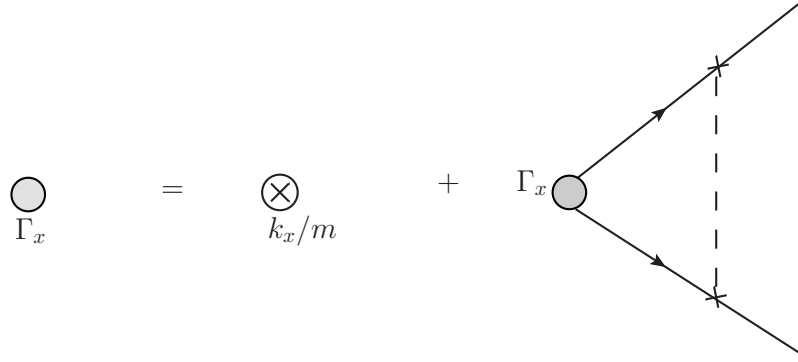


Figure 3.3: Feynman diagram for the vertex corrections.

real part which can be absorbed by a redefinition of the chemical potential. From now on we will ignore the real part of the self-energy understanding that it has been absorbed in a shift of the chemical potential.

Now we introduce Σ^1 in Eq.(3.2.39) and calculate G^1 . Then we reintroduce this value of G^1 in Eq.(3.2.40) to calculate Σ^2 . We have to pay attention to the fact that the differences between the Eq.(3.2.39) integrals when we integrate G^1 or G^0 are only in the absolute value of the imaginary part of both integrands. But as the integral only depends on the sign of the imaginary part and not on its modulus we obtain the same value for Σ^2 as the one we obtained for Σ^1 . So we can conclude that in the Born approximation the total self-energy and the total Green function can be written as follows

$$\begin{aligned} \Sigma &= -\frac{i}{2\tau} \text{sgn}(\omega) \\ G &= \frac{1}{\omega - \xi(\mathbf{k}) + \frac{i}{2\tau} \text{sgn}(\omega)}. \end{aligned} \quad (3.2.41)$$

Impurities affect the Green functions and they affect vertex through the so-called vertex corrections, Fig.3.3. The techniques we have applied to the

diagrams for the Green function can be extended also for those for the evaluations of the vertex. The equation for the corrected vertex Γ_x is

$$\Gamma_x = \frac{k_x}{m} + \sum_{\mathbf{k}'} |u(\mathbf{k} - \mathbf{k}')|^2 G_{\mathbf{k}'}^R \Gamma_x G_{\mathbf{k}'}^A, \quad (3.2.42)$$

where we have introduced the retarded and advanced zero-energy Green functions at the Fermi level

$$G_{\mathbf{k}}^{R,A} = \frac{1}{-E_{\mathbf{k}} + \mu \pm i/2\tau}. \quad (3.2.43)$$

Eq.(3.2.42) like Eq.(3.2.36) can be solved in a perturbative way, $\Gamma_x = k_x/m + \Gamma_x^1 + \Gamma_x^2 + \dots$ with

$$\Gamma_x^1 = \sum_{\mathbf{k}'} |u(\mathbf{k} - \mathbf{k}')|^2 G_{\mathbf{k}'}^R \frac{k'_x}{m} G_{\mathbf{k}'}^A. \quad (3.2.44)$$

But if $|u(\mathbf{k} - \mathbf{k}')|^2$ does not depend on the direction of the momentum (s-wave scattering), the integral over the solid angle makes $\Gamma_x^1 = 0$ and we are able to write $\Gamma_x = k_x/m$. It is important to notice that if $|u(\mathbf{k} - \mathbf{k}')|^2 G_{\mathbf{k}'}^R G_{\mathbf{k}'}^A$ depends on the direction of the momentum the vertex corrections become important.

3.3 The spin Hall and Edelstein conductivities in the 2DEG Rashba model

In this Section we calculate both the Edelstein and the spin-Hall conductivities in a 2DEG with Rashba SOC, in the presence of disorder due to impurities, with the techniques shown in the previous Sections. The Hamiltonian of the model reads

$$H = \frac{k^2}{2m} + U(\mathbf{r}) + \alpha(\sigma_x k_y - \sigma_y k_x). \quad (3.3.45)$$

Firstly we evaluate G^0 in the presence of the Rashba SOC without including disorder. From Eq.(3.1.4) we have

$$G^{-1}(t, \mathbf{k}) = i\partial_t - H = i\partial_t - \frac{k^2}{2m} - \alpha(k_x\sigma_y - k_y\sigma_x). \quad (3.3.46)$$

G has a matrix structure $G = G_0\sigma_0 + \sum_i G_i\sigma_i$. Its matrix elements in the basis of the eigenstates with quantum numbers k and s are

$$G_{\mathbf{k}s}^0(\omega) = \frac{1}{\omega - E_{ks} + \mu + i\text{sgn}(|\mathbf{k}| - k_F)0^+}. \quad (3.3.47)$$

Following Eq.(3.2.40) one should expect that the self-energy has a matrix structure in spin space too. But it can be proved that inside the self-consistent Born approximation only Σ_0 survives due to the symmetry properties $k_x \rightarrow -k_x$ and $k_y \rightarrow -k_y$ of the spin-components of the Green function [97]. These properties allow us to write the Green function matrix element k, s in the presence of disorder as

$$G_{\mathbf{k}s}(\omega) = \frac{1}{\omega - E_{ks} + \mu + \frac{i}{2\tau}\text{sgn}(\omega)}. \quad (3.3.48)$$

Now we calculate the spin Hall conductivity, Eq.(3.1.30). The number current operator, j_x , besides the standard velocity component, includes a spin-orbit induced anomalous contribution $\hat{v}_x = k_x/m + \hat{\Gamma}_x$. Without vertex corrections, the anomalous contribution, in this model, reads

$$\hat{\Gamma}_x = \delta\hat{v}_x = -\alpha\sigma_y. \quad (3.3.49)$$

it is important to notice that the trace of Eq.(3.1.30) implies not only the sum over momentum but also the average over disorder. So taking into account disorder, we project Eq.(3.1.30) over the eigenstates and we explicit its trace

$$\sigma^{SHE} = -\lim_{\omega \rightarrow 0} \text{Im} \frac{e}{\omega} \sum_{\mathbf{k}\mathbf{k}'s's'} \langle \mathbf{k}'s' | \hat{v}_x | \mathbf{k}s \rangle \langle \mathbf{k}s | j_y^z | \mathbf{k}'s' \rangle \int_{-\infty}^{\infty} \frac{d\epsilon}{2\pi} G_s(\epsilon_+, \mathbf{k}) G_{s'}(\epsilon_-, \mathbf{k}'). \quad (3.3.50)$$

After performing the integral over ϵ and the $\omega \rightarrow 0$ limit we obtain

$$\sigma^{SHE} = -\frac{e}{2\pi} \sum_{\mathbf{k}ss'} \langle \mathbf{k}s' | \hat{v}_x | \mathbf{k}s \rangle \langle \mathbf{k}s | j_y^z | \mathbf{k}s' \rangle G_{\mathbf{k}s}^R G_{\mathbf{k}s'}^A, \quad (3.3.51)$$

where we have exploited the fact that plane waves at different momentum \mathbf{k} are orthogonal.

To proceed further we need the expression for the vertices. It is easy to recognize that the standard part of the velocity operator k_x/m does not contribute since it requires $s = s'$, whereas the matrix elements of j_y^z differ from zero only for $s \neq s'$. Explicitly we have

$$\langle \mathbf{k}s' | k_x | \mathbf{k}s \rangle = k_x \delta_{s's} \quad (3.3.52)$$

$$\langle \mathbf{k}s' | \delta \hat{v}_x | \mathbf{k}s \rangle = -\alpha (\cos \theta_{\mathbf{k}} \sigma_{z,s's} + \sin \theta_{\mathbf{k}} \sigma_{y,s's}) \quad (3.3.53)$$

$$\langle \mathbf{k}s | j_y^z | \mathbf{k}s' \rangle = \frac{k}{2m} \sin \theta_{\mathbf{k}} \sigma_{x,ss'}. \quad (3.3.54)$$

Introducing these quantities in Eq.(3.3.51)

$$\sigma^{SHE} = +\frac{e\alpha}{4\pi m} \sum_{\mathbf{k}ss'} k \sin^2 \theta_{\mathbf{k}} \sigma_{y,s's} G_{\mathbf{k}s}^R G_{\mathbf{k}s'}^A, \quad (3.3.55)$$

which is equal to

$$\sigma^{SHE} = +\frac{e\alpha}{8\pi m} \sum_k \text{Im} [k (G_{k+}^R G_{k-}^A - G_{k-}^R G_{k+}^A)]. \quad (3.3.56)$$

To perform the k integral we make the following considerations. Those considerations are based on the idea that the Fermi energy is the biggest energy scale, i.e. $\epsilon_F \gg \alpha k_F$, $\epsilon_F \gg 1/\tau$. Using the residue theorem, (see Appendix B), we obtain

$$\sigma_{bare}^{SHE} = \frac{e}{8\pi} \frac{4\alpha^2 k_F^2 \tau^2}{1 + 4\alpha^2 k_F^2 \tau^2} = \frac{e}{8\pi} \frac{2\tau}{\tau_{DP}}, \quad (3.3.57)$$

where we have introduced the Dyakonov-Perel time τ_{DP} , which is the spin relaxation time due to the Rashba spin-orbit coupling. In the weak disorder limit, i.e. $\tau \rightarrow \infty$, the SHC, Eq.(3.3.57), takes the universal value of $\sigma^{SHE} = e/8\pi$, like the one found by Sinova et al. in 2004. [11]

This result does not take into account vertex corrections. As we pointed out in the previous Section if $|u(\mathbf{k} - \mathbf{k}')|^2 G_{\mathbf{k}'}^R G_{\mathbf{k}'}^A$ does not depend on the momentum they are negligible. But the new k-dependence of the Green functions when Rashba SOC is present changes drastically the situation as we will see below.

The anomalous contribution to the velocity vertex, $\hat{\Gamma}_x$, can be computed following the procedure described in [31] according to the equations

$$\begin{aligned}\hat{\Gamma}_x &= \tilde{\gamma}_x + \frac{1}{2\pi N_0 \tau} \sum_{\mathbf{k}'} G_{\mathbf{k}'}^R \hat{\Gamma}_x G_{\mathbf{k}'}^A, \\ \tilde{\gamma}_x &= \hat{\delta}v_x + \frac{1}{2\pi N_0 \tau} \sum_{\mathbf{k}'} G_{\mathbf{k}'}^R \frac{k'_x}{m} G_{\mathbf{k}'}^A \equiv \tilde{\gamma}^{(1)} + \tilde{\gamma}^{(2)}.\end{aligned}\quad (3.3.58)$$

Then projecting over the states $|\mathbf{k}s\rangle$, the matrix elements of the effective vertex $\tilde{\gamma}^{(2)}$ are:

$$\gamma_{ss'}^{(2)}(k) \equiv \langle \mathbf{k}s | \tilde{\gamma}^{(2)} | \mathbf{k}s' \rangle = \frac{1}{2\pi N_0 \tau} \sum_{\mathbf{k}'s_1} \langle \mathbf{k}s | \mathbf{k}'s_1 \rangle G_{\mathbf{k}'s_1}^R \frac{k'_x}{m} G_{\mathbf{k}'s_1}^A \langle \mathbf{k}'s_1 | \mathbf{k}s' \rangle, \quad (3.3.59)$$

and $\gamma_{ss'}^{(1)}(k) \equiv \langle \mathbf{k}s | \tilde{\gamma}^{(1)} | \mathbf{k}s' \rangle$ is given by Eq.(3.3.54). The matrix elements $\langle \mathbf{k}s | \mathbf{k}'s_1 \rangle$ and $\langle \mathbf{k}'s_1 | \mathbf{k}s' \rangle$ are those of the impurity potential:

$$\langle \mathbf{k}s | \mathbf{k}'s_1 \rangle = \frac{1}{2} [1 + s s_1 e^{i(\theta_{\mathbf{k}'} - \theta_{\mathbf{k}})}] \quad (3.3.60)$$

$$\langle \mathbf{k}'s_1 | \mathbf{k}s' \rangle = \frac{1}{2} [1 + s' s_1 e^{-i(\theta_{\mathbf{k}'} - \theta_{\mathbf{k}})}]. \quad (3.3.61)$$

By observing that $k'_x = k' \cos \theta_{\mathbf{k}'}$, one can perform the integration over the

direction of \mathbf{k}' in the expression of $\gamma_{ss'}^{(2)}(k)$

$$\frac{1}{4} \int_0^{2\pi} \frac{d\theta_{\mathbf{k}'}}{2\pi} [1 + s s_1 e^{i(\theta_{\mathbf{k}'} - \theta_{\mathbf{k}})}] \cos \theta_{\mathbf{k}'} [1 + s' s_1 e^{-i(\theta_{\mathbf{k}'} - \theta_{\mathbf{k}})}] = \frac{s_1}{8} [s e^{-i\theta_{\mathbf{k}}} + s' e^{i\theta_{\mathbf{k}}}], \quad (3.3.62)$$

to get

$$\gamma_{ss'}^{(2)}(k) = \frac{(\cos \theta_{\mathbf{k}} \sigma_{z,ss'} + \sin \theta_{\mathbf{k}} \sigma_{y,ss'})}{16\pi N_0 \tau} \sum_{\mathbf{k}' s_1} s_1 G_{\mathbf{k}' s_1}^R \frac{k'}{m} G_{\mathbf{k}' s_1}^A, \quad (3.3.63)$$

that summing over s_1 , and integrating over k yields

$$\gamma_{ss'}^{(2)}(k) = \alpha (\cos \theta_{\mathbf{k}} \sigma_{z,ss'} + \sin \theta_{\mathbf{k}} \sigma_{y,ss'}), \quad (3.3.64)$$

which cancels exactly $\gamma_{ss'}^{(1)}(k)$. This is the cancellation of the dressed current. As we can see vertex corrections play a very important role in the calculation of the SHC. It is important to notice that this cancellation is a particular characteristic of the Rashba 2DEG model. When we deal with other spin-orbit interactions, like *extrinsic* SOC, this cancellation does not happen anymore, [19, 24, 34–38, 40–42], but vertex corrections remain still important.

There is a very interesting way to understand this vanishing SHC in the Rashba model proposed by Dimitrova [98]. The commutation relation allows us to write

$$-i \frac{ds^y}{dt} = [H, s^y] = i2m\alpha \frac{p_y}{m} s^z = i2m\alpha j_y^z. \quad (3.3.65)$$

This relation implies that in static circumstances

$$\left\langle \frac{ds^y}{dt} \right\rangle = 0 \rightarrow \langle 2m\alpha j_y^z \rangle = 0. \quad (3.3.66)$$

If α is constant, Eq.(3.3.66) implies that $j_y^z = 0$.

Now we calculate the Edelstein conductivity in the 2DEG Rashba model. First of all we will project Eq.(3.1.31) over the eigenstates and calculate its trace

$$\sigma^{EE} = -\lim_{\omega \rightarrow 0} \text{Im} \frac{e}{\omega} \sum_{\mathbf{k}\mathbf{k}'s's'} \langle \mathbf{k}'s' | \hat{v}_x | \mathbf{k}s \rangle \langle \mathbf{k}s | s^y | \mathbf{k}'s' \rangle \int_{-\infty}^{\infty} \frac{d\epsilon}{2\pi} G_s(\epsilon_+, \mathbf{k}) G_{s'}(\epsilon_-, \mathbf{k}'), \quad (3.3.67)$$

with $s^y = \sigma_y/2$. After performing the integral over ϵ and taking the $\omega \rightarrow 0$ limit we obtain

$$\sigma^{EE} = -\frac{e}{4\pi} \sum_{\mathbf{k}ss'} \langle \mathbf{k}s' | \hat{v}_x | \mathbf{k}s \rangle \langle \mathbf{k}s | \sigma^y | \mathbf{k}s' \rangle G_{\mathbf{k}s}^R G_{\mathbf{k}s'}^A. \quad (3.3.68)$$

The matrix elements of the spin vertex are

$$\langle \mathbf{k}s | \sigma_y | \mathbf{k}s' \rangle = \cos \theta_{\mathbf{k}} \sigma_{z,ss'} - \sin \theta_{\mathbf{k}} \sigma_{y,ss'}. \quad (3.3.69)$$

It is important to notice that now $\hat{v}_x = k_x$ so we should substitute Eqs.(3.3.52) and (3.3.69) in Eq.(3.3.67) and calculate the integral that gives us the final result

$$\sigma^{EE} = -eN_0\alpha\tau. \quad (3.3.70)$$

Both the Edelstein and the spin Hall conductivities are deeply connected through the following equation

$$j_y^z = \frac{D}{L_{so}} s^y + \sigma_{drift}^{SHE} E_x, \quad (3.3.71)$$

where $L_{so} = (2m\alpha)^{-1}$ plays the role of an ‘‘orientational spin diffusion length’’, related to the different Fermi momenta in the two spin-orbit split bands. For a detailed justification of Eq.(3.3.71) see Appendix C. The factor in front of the spin density in the first term of Eq.(3.3.71) can also be written in terms

of the Dyakonov-Perel spin relaxation time, i.e. the "orientational spin diffusion time" given by $\tau_{DP} = L_{so}^2/D$. Now we know that in the 2DEG Rashba model $j_y^z = 0$, so we may rewrite Eq.(3.3.71)

$$\sigma^{EE} = -\frac{\tau_{DP}}{L_{so}}\sigma_{drift}^{SHE} = -e\frac{m}{2\pi}\alpha\tau = -eN_0\alpha\tau, \quad (3.3.72)$$

where σ_{drift}^{SHE} is the value of the SHC before vertex corrections, Eq.(3.3.57).

We have seen that this deep relation allows us to calculate the Edelstein conductivity in an elegant way.

3.4 The spin-Hall conductivity and extrinsic SOC

In this Section we will calculate the spin Hall conductivity taking into account the so-called extrinsic spin-orbit coupling in a 2DEG. We will calculate the contribution of this interaction to the SHC, firstly, in the absence of Rashba SOC [99], and then, when both types of interaction are present.

We have seen in Eq.(2.2.19) that the spin-orbit coupling appears as the gradient of the potential. In the case of the Rashba model, this potential was the confinement one $\nabla V(\mathbf{r}) \rightarrow eE_z$, in the extrinsic SOC case the potential is due to the impurities, so $\nabla V(\mathbf{r}) \rightarrow \nabla U(\mathbf{r})$. The total Hamiltonian can be written as

$$H = \frac{k^2}{2m} + U(\mathbf{r}) - \frac{\lambda_e^2}{4}\boldsymbol{\sigma} \times \nabla U(\mathbf{r}) \cdot \mathbf{k}, \quad (3.4.73)$$

where λ_e is the effective spin-orbit wavelength (the renormalized Compton wavelength of Chapter 2). This new SOC term affects the SHC through two different mechanisms, the side jump and the skew scattering.

The side jump mechanism [100] describes the lateral displacement of the wave function during the scattering event. This effect is originated by the

anomalous part of both, the charge and the spin currents. As in the Rashba case the velocity operator has two terms

$$\hat{\mathbf{v}} = i[H, \mathbf{r}] = \frac{\mathbf{k}}{m} - \frac{\lambda_e^2}{4} \nabla U(\mathbf{r}) \times \boldsymbol{\sigma}. \quad (3.4.74)$$

When an electron is scattered by an impurity potential U , the scattering cross section depends on the spin state. This is the skew scattering mechanism, predicted by Mott [29], which does not appear in the first order Born approximation.

Both mechanisms depend on the impurity potential. We will have to average over the different configurations as we did in Section 2, but now we will need to go beyond the Born approximation. The impurity average in momentum space reads

$$\begin{aligned} \overline{U(\mathbf{q}_1)U(\mathbf{q}_2)} &= n_i v_0^2 \delta(\mathbf{q}_1 + \mathbf{q}_2) \\ \overline{U(\mathbf{q}_1)U(\mathbf{q}_2)U(\mathbf{q}_3)} &= n_i v_0^3 \delta(\mathbf{q}_1 + \mathbf{q}_2 + \mathbf{q}_3), \end{aligned} \quad (3.4.75)$$

and the impurity potential in momentum space, which appears in the second and third terms of Eq.(3.4.73), reads

$$U(\mathbf{k} - \mathbf{k}') \left[1 - i \frac{\lambda_e^2}{4} \mathbf{k} \times \mathbf{k}' \cdot \boldsymbol{\sigma} \right] \quad (3.4.76)$$

Firstly we will calculate the self-energy, and then the Green function. The most important contributions to the self-energy are shown in Fig.(3.4). It is easily shown that, as G^0 does not depend on the direction of the momentum, only diagrams I and IV are non-zero. Diagrams II, III, V, VI, VII depend linearly on momentum, so when we integrate over the direction of it, both vanish. Diagram IV, which depends quadratically on momentum, is of order

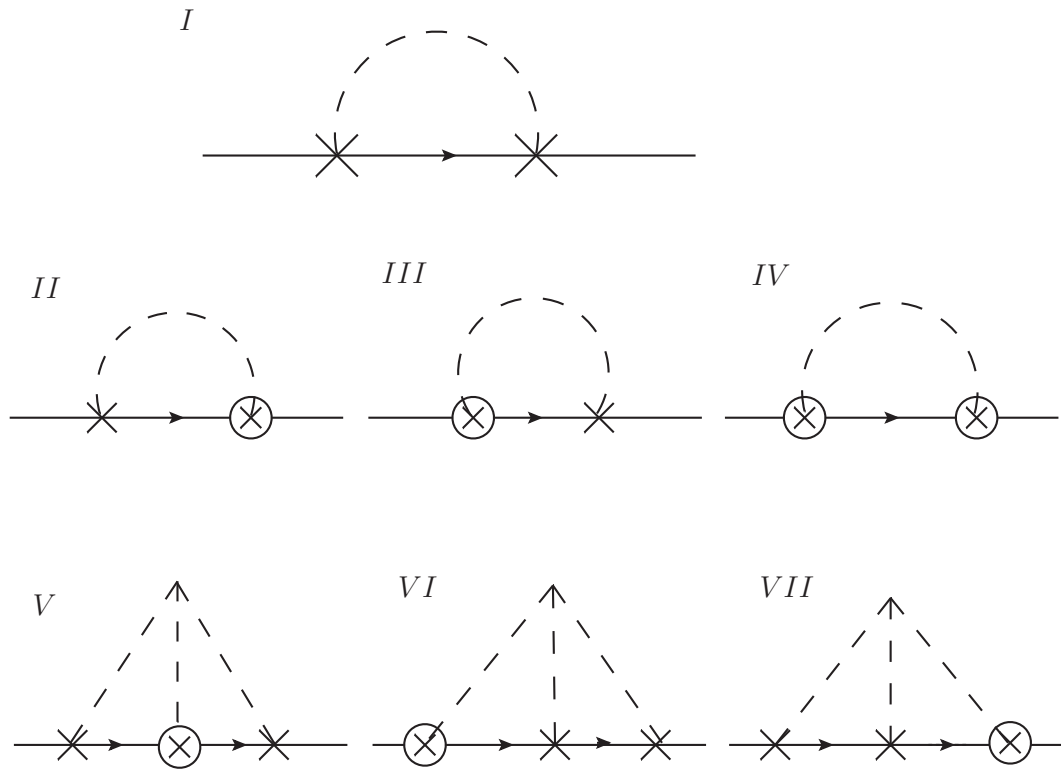


Figure 3.4: Different Feynman diagrams of the self-energy to first order in the spin-orbit interaction. The normal impurity site is denoted by a cross and the spin-orbit one by a cross inside a circle.

λ_e^4 , so we can neglect it. We will see later that when extrinsic and Rashba SOC are present, this diagram becomes important. The self-energy at zero order in the spin-orbit interaction, and the Green function have the same form as the ones of Eq.(3.2.41) which we recall here

$$\begin{aligned}\Sigma &= -\frac{i}{2\tau} \text{sign}(\omega) \\ G &= \frac{1}{\omega - \xi(\mathbf{k}) + \frac{i}{2\tau} \text{sgn}(\omega)}.\end{aligned}\quad (3.4.77)$$

Now we are able to calculate the spin Hall conductivity, which will consist of six terms, Fig.(3.5), diagrams I-IV correspond to the side jump contribution and the V, VI to the skew scattering one.

Before calculating the side jump diagrams we must write explicitly the anomalous spin, and charge currents.

$$\begin{aligned}\delta j_x &= -e \left[\frac{i\lambda_e^2}{4} \varepsilon_{xmn} (k_m - k'_m) \sigma_n U(k_m - k'_m) \right] \\ \delta j_y^z &= \frac{i\lambda_e^2}{8} \varepsilon_{ymz} (k_m - k'_m) U(k_m - k'_m),\end{aligned}\quad (3.4.78)$$

where ε_{ijk} is the Levi-Civita tensor. It can be easily proved that, in the absence of Rashba SOC, vertex corrections are negligible. The side jump contribution, Fig.(3.5(I-IV)), reads

$$\begin{aligned}\sigma_{I+II}^{SHC} &= -i \frac{e\lambda_e^2}{16\pi m} n_i v_0^2 \text{Tr} \left[\sum_{k_1 k_2} k_{1x}^2 [G^A(k_2) - G^R(k_1)] G^R(k_1) G^A(k_1) \right] = \frac{e\lambda_e^2}{8m} N_0 k_F^2 \\ \sigma_{III+IV}^{SHC} &= -i \frac{e\lambda_e^2}{16\pi m} n_i v_0^2 \text{Tr} \left[\sum_{k_1 k_2} k_{1y}^2 [\sigma_z G^A(k_2) - G^R(k_1) \sigma_z] G^R(k_1) \sigma_z G^A(k_1) \right] = \frac{e\lambda_e^2}{8m} N_0 k_F^2 \\ \sigma_{sj}^{SHC} &= \sigma_{I+II}^{SHC} + \sigma_{III+IV}^{SHC} = \frac{e\lambda_e^2}{4m} N_0 k_F^2.\end{aligned}\quad (3.4.79)$$

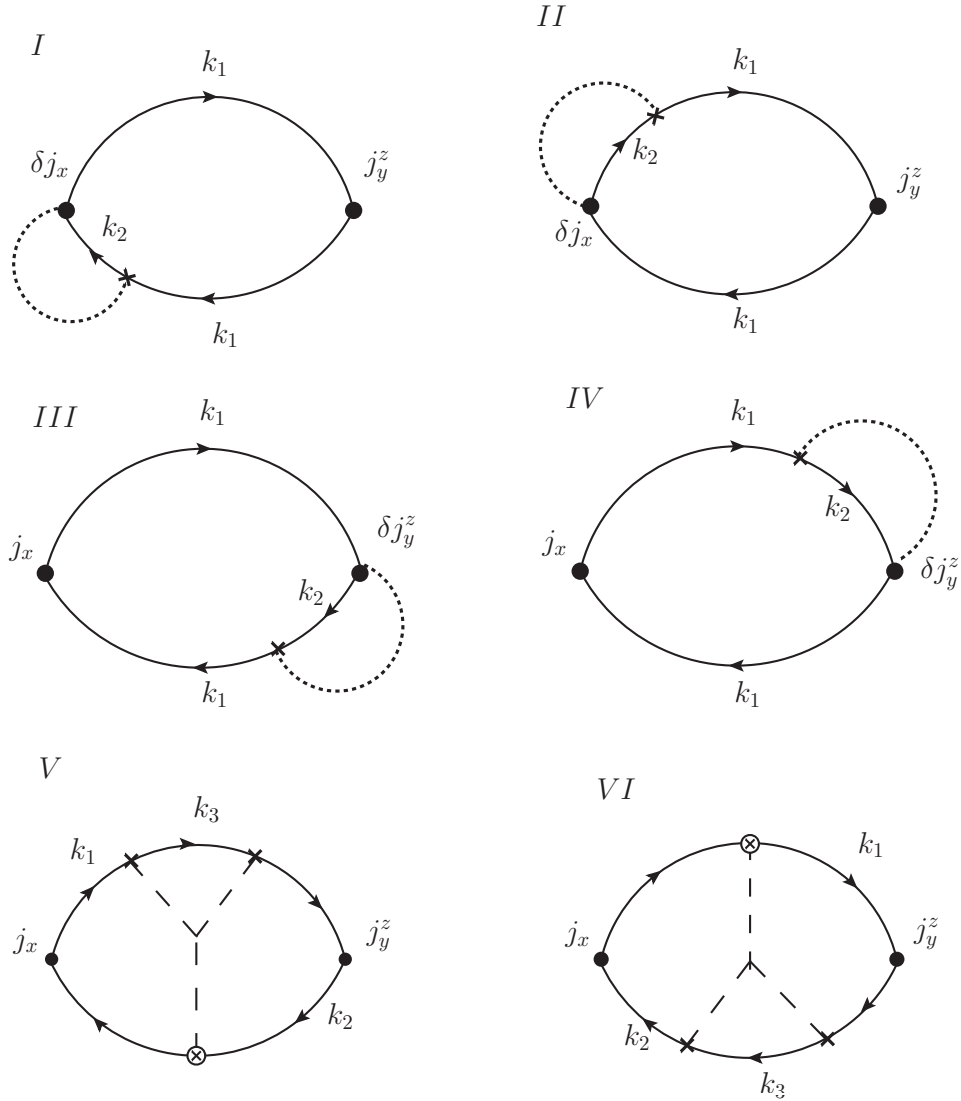


Figure 3.5: Feynman diagrams for the side jump and skew scattering contributions to the SHC to first order in the spin-orbit coupling. The normal impurity site is denoted by a cross and the spin-orbit one by a cross inside a circle.

The skew scattering diagrams, Fig.(3.5)(V, VI), read

$$\begin{aligned}\sigma_{V+VI}^{SHC} &= -i\frac{e\lambda_e^2}{16\pi m^2}n_i v_0^3 \text{Tr} \left[\sum_{k_1 k_2 k_3} k_{1x}^2 [G^A(k_3) - G^R(k_3)] G^R(k_1) G^A(k_1) k_{2y}^2 G^R(k_2) G^A(k_2) \right] \\ \sigma_{ss}^{SHC} &= \frac{e\pi\lambda_e^2}{8m^2} v_0 N_0^2 k_F^4 \tau,\end{aligned}\tag{3.4.80}$$

and the total SHC reads

$$\sigma^{SHC} = \sigma_{sj}^{SHC} + \sigma_{ss}^{SHC} = \frac{e\lambda_e^2}{4m} N_0 k_F^2 \left(1 + \frac{v_0 k_F^2 \tau}{4} \right).\tag{3.4.81}$$

We can see that the ratio between both contributions is $\sigma_{ss}^{SHC}/\sigma_{sj}^{SHC} \sim \epsilon_F \tau$, so the skew scattering mechanism will be dominant. We should remember that the impurities technique shown in Section 2 is only valid if $\epsilon_F \gg 1/\tau$

Now we should calculate the SHC when both Rashba and extrinsic SOC are present. It is important to notice that now G^0 has a matrix structure in spin space, because of Rashba SOC, so G will have it too. The self-energy diagrams are the same of Fig.(3.4) but we will take them into account not in the Green function but only in the two last diagrams of Fig.(3.6). The Green function in spin space, $G = G_0 + \sum_i G_i \sigma_i$, taking into account diagrams I and IV of Fig.(3.4), is

$$\begin{aligned}G_0 &= \frac{1}{2}(G_+ + G_-) \\ G_1 &= \hat{k}_y \frac{1}{2}(G_+ - G_-) \\ G_2 &= -\hat{k}_x \frac{1}{2}(G_+ - G_-),\end{aligned}\tag{3.4.82}$$

with

$$G_{\pm}^{R,A} = \left(\omega - \xi_k \mp \alpha k \pm \frac{i}{2\tau_t} \right)^{-1},\tag{3.4.83}$$

and

$$\frac{1}{\tau_t} = \frac{1}{\tau} + \frac{1}{2\tau_{so}}, \quad \frac{1}{\tau_{so}} \equiv \frac{1}{\tau_{EY}} = \frac{1}{\tau} \left(\frac{\lambda_e k_F}{2} \right)^4. \quad (3.4.84)$$

When Rashba SOC was absent we were able to neglect terms of order λ_e^4 , Fig.(3.4)(IV). This is no longer possible because, as we will see below, when both types of SOC are present these terms become crucial. Ignoring these terms gives rise to an analytic problem as we will see later on [38].

In this case vertex corrections become crucial again, as they were when only Rashba SOC was present. The appearance of vertex corrections gives rise to ten new diagrams shown in Figs.(3.6)(I-IV),(3.7). The charge and spin currents reads

$$j_x \equiv j^{x0} = -e \left(\frac{k_x}{m} + \Gamma^{x0} \right) + \delta j_x \quad (3.4.85)$$

$$j_y^z \equiv j^{yz} = \frac{k_y}{2m} \sigma_z + \Gamma^{yz} + \delta j_y^z, \quad (3.4.86)$$

with $\Gamma^{\alpha\beta} = \Gamma_0^{\alpha\beta} + \sum_i \Gamma_i^{\alpha\beta} \sigma_i$.

The vertex correction equations reads

$$\begin{aligned} \Gamma_\rho^{\alpha\beta} &= \gamma_\rho^{\alpha\beta} + \frac{1}{2} \sum_{\mu\nu} I_{\mu\nu} \text{Tr}(\sigma_\rho \sigma_\mu \sigma_\lambda \sigma_\nu) \Gamma_\lambda^{\alpha\beta} + \frac{1}{2} \sum_{\mu\lambda\nu} J_{\mu\lambda\nu} \text{Tr}(\sigma_\rho \sigma_z \sigma_\mu \sigma_\lambda \sigma_\nu \sigma_z) \Gamma_\lambda^{\alpha\beta} \\ \gamma^{x0} &= -\alpha \sigma_y + \frac{1}{2\pi N_0 \tau} \sum_k \frac{k_x}{m} G_\mu^A G_\nu^R + \frac{1}{2} \frac{1}{2\pi N_0 \tau_{so}} \sum_k \frac{k_x}{m} \sigma_z G_\mu^A G_\nu^R \sigma_z \\ \gamma^{yz} &= \frac{1}{2\pi N_0 \tau} \sum_k \frac{k_y}{2m} G_\mu^A \sigma_z G_\nu^R + \frac{1}{2} \frac{1}{2\pi N_0 \tau_{so}} \sum_k \frac{k_y}{2m} \sigma_z G_\mu^A \sigma_z G_\nu^R \sigma_z, \end{aligned} \quad (3.4.87)$$

where

$$\begin{aligned} I_{\mu\nu} &= \frac{1}{2\pi N_0 \tau} \sum_k G_\mu^A G_\nu^R \\ J_{\mu\nu} &= \frac{1}{2} \frac{1}{2\pi N_0 \tau_{so}} \sum_k G_\mu^A G_\nu^R = \frac{\tau}{2\tau_{so}} I_{\mu\nu}. \end{aligned} \quad (3.4.88)$$

The only component of the corrected current we are interested in is Γ_2 . After some calculations we obtain

$$\begin{aligned} \Gamma_2^x &= -\alpha \frac{1}{\frac{\tau_{so}}{\tau_{DP}} + 1} \\ \Gamma_2^{yz} &= \frac{v_F}{4} \frac{a}{1+a^2} \left(1 - \frac{\tau_t}{\tau_{so}}\right) \frac{1}{\frac{\tau_t}{\tau_{DP}} + \frac{\tau_t}{\tau_{so}}}. \end{aligned} \quad (3.4.89)$$

When we calculate all diagrams Figs.(3.1)(a),(3.5),(3.6),(3.7), we obtain the following value for the SHC

$$\sigma^{SHC} = \frac{1}{\frac{\tau_{so}}{\tau_{DP}} + 1} \left(\frac{e}{8\pi} \frac{2\tau}{\tau_{DP}} + \frac{e\lambda_e^2}{4m} N_0 k_F^2 + \frac{e\pi\lambda_e^2}{8m^2} v_0 N_0^2 k_F^4 \tau \right), \quad (3.4.90)$$

which can be written in a very elegant and condensate way

$$\sigma^{SHC} = \frac{1}{\frac{\tau_{so}}{\tau_{DP}} + 1} \left(\sigma_{int}^{SHC} + \sigma_{sj}^{SHC} + \sigma_{ss}^{SHC} \right), \quad (3.4.91)$$

with σ_{int}^{SHC} the intrinsic SHC before vertex corrections of Eq.(3.3.57).

It is important to notice that if we take the limit $\tau_{so} \rightarrow \infty$, which means not to take into account second order extrinsic terms, $\sigma_{SHC} = 0$ for any $\alpha \neq 0$. But if $\alpha = 0$ we have $\sigma^{SHC} = \sigma_{sj}^{SHC} + \sigma_{ss}^{SHC}$ recovering the result obtained when Rashba SOC was absent Eq.(3.4.81). As we pointed before if we ignore terms of order λ_e^4 from the beginning we find $\sigma^{SHC} = 0$ for any α , including $\alpha = 0$, which is clearly different from the result that we obtain if we take the limit $\alpha \rightarrow 0$ in Eq.(3.4.91).

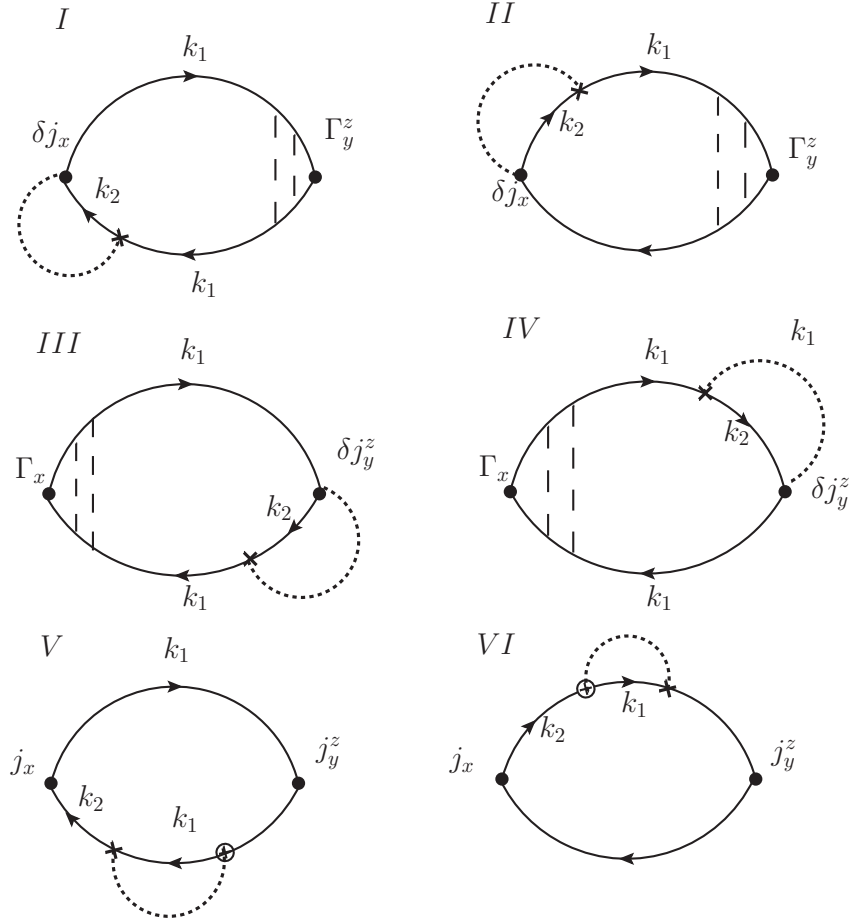


Figure 3.6: The new Feynman diagrams for the side jump contributions in the presence of Rashba SOC. The vertices j_x, j_y^z have two parts $j_x = k_x/m + \Gamma_x$, $j_y^z = k_y\sigma_z/2m + \Gamma_y^z$.

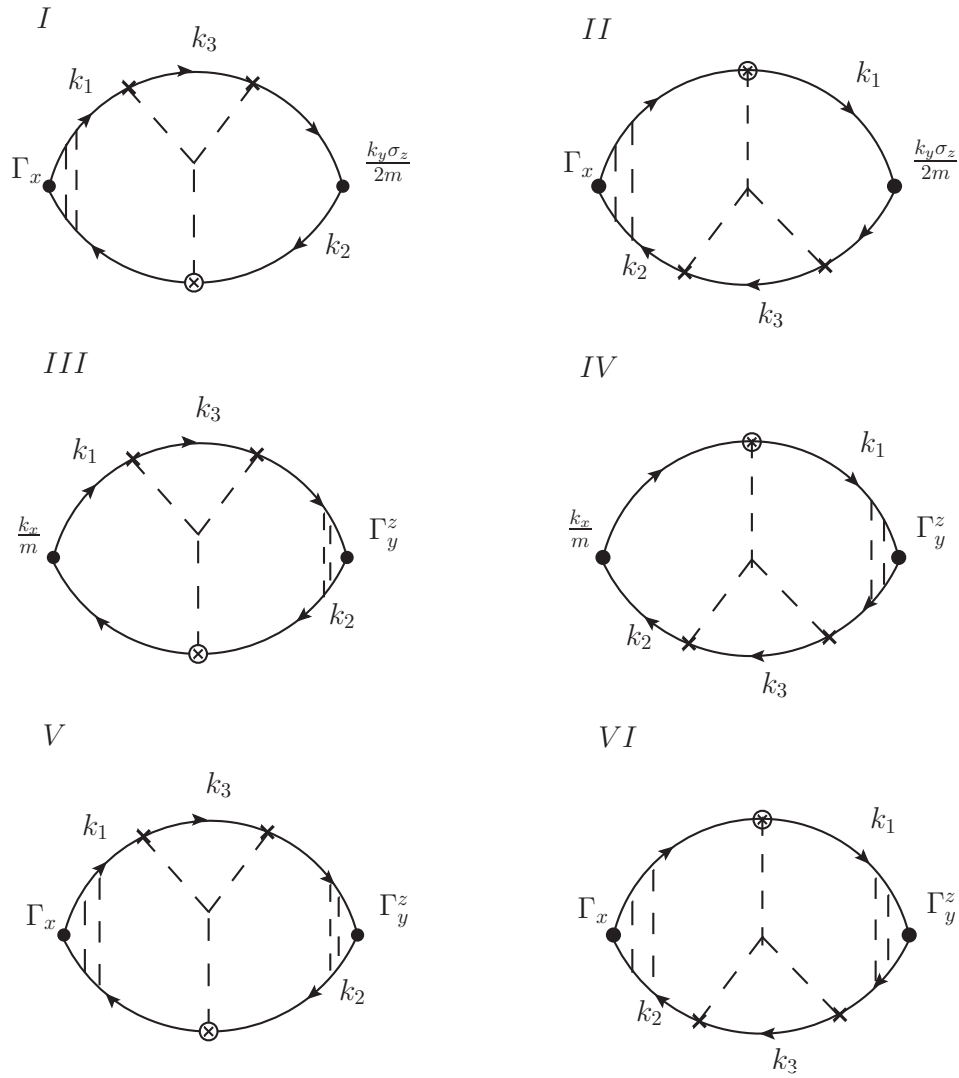


Figure 3.7: The new Feynman diagrams for the skew scattering contributions in the presence of Rashba SOC.

We have pointed in Section 3 how the continuity equation shows us that the SHC vanishes in the 2DEG Rashba case, Eq.(3.3.65). When extrinsic SOC is present the continuity equation reads [43]

$$\partial_t s^y + \frac{1}{\tau_{so}} s^y = -2m\alpha j_y^z. \quad (3.4.92)$$

Which implies that if $\tau_{so} \neq 0$, the SHC should not vanish anymore.

Chapter 4

Spin Hall and Edelstein effects in metallic films: From two to three dimensions

The research of materials which present a large spin Hall conductivity has been one of the most important topics inside the field of spintronics. In this Chapter we describe a model which consists on a thin metallic film sandwiched by two different insulators. The inversion symmetry breaking across the interfaces produces giant spin-orbit coupling. We will calculate the spin Hall and Edelstein conductivities due to these interactions and show that they provide high values for the SHC. We will also discuss the relation which exists between these two effects. At the end of the Chapter, we will describe some interesting physical limits and the regime of applications of the theoretical model here proposed. We will work in natural units $\hbar = c = 1$.

These results have been published in Phys. Rev. B 89, 245443, 2014

[101].

4.1 The model

As we saw in Chapters 2 and 3, the Rashba 2DEG model is one of the most studied systems inside the field of spintronics. One of the best-known results concerning this system is the vanishing of the spin Hall conductivity [31–33]. By recalling the Dimitrova’s results [98] we have

$$\left\langle \frac{ds^y}{dt} \right\rangle = 0 \rightarrow \langle 2m\alpha j_y^z \rangle = 0. \quad (4.1.1)$$

If α is constant, i.e. spatially uniform, Eq.(4.1.1) implies that $j_y^z = 0$. But if α is not uniform anymore, i.e. $\alpha = \alpha(z)$, Eq.(4.1.1) only implies that $\langle 2m\alpha j_y^z \rangle = 0$, but not $j_y^z = 0$. Moreover, it has been recently pointed out that the vanishing of the SHC need not occur in systems which present Rashba-like SOC but are not strictly two-dimensional, as explicitly shown in a model schematically describing the interface of the two insulating oxides LaAlO₃ and SrTiO₃ (LAO/STO) [39]. Even more recently [60], it has been suggested that a large SHC could be realized in a thin metal (Cu) film that is sandwiched between two different insulators, such as oxides or even the vacuum. A very large spin Hall angle of extrinsic origin has been observed [102] in thin films of Cu doped with bismuth impurities. In [60], however, the Bi impurities are absent. Such a system is shown schematically in Fig.4.2.

We will describe this insulator-metal-insulator model. Then we will calculate both the Edelstein and spin Hall conductivities showing the deep connection that exists between them.

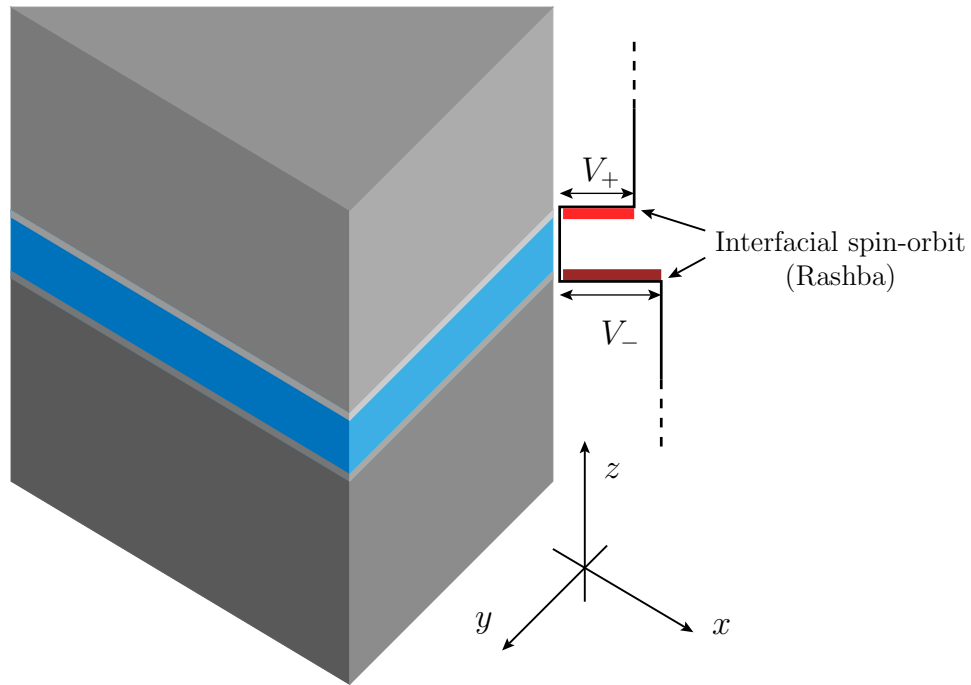


Figure 4.1: Schematic representation of a thin metal film sandwiched between insulators with asymmetric interfacial spin-orbit couplings. V_+ and V_- are the heights of the two interfacial potential barriers. These potentials generate interfacial spin-orbit interactions of the Rashba type, whose strength is controlled by the effective Compton wavelengths λ_+ and λ_- respectively.

Firstly we will calculate the eigenvalues and eigenfunctions of this junction. To this end, following Ref. [60], we model this metallic film via the following Hamiltonian

$$H = \frac{k^2}{2m} + \frac{k_z^2}{2m} + V_C(z) + H_R + U(\mathbf{r}), \quad (4.1.2)$$

where the first term represents the kinetic energy associated to the unconstrained motion in the xy plane and $\mathbf{k} = (k_x, k_y)$ is the two-dimensional momentum operator. The second term is the kinetic energy of the motion in the perpendicular direction, with k_z the momentum operator in the z direction (we ignore the possibility of different effective masses in plane and out of plane). The finite thickness d of the metallic film is taken into account by a confining potential

$$V_C = V_+\theta(z - z_+) + V_-\theta(z_- - z), \quad (4.1.3)$$

where V_\pm is the height of the potential barrier at $z_\pm = \pm d/2$ and $\theta(z)$ is the Heaviside function. The third term in Eq.(4.1.2) describes the Rashba interfacial spin-orbit interaction in the xy plane located at $z_\pm = \pm d/2$. We saw in Chapter 2 that the spin-orbit coupling terms arise as the gradient of the confining potential in the Kane model. The confining potential, Eq.(4.1.3), consists on two Heaviside functions so the spin-orbit interaction term consists in two Dirac delta functions

$$H_R = [\lambda_-^2 V_- \delta(z - z_-) - \lambda_+^2 V_+ \delta(z - z_+)] (k_y \sigma_x - k_x \sigma_y), \quad (4.1.4)$$

where λ_\pm are the effective Compton wavelengths for the two interfaces, $\sigma_x, \sigma_y, \sigma_z$ are the Pauli matrices. The last term in Eq.(4.1.2) represents the scattering from impurities affecting the motion in the $x - y$ plane and

$\mathbf{r} = (x, y)$ is the coordinate operator. The impurity potential is taken in a standard way as a white-noise disorder with variance $\langle U(\mathbf{r})U(\mathbf{r}') \rangle = (2\pi N_0\tau)^{-1}\delta(\mathbf{r} - \mathbf{r}')$, as the one we defined in Chapter 3. As we did before we will assume that the Fermi energy $E_{nk_{Fn}}$ in each subband is much larger than the level broadening $1/\tau$ and we will use the self-consistent Born approximation.

It is important to remember that in this thesis we are describing intrinsic spin-orbit induced effects. This means that the impurities (while, of course, needed to give the system a finite electrical conductivity) do not couple to the electron spin.

The eigenfunctions of the Hamiltonian (4.1.2) have the form

$$\psi_{n\mathbf{k}s}(\mathbf{r}, z) = \frac{e^{i\mathbf{k}\cdot\mathbf{r}}}{\sqrt{\mathcal{A}}} \frac{1}{\sqrt{2}} \begin{pmatrix} 1 \\ i s e^{i\theta_{\mathbf{k}}} \end{pmatrix} f_{n\mathbf{k}s}(z), \quad (4.1.5)$$

where \mathcal{A} is the area of the interface, $\mathbf{k} = (k_x, k_y)$ is the in-plane wave vector, \mathbf{r} is the position in the interfacial plane and z is the coordinate perpendicular to the plane. $\theta_{\mathbf{k}}$ is the angle between \mathbf{k} and the x axis. These states are classified by a *subband index* $n = 1, 2, \dots$, which plays the role of a principal quantum number, an in-plane wave vector \mathbf{k} , and an *helicity index*, $s = +1$ or -1 which determines the form of the spin-dependent part of the wave function.

By inserting the wave function (4.1.5) into the Schrödinger equation for the Hamiltonian (4.1.2) we find the following equation for the functions $f_{n\mathbf{k}s}(z)$ describing the motion along the z -axis

$$-\frac{1}{2m} f_{n\mathbf{k}s}''(z) + \{V_C(z) - ks [\lambda_-^2 V_- \delta(z + d/2) - \lambda_+^2 V_+ \delta(z - d/2)]\} f_{n\mathbf{k}s}(z) = \epsilon_{n\mathbf{k}s} f_{n\mathbf{k}s}(z), \quad (4.1.6)$$

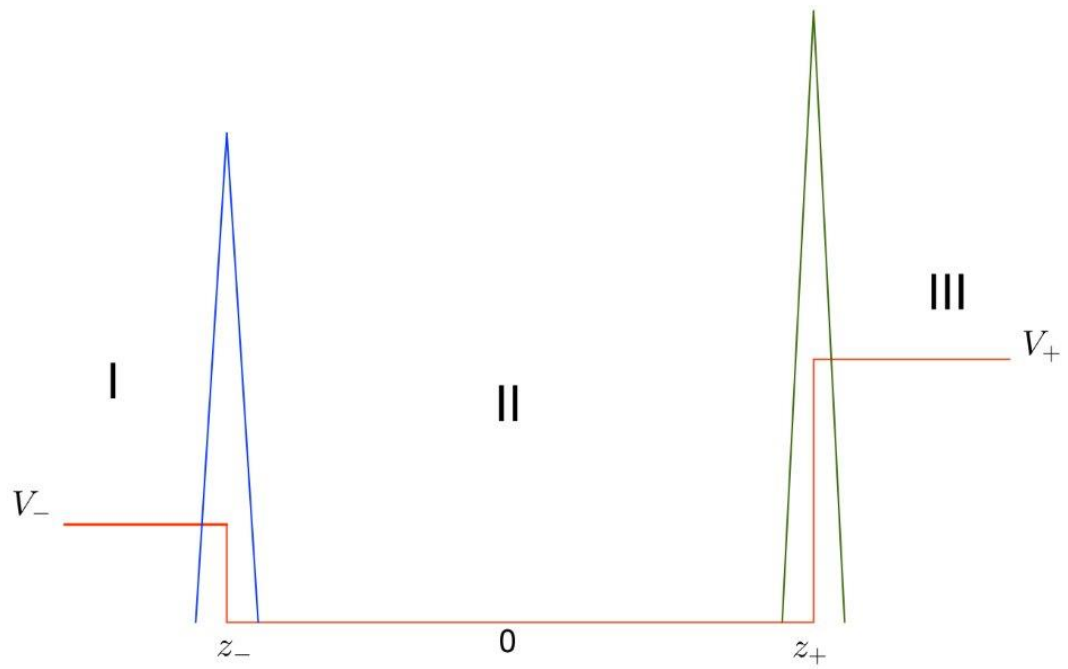


Figure 4.2: The confining potential V_c and the spin-orbit interaction along the confinement direction (i.e., z axis).

where the full energy eigenvalues are

$$E_{n\mathbf{k}s} = \frac{k^2}{2m} + \epsilon_{n\mathbf{k}s}. \quad (4.1.7)$$

We then solve (4.1.7) and find the following solution for $f_{n\mathbf{k}s}(z)$

$$f_{n\mathbf{k}s}(z) = \begin{cases} B_I e^{\xi_I x} & \text{if } z < z_- \\ B_{II} e^{i\xi_{II} x} + B'_{II} e^{-i\xi_{II} x} & \text{if } z_- < z < z_+ \\ B_{III} e^{-\xi_{III} x} & \text{if } z > z_+ \end{cases}, \quad (4.1.8)$$

where $\xi_I = \sqrt{2m(V_- - \epsilon_{n\mathbf{k}s})}$, $\xi_{II} = \sqrt{2m\epsilon_{n\mathbf{k}s}}$ and $\xi_{III} = \sqrt{2m(V_+ - \epsilon_{n\mathbf{k}s})}$ and B_I, B_{II}, B'_{II} and B_{III} normalization constants which eventually could depend on n, \mathbf{k}, s . By taking into account the continuity of the wave function $f_{n\mathbf{k}s}(z)$ at $z = \pm d/2$ and the discontinuities of its derivatives, produced by the Dirac delta functions, we obtain for the eigenvalue $\epsilon_{n\mathbf{k}s}$ the following transcendental equation

$$\arctan \left(\frac{\sqrt{\epsilon}}{\sqrt{\left(\frac{d_-^2}{d_-^2} - \epsilon\right) - \frac{d_-}{d_-} \alpha_- s k}} \right) + \arctan \left(\frac{\sqrt{\epsilon}}{\sqrt{\left(\frac{d_+^2}{d_+^2} - \epsilon\right) + \frac{d_+}{d_+} \alpha_+ s k}} \right) + \sqrt{\epsilon} = n\pi, \quad (4.1.9)$$

where the energy ϵ is measured in units of $E_0 = \pi^2/(2md^2)$ set by the thickness of the film. In the absence of spin-orbit coupling ($\lambda_{\pm} = 0$) and for infinite heights of the potential ($V_{\pm} \rightarrow \infty$), the solution reduces to the well-known energy levels $\epsilon_{n\mathbf{k}s} = E_0 n^2$.

In the general case with both λ_{\pm} and V_{\pm} finite we use perturbation theory by assuming d large. There are two natural length scales associated with the confining potential $d_{\pm} = 1/\sqrt{2mV_{\pm}}$ so that we expand in the small parameters d_{\pm}/d . Since all the energy scales are set by E_0 , we find useful to describe

the spin-orbit coupling in terms of the parameters $\alpha_{\pm} = \lambda_{\pm}^2/d_{\pm}$, which have the dimensions of a length. The product $E_0\alpha_{\pm}$ has the dimensions of a velocity and plays the role of the Rashba coupling parameter. In the following we make an expansion to first order in d_{\pm}/d and up to third order in $\alpha_{\pm}k$. For the eigenvalues of Eq.(4.1.6) we find

$$\epsilon_{n\mathbf{k}s} = E_0 n^2 \left[1 - 2 \frac{d_- + d_+}{d} + s e_1 k + e_2 k^2 + s e_3 k^3 \right] \quad (4.1.10)$$

and the eigenfunctions

$$f_{n\mathbf{k}s}(z) = c_{n\mathbf{k}s} \sin \left[\frac{n\pi}{d + \frac{d_-}{1-\alpha_-ks} + \frac{d_+}{1+\alpha_+ks}} \left(\frac{d}{2} + z + \frac{d_-}{1-\alpha_-ks} \right) \right], \quad (4.1.11)$$

with $n = 1, 2, \dots$, where

$$\begin{aligned} c_{n\mathbf{k}s} &= \sqrt{\frac{4}{d_e [2 - (s e_1 k + e_2 k^2 + s e_3 k^3)]}}, \quad d_e = d + d_+ + d_-; \\ e_1 &= 2 \left(\frac{d_+}{d} \alpha_+ - \frac{d_-}{d} \alpha_- \right), \quad e_2 = -2 \left(\frac{d_+}{d} \alpha_+^2 + \frac{d_-}{d} \alpha_-^2 \right), \quad e_3 = 2 \left(\frac{d_+}{d} \alpha_+^3 - \frac{d_-}{d} \alpha_-^3 \right). \end{aligned} \quad (4.1.12)$$

Notice that the sign of the coefficients e_1 and e_3 depends on the relative strength of the spin-orbit coupling λ_{\pm} and barrier heights V_{\pm} . To avoid trouble with negative signs in the following calculations, we assume that the couplings are labeled in such a way that $\lambda_+ > \lambda_-$, and $V_+ > V_-$ so that $e_1, e_3 > 0$. We will also assume that $n = n_c$ is the topmost occupied subband.

We define the spin splitting energy as

$$\begin{aligned} \Delta E_{nk_{Fn}} &= (2E_0 n^2/d) [k_{Fn}(\lambda_+^2 - \lambda_-^2) + \frac{2mk_{Fn}^3}{\hbar^2} (\lambda_+^6 V_+ - \lambda_-^6 V_-)] \\ &\equiv \Delta E_{nk_{Fn}}^{(1)} + \Delta E_{nk_{Fn}}^{(3)} \end{aligned} \quad (4.1.13)$$

In the next Section we will calculate the spin Hall and the Edelstein conductivities including vertex corrections.

4.2 The transport coefficients

In this Section we will calculate two important and deeply connected coefficients, the spin Hall and the Edelstein conductivities. We will use all the techniques explained in Chapter 3. It is important to keep in mind that these formulas will be derived under the following assumptions:

1. The spin-orbit interaction produces only a small correction to the energy levels: in particular, the spin splittings, ΔE_{nk} , in the various subbands are small in comparison with the energy separation between the subbands, which we denote by ΔE_{IB} .

By considering the first term in Eq.(4.1.13) and assuming the inter-band spacing scaling as E_0 , this assumption requires the effective Compton wavelength to be smaller than the geometrical average between the film thickness and the Fermi wavelength, $\lambda_{\pm} < \sqrt{d\lambda_{F_n}}$ with $\lambda_{F_n} = 2\pi/k_{F_n}$. The second term in Eq.(4.1.13) is also assumed small with respect to the first as required for the validity of the expansion, implying the condition $2mk_{F_n}^2 V_{\pm}\lambda_{\pm}^4/\hbar^2 < 1$. Hence, in summary, one requires the conditions

$$\frac{\lambda_{\pm}^2}{d\lambda_{F_n}} < 1, \quad \frac{V}{E_0} < \frac{d^2\lambda_{F_n}^2}{\lambda_{\pm}^4}. \quad (4.2.14)$$

As a rough estimate with $d \sim 10^{-9}$ m, $\lambda_{\pm} \sim 10^{-10}$ m, $\lambda_{F_n} \sim 10^{-9}$ m, we have $\lambda_{\pm}^2/(d\lambda_{F_n}) \sim 10^{-2}$, which makes the assumption (4.2.14) reasonable.

2. In addition, the spacing between subbands must be large compared to the broadening caused by disorder, meaning that inter-band transitions

caused by impurity scattering are rare. Mathematically, this condition is expressed by the inequality

$$\frac{1}{\tau} < \Delta E_{IB}, \quad (4.2.15)$$

where τ is the typical electron-impurity scattering time. This condition implies, in particular, that the metallic film cannot be too large, otherwise the intersubband spacing, scaling as $E_0 \sim 1/d^2$, would become smaller than $1/\tau$. A corollary to this is that the number of occupied subbands must remain small – for example one has $n_c = 4$ in a typical 1-nm wide Al film [103]. Roughly one expects $\Delta E_{IB}\tau \sim 10$.

We have made explicit \hbar to give clarity to the assumptions, from now on we will turn to natural units $\hbar = 1$. This assumption and the fact that we are truncating our expansion up to first order in d_{\pm}/d , implies, as we will see later on, that we will only take into account the intra-band contributions (inside the same band), and we will neglect the inter-band ones among this Section.

The SHC is the non-equilibrium spin response to an applied electric field. As we defined in Eq.(3.1.30) the Kubo formula corresponds to the diagram (c) of Fig.4.3, and it reads

$$\sigma^{SHE} = \lim_{\omega \rightarrow 0} \frac{\text{Im} \langle \langle j_y^z, j_x \rangle \rangle}{\omega}, \quad (4.2.16)$$

where the spin current operator reads $j_y^z = \sigma_z k_y / 2m$ and the charge current operator $j_x = -e\hat{v}_x$. The number current operator, as it happens in the 2DEG Rashba case, besides the standard velocity component, includes a

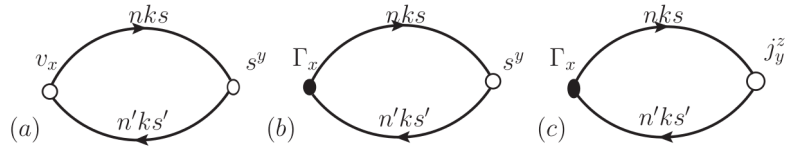


Figure 4.3: Feynman bubble diagram for the EC(a+b) or SHC(c). The empty right dot indicates the spin density (EC) or the spin current density (SHC) bare vertex, the left empty one indicates the normal velocity operator, and the full dot is the dressed charge current density vertex.

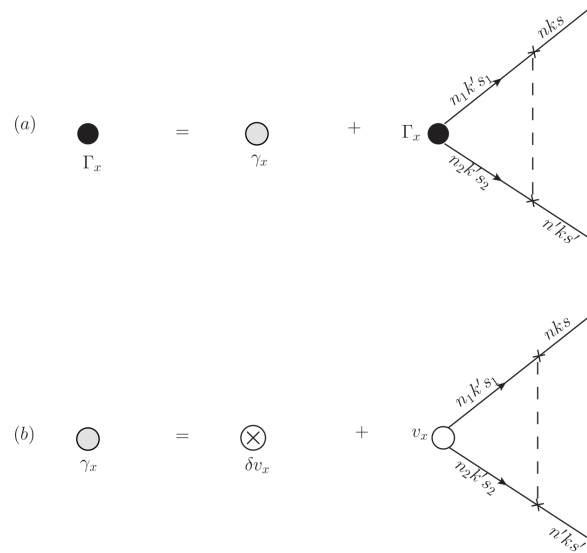


Figure 4.4: Ladder resummation for the spin-dependent part of the dressed charge current density vertex. The dashed line represents the correlation between propagators scattering off the same impurity site.

spin-orbit induced anomalous contribution $\hat{v}_x = k_x/m + \hat{\Gamma}_x$. Without vertex corrections, the anomalous contribution reads

$$\hat{\Gamma}_x = \delta\hat{v}_x = [\lambda_+^2 V_+ \delta(z - z_+) - \lambda_-^2 V_- \delta(z - z_-)] \sigma_y. \quad (4.2.17)$$

This expression can be written in terms of the exact Green functions and vertices as

$$\sigma^{SHE} = - \lim_{\omega \rightarrow 0} \text{Im} \frac{e}{\omega} \sum_{nn'\mathbf{k}\mathbf{k}'ss'} \langle n'\mathbf{k}'s' | \hat{v}_x | n\mathbf{k}s \rangle \langle n\mathbf{k}s | j_y^z | n'\mathbf{k}'s' \rangle \int_{-\infty}^{\infty} \frac{d\epsilon}{2\pi} G_{ns}(\epsilon_+, \mathbf{k}) G_{n's'}(\epsilon_-, \mathbf{k}'). \quad (4.2.18)$$

where $e > 0$ is the unit charge, $\epsilon_{\pm} = \epsilon \pm \omega/2$ and $G_{ns}(\epsilon, \mathbf{k}) = (\epsilon - E_{n\mathbf{k}s} + i \text{sgn}\epsilon/2\tau)^{-1}$ is the Green function averaged over disorder in the self-consistent Born approximation with self energy

$$\Sigma_{ns}(\mathbf{r}, \mathbf{r}'; \epsilon) = \frac{\delta(\mathbf{r} - \mathbf{r}')}{2\pi N_0 \tau} G_{ns}(\mathbf{r}, \mathbf{r}; \epsilon). \quad (4.2.19)$$

After performing the integral over the frequency we obtain

$$\sigma^{SHE} = - \frac{e}{2\pi} \sum_{nn'\mathbf{k}\mathbf{k}'ss'} \langle n'\mathbf{k}'s' | \hat{v}_x | n\mathbf{k}s \rangle \langle n\mathbf{k}s | j_y^z | n'\mathbf{k}'s' \rangle G_{n\mathbf{k}s}^R G_{n'\mathbf{k}'s'}^A, \quad (4.2.20)$$

where we have introduced the retarded and advanced zero-energy Green functions at the Fermi level

$$G_{n\mathbf{k}s}^{R,A} = \frac{1}{-E_{n\mathbf{k}s} + \mu \pm i/2\tau} \quad (4.2.21)$$

and exploited the fact that plane waves at different momentum \mathbf{k} are orthogonal.

To proceed further we need the expression for the vertices. It is easy to recognize that the standard part of the velocity operator k_x/m does not

contribute since it requires $s = s'$, whereas the matrix elements of j_y^z differ from zero only for $s \neq s'$. Explicitly we have

$$\langle n'\mathbf{k}s' | k_x | n\mathbf{k}s \rangle = k_x \langle f_{n'\mathbf{k}s'} | f_{n\mathbf{k}s} \rangle \delta_{s's} = \langle f_{n'\mathbf{k}s'} | f_{n\mathbf{k}s} \rangle k \cos \theta_{\mathbf{k}} \delta_{s's} \quad (4.2.22)$$

$$\begin{aligned} \langle n'\mathbf{k}s' | \delta \hat{v}_x | n\mathbf{k}s \rangle &= (\cos \theta_{\mathbf{k}} \sigma_{z,s's} + \sin \theta_{\mathbf{k}} \sigma_{y,s's}) \frac{\Delta E_{nk}}{k} \langle f_{n'\mathbf{k}s'} | f_{n\mathbf{k}s} \rangle \\ &\quad + 2 \cos \theta_{\mathbf{k}} \sigma_{z,s's} \frac{\Delta E_{nk}^{(3)}}{k} \langle f_{n'\mathbf{k}s'} | f_{n\mathbf{k}s} \rangle \end{aligned} \quad (4.2.23)$$

$$\langle n'\mathbf{k}s | j_y^z | n'\mathbf{k}s' \rangle = \langle f_{n\mathbf{k}s} | f_{n'\mathbf{k}s'} \rangle \frac{k}{2m} \sin \theta_{\mathbf{k}} \sigma_{x,ss'} , \quad (4.2.24)$$

where $\Delta E_{nk} = (E_{nk+} - E_{nk-})/2 = E_0 n^2 (e_1 k + e_3 k^3)$ is half the spin-splitting energy in the n -th band. Equation (4.2.23) is straightforwardly obtained from the eigenvalue equation (4.1.6) for the functions $f_{n\mathbf{k}s}(z)$ when $s \neq s'$. When $s = s'$ we have to calculate the matrix element explicitly.

Let us now discuss the overlaps between the wave functions $\langle f_{n\mathbf{k}s} | f_{n'\mathbf{k}s'} \rangle$. If $n = n'$ we have

$$\langle f_{n\mathbf{k}s} | f_{n'\mathbf{k}s'} \rangle = \frac{d_e}{2} c_{n\mathbf{k}s} c_{n'\mathbf{k}s'} \left[1 - \frac{e_1 (ks + k's') + e_2 (k^2 + k'^2) + e_3 (k^3 s + k'^3 s')}{4} \right], \quad (4.2.25)$$

which is unity plus corrections of order (d_{\pm}/d) when $s, k \neq s', k'$. If $n \neq n'$ $\langle f_{n\mathbf{k}s} | f_{n'\mathbf{k}s'} \rangle$ is at least of order (d_{\pm}/d) . Before continuing our calculation we observe that it is important to distinguish between the intra-band ($n = n'$) and the inter-band ($n \neq n'$) contributions. The inter-band contributions are of second order in d_{\pm}/d , because they are proportional to $\langle f_{n\mathbf{k}s} | f_{n'\mathbf{k}s'} \rangle^2$. Since we limit our expansion to the first order in d_{\pm}/d we will from now on neglect these contributions. Notice, however, that this approximation is no longer valid when the intra-band splitting controlled by e_1 and e_3 vanishes. In this case one cannot avoid taking into account the inter-band contributions. In

the same spirit, we also approximate the intra-band overlap $\langle f_{n\mathbf{k}s} | f_{n\mathbf{k}'s'} \rangle \simeq 1$, because all of our results are at least linear in (d_{\pm}/d) and we neglect higher order terms.

The anomalous contribution to the velocity vertex, $\hat{\Gamma}_x$, can be computed following the procedure described in Ref. [31] according to the equations (see Fig.4.4)

$$\begin{aligned}\hat{\Gamma}_x &= \tilde{\gamma}_x + \frac{1}{2\pi N_0\tau} \sum_{\mathbf{k}'} G_{\mathbf{k}'}^R \hat{\Gamma}_x G_{\mathbf{k}'}^A, \\ \tilde{\gamma}_x &= \hat{\delta}v_x + \frac{1}{2\pi N_0\tau} \sum_{\mathbf{k}'} G_{\mathbf{k}'}^R \frac{k'_x}{m} G_{\mathbf{k}'}^A \equiv \tilde{\gamma}^{(1)} + \tilde{\gamma}^{(2)}\end{aligned}\quad (4.2.26)$$

To extend the treatment to the present case, the projection must be made over the states $|n\mathbf{k}s\rangle$. Assuming that the impurity potential does not depend on z , the matrix elements of the effective vertex $\tilde{\gamma}^{(2)}$ are:

$$\gamma_{ss'}^{(2)nn}(k) \equiv \langle n\mathbf{k}s | \tilde{\gamma}^{(2)} | n\mathbf{k}s' \rangle = \frac{1}{2\pi N_0\tau} \sum_{n_1\mathbf{k}'s_1} \langle n\mathbf{k}s | n_1\mathbf{k}'s_1 \rangle G_{n_1\mathbf{k}'s_1}^R \frac{k'_x}{m} G_{n_1\mathbf{k}'s_1}^A \langle n_1\mathbf{k}'s_1 | n\mathbf{k}s' \rangle, \quad (4.2.27)$$

and $\gamma_{ss'}^{(1)nn}(k) \equiv \langle n\mathbf{k}s | \tilde{\gamma}^{(1)} | n\mathbf{k}s' \rangle$ is given by Eq.(4.2.23). The matrix elements $\langle n\mathbf{k}s | n_1\mathbf{k}'s_1 \rangle$ and $\langle n_1\mathbf{k}'s_1 | n\mathbf{k}s' \rangle$ are those of the impurity potential:

$$\langle n\mathbf{k}s | n_1\mathbf{k}'s_1 \rangle = \frac{1}{2} \langle f_{n\mathbf{k}s} | f_{n_1\mathbf{k}'s_1} \rangle [1 + s s_1 e^{i(\theta_{\mathbf{k}'} - \theta_{\mathbf{k}})}] \quad (4.2.28)$$

$$\langle n_1\mathbf{k}'s_1 | n\mathbf{k}s' \rangle = \frac{1}{2} \langle f_{n_1\mathbf{k}'s_1} | f_{n\mathbf{k}s'} \rangle [1 + s' s_1 e^{-i(\theta_{\mathbf{k}'} - \theta_{\mathbf{k}})}]. \quad (4.2.29)$$

By observing that $k'_x = k' \cos \theta_{\mathbf{k}'}$, one can perform the integration over the direction of \mathbf{k}' in the expression of $\gamma_{ss'}^{(2)nn}(k)$

$$\frac{1}{4} \int_0^{2\pi} \frac{d\theta_{\mathbf{k}'}}{2\pi} [1 + s s_1 e^{i(\theta_{\mathbf{k}'} - \theta_{\mathbf{k}})}] \cos \theta_{\mathbf{k}'} [1 + s' s_1 e^{-i(\theta_{\mathbf{k}'} - \theta_{\mathbf{k}})}] = \frac{s_1}{8} [s e^{-i\theta_{\mathbf{k}}} + s' e^{i\theta_{\mathbf{k}}}], \quad (4.2.30)$$

to get

$$\gamma_{ss'}^{(2)nn}(k) = \frac{(\cos \theta_{\mathbf{k}} \sigma_{z,ss'} + \sin \theta_{\mathbf{k}} \sigma_{y,ss'})}{16\pi N_0 \tau} \sum_{n_1 \mathbf{k}' s_1} s_1 \langle f_{n\mathbf{k}s} | f_{n_1 \mathbf{k}' s_1} \rangle \langle f_{n_1 \mathbf{k}' s_1} | f_{n\mathbf{k}s'} \rangle G_{n_1 \mathbf{k}' s_1}^R \frac{k'}{m} G_{n_1 \mathbf{k}' s_1}^A. \quad (4.2.31)$$

Approximating $\langle f_{n\mathbf{k}s} | f_{n_1 \mathbf{k}' s_1} \rangle \sim \delta_{nn_1}$, summing over s_1 , and integrating over k with the technique shown in Appendix B yields

$$\gamma_{ss'}^{(2)nn}(k) = -(\cos \theta_{\mathbf{k}} \sigma_{z,ss'} + \sin \theta_{\mathbf{k}} \sigma_{y,ss'}) E_0 n^2 (e_1 + 2e_3 k_{Fn}^2), \quad (4.2.32)$$

where we have introduced the spin-averaged Fermi momentum in the n -th subband

$$\frac{k_{Fn}^2}{2m} = \mu - E_0 n^2. \quad (4.2.33)$$

On the other hand $\gamma_{ss'}^{(1)nn}(k)$ is given by

$$\begin{aligned} \gamma_{ss'}^{(1)nn}(k) &= (\cos \theta_{\mathbf{k}} \sigma_{z,ss'} + \sin \theta_{\mathbf{k}} \sigma_{y,ss'}) E_0 n^2 (e_1 + e_3 k_{Fn}^2) \\ &\quad + 2 \cos \theta_{\mathbf{k}} \sigma_{z,ss'} E_0 n^2 e_3 k_{Fn}^2 \end{aligned} \quad (4.2.34)$$

where k has been replaced by k_{Fn} at the required level of accuracy. Combining $\gamma_{ss'}^{(1)nn}(k)$ and $\gamma_{ss'}^{(2)nn}(k)$ as mandated by Eq.(4.2.26) we finally obtain

$$\gamma_{x,ss'}^{nn}(k) = (\cos \theta_{\mathbf{k}} \sigma_{z,ss'} - \sin \theta_{\mathbf{k}} \sigma_{y,ss'}) E_0 n^2 e_3 k_{Fn}^2. \quad (4.2.35)$$

Next we project the equation for the vertex corrections in the basis of the eigenstates and get the following integral equation:

$$\Gamma_{x,ss'}^{nn}(k) = \gamma_{x,ss'}^{nn}(k) + \frac{1}{2\pi N_0 \tau} \sum_{n_1 n_2 \mathbf{k}' s_1 s_2} \langle n\mathbf{k}s | n_1 \mathbf{k}' s_1 \rangle G_{n_1 \mathbf{k}' s_1}^R \Gamma_{x,s_1 s_2}^{n_1 n_2}(k') G_{n_2 \mathbf{k}' s_2}^A \langle n_2 \mathbf{k}' s_2 | n\mathbf{k}s' \rangle, \quad (4.2.36)$$

which, by confining to intra-band processes only, can be solved with the ansatz $\Gamma_{x,ss'}^{nn}(k) = \Gamma^n(k_{Fn})(\cos(\theta_{\mathbf{k}})(\sigma_z)_{ss'} + \sin(\theta_{\mathbf{k}})(\sigma_y)_{ss'})$ yielding

$$\Gamma_{x,ss'}^{nn}(k) = \gamma_{x,ss'}^{nn}(k) \frac{\tau_{DP}^{(n)}}{\tau}, \quad (4.2.37)$$

with the Dyakonov-Perel spin relaxation time for each subband defined as

$$\frac{\tau_{DP}^{(n)}}{\tau} = 2 \left[\frac{1 + (2\tau \Delta E_{nk_{Fn}})^2}{(2\tau \Delta E_{nk_{Fn}})^2} \right]. \quad (4.2.38)$$

By performing the integral over momentum and summing over the spin indices in Eq.(4.2.16), one obtains the SHC as

$$\sigma^{SHE} = \sum_{n=1}^{n_c} \frac{e}{8\pi} \frac{2\tau}{\tau_{DP}^{(n)}} \frac{\Gamma^n(k_{Fn})}{\Delta E_{nk_{Fn}}/k_{Fn}}, \quad (4.2.39)$$

where n_c is the number of occupied bands.

If vertex corrections are ignored, i.e. if we approximate $\Gamma^n(k_{Fn}) = \Delta E_{nk_{Fn}}/k_{Fn}$ (cf. Eq.(4.2.30)), Eq.(4.2.18) gives us

$$\sigma_{drift}^{SHE} = \sum_{n=1}^{n_c} \frac{e}{8\pi} \frac{2\tau}{\tau_{DP}^{(n)}}, \quad (4.2.40)$$

which, in the weak disorder limit ($\tau \rightarrow \infty$), reproduces the result of Ref. [60], i.e. $\sigma_{drift}^{SHE} = (e/8\pi)n_c$.

If instead the renormalized vertex (4.2.37) is properly taken into account, we obtain

$$\sigma^{SHE} = - \sum_n^{n_c} \frac{e}{4\pi} \frac{e_3 k_{Fn}^2}{e_1 + e_3 k_{Fn}^2}. \quad (4.2.41)$$

Notice that, being proportional to λ_{\pm}^4 ($e_1 \propto \lambda_{\pm}^2$, $e_3 \propto \lambda_{\pm}^6$), this result is consistent with the result obtained in Ref. [39], where the SHC is calculated in an asymmetric triangular potential well, which represents the mobile electrons at the interface between two insulating oxides, such as $LaAlO_3$ and $SrTiO_3$.

Now we will calculate the Edelstein conductivity (EC). The Kubo formula for the DC EC is

$$\sigma^{EE} = \lim_{\omega \rightarrow 0} \frac{\text{Im} \langle \langle s^y; j_x \rangle \rangle}{\omega}, \quad (4.2.42)$$

which corresponds with diagrams a) and b) of Fig.(4.3). It can be written as

$$\sigma^{EE} = - \lim_{\omega \rightarrow 0} \text{Im} \frac{e}{\omega} \sum_{nn'\mathbf{k}\mathbf{k}'ss'} \langle n'\mathbf{k}'s' | \hat{v}_x | n\mathbf{k}s \rangle \langle n\mathbf{k}s | s^y | n'\mathbf{k}'s' \rangle \int_{-\infty}^{\infty} \frac{d\epsilon}{2\pi} G_{ns}(\epsilon_+, \mathbf{k}) G_{n's'}(\epsilon_-, \mathbf{k}'), \quad (4.2.43)$$

After performing the integral over frequency we get

$$\sigma^{EE} = - \frac{e}{2\pi} \sum_{nn'\mathbf{k}ss'} \langle n'\mathbf{k}'s' | \hat{v}_x | n\mathbf{k}s \rangle \langle n\mathbf{k}s | s^y | n'\mathbf{k}'s' \rangle G_{n\mathbf{k}s}^R G_{n'\mathbf{k}'s'}^A, \quad (4.2.44)$$

where we have used again the orthogonality of the eigenvectors with different momentum. As shown in Fig.4.3, we consider the bare vertex for the spin density $s^y = \sigma_y/2$ and the two vertices for the number current density $\hat{v}_x = \hat{\Gamma}_x + k_x/m$. In clear contrast with the 2DEG Rashba case, the two parts of the number current vertex yield two separate contributions to the EC and we are now going to evaluate them separately. We then evaluate Fig.(4.3)(a) as:

$$\sigma^{EE,(a)} = - \frac{e}{4\pi m} \sum_{nn'\mathbf{k}ss'} \langle n'\mathbf{k}'s' | k_x | n\mathbf{k}s \rangle \langle n\mathbf{k}s | \sigma_y | n'\mathbf{k}'s' \rangle G_{n\mathbf{k}s}^R G_{n'\mathbf{k}'s'}^A, \quad (4.2.45)$$

where the matrix elements of the spin vertex are

$$\langle n\mathbf{k}s | \sigma_y | n'\mathbf{k}'s' \rangle = \langle f_{n\mathbf{k}s} | f_{n'\mathbf{k}'s'} \rangle (\cos \theta_{\mathbf{k}} \sigma_{z,ss'} + \sin \theta_{\mathbf{k}} \sigma_{y,ss'}). \quad (4.2.46)$$

Setting $n' = n$ and using Eq.(4.1.10) for the energy eigenvalues, we can perform the integration over the momentum in Eq.(4.2.45) obtaining for $\sigma^{EE,(a)}$ the expression

$$\sigma^{EE,(a)} = \sum_{n=1}^{n_c} e N_0 \tau E_0 n^2 (e_1 + 2e_3 k_{Fn}^2), \quad (4.2.47)$$

Next, we evaluate Fig.(4.3)(b) as:

$$\sigma^{EE,(b)} = -\frac{e}{4\pi} \sum_{nn'\mathbf{k}s s'} \langle n'\mathbf{k}s' | \hat{\Gamma}_x | n\mathbf{k}s \rangle \langle n\mathbf{k}s | \sigma_y | n'\mathbf{k}s' \rangle G_{n\mathbf{k}s}^R G_{n'\mathbf{k}s'}^A \quad (4.2.48)$$

We set $n = n'$ and insert the result obtained in Eq.(4.2.37) for $\langle n\mathbf{k}s' | \hat{\Gamma}_x | n\mathbf{k}s \rangle$. Since both the matrix elements of $\hat{\Gamma}_x$ and σ_y contain terms proportional to $\cos(\theta_{\mathbf{k}})$ and $\sin(\theta_{\mathbf{k}})$, we must distinguish between $s = s'$ (first term in Eq.(4.2.35)) and $s \neq s'$ (second term in Eq.(4.2.35)). If $s = s'$ we have

$$\sigma_1^{EE,(b)} = -\frac{e}{4\pi} \sum_{n\mathbf{k}s} \langle n\mathbf{k}s | \hat{\Gamma}_x | n\mathbf{k}s \rangle \langle n\mathbf{k}s | \sigma_y | n\mathbf{k}s \rangle G_{n\mathbf{k}s}^R G_{n\mathbf{k}s}^A \quad (4.2.49)$$

The integral over the momentum can be done with the technique shown in Chapter 3

$$\sigma_1^{EE,(b)} = -\sum_n^{n_c} eN_0\tau E_0 n^2 e_3 k_{Fn}^2 \frac{\tau_{DP}^{(n)}}{2\tau}. \quad (4.2.50)$$

If $s \neq s'$ we have instead

$$\sigma_2^{EE,(b)} = -\frac{e}{4\pi} \sum_{n\mathbf{k}s} \langle n\mathbf{k}\bar{s} | \hat{\Gamma}_x | n\mathbf{k}s \rangle \langle n\mathbf{k}s | \sigma_y | n\mathbf{k}\bar{s} \rangle G_{n\mathbf{k}s}^R G_{n\mathbf{k}\bar{s}}^A. \quad (4.2.51)$$

So we can conclude that

$$\sigma_2^{EE,(b)} = \sum_{n=1}^{n_c} eN_0\tau E_0 n^2 \frac{e_3 k_{Fn}^2}{(2\tau \Delta E_{nk_{Fn}})^2} \quad (4.2.52)$$

with $\Delta E_{nk_{Fn}} = E_0 n^2 (e_1 k_{Fn} + e_3 k_{Fn}^3)$ as the one defined before. Combining the (a) and (b) contributions, the final result for the Edelman conductivity is found to be:

$$\sigma^{EE} = \sum_{n=1}^{n_c} eN_0\tau E_0 n^2 (e_1 + e_3 k_{Fn}^2). \quad (4.2.53)$$

4.3 Discussion of the results

In this Section we will make \hbar explicit to give clarity to the results.

We now examine two physically interesting limiting cases of the general solution:

1. the insulator-metal-vacuum junction,
2. films with the same spin orbit constant coupling at the two interfaces

The insulator-metal-vacuum junction corresponds in our model to $\lambda_- \ll \lambda_+ \equiv \lambda$, $V_- \gg V_+ \equiv V$. We will neglect the so-called Vasko effect [104], which consists in the appearance of an induced spin-orbit coupling due to the inversion symmetry breaking across the metal-vacuum interface, because the induced SOC due to this effect is much smaller than the one induced by the insulator. This fact justifies the limits referred before. In this case we obtain the following values for the SHC and EC

$$\sigma^{EE} = \sum_n^{n_c} \frac{2eN_0\tau E_0 n^2 \lambda^2}{d\hbar}, \quad (4.3.54)$$

$$\sigma^{SHE} = - \sum_n^{n_c} \frac{e}{4\pi\hbar^3} 2mk_{Fn}^2 V \lambda^4. \quad (4.3.55)$$

There are some experimental studies of metal-metal-vacuum junctions that shows giant spin-orbit coupling [103, 105], and where one could test the prediction of Eqs.(4.3.54), (4.3.55). Following Ref. [103], where the dispersion of electrons in a Al/W junction is studied through the ARPES techniques resolved in spin, the metallic film is made of ten monatomic layers of Al, ($d \approx 1$ nm), it shows a large spin splitting energy of $\Delta E_{nk_{Fn}} = 240$ meV in the second band ($n = 2$). Introducing these values in our model, with a

barrier of $V \approx 4$ eV, one can find a value for $\lambda \approx 4.9 \times 10^{-9}$ cm. We should remember that in this experiment there is only one interfacial barrier (the other barrier is the vacuum) so we assume that only λ_+ survives.

Though Eq.(4.3.55) is obtained for small values of the parameter $2mk_{F_n}^2 V \lambda^4 / \hbar^2 \ll 1$, the structure of the result is quite interesting: it suggests that this kind of device, the insulator-metal-vacuum junction, could be an efficient spintronic device, its transport properties being proportional to the barrier height V . With these values one obtains the following value for the SHC, $\sigma^{SHE} \approx -0.29 \times e/(8\pi)$ which, as we said before, is smaller than one, but seems an encouraging result. In Fig.?? we report the EC in values of the "normal" value as a function of $2\Delta E_{nk_{F_n}} \tau$.

These experimental data, Ref. [103], refer to the specific device metal-metal-vacuum junction, but it provides good experimental data to expect giant spin orbit coupling on insulator-metal-insulator junctions.

Lets discuss the "quasi-symmetric" configuration, i.e. though $\lambda_+ = \lambda_- \equiv \lambda$ and different barrier heights, $V_+ \neq V_-$. We then obtain that the spin splitting of the bands vanishes to linear order in k ($e_1 = 0$), due to Ehrenfest's theorem¹. When we substitute this result in Eq.(4.2.41) we obtain the following result

$$\sigma^{SHE} = - \sum_{n=1}^{n_c} \frac{e}{4\pi\hbar}. \quad (4.3.56)$$

¹This is because the splitting of the energy levels to first order in k is shown by perturbation theory to be proportional to the expectation value of $V'(z)$, i.e. the force, in the ground-state in the absence of spin-orbit coupling. By Ehrenfest's theorem, i.e. $\frac{d}{dt} \langle k \rangle = - \langle \frac{\partial V}{\partial r} \rangle$, this is the expectation value of the time derivative of the z -component of the momentum, and therefore must vanish [76].

The SHC in this limit is independent of λ . This very striking result is reminiscent of the universal result $\frac{e}{8\pi\hbar}$ obtained for a single Bychkov-Rashba band when vertex corrections are ignored [11]. However vertex corrections are now fully included, yet the SHC is not only finite, but *independent* of λ and equal to the single band universal result multiplied by a factor -2 ! We emphasize that this result has nothing to do with the non-vanishing intrinsic SHC that arises in certain generalized models of spin-orbit coupling with winding number higher than 1 [106]. Rather, it has to do with the k -dependence of the transverse subbands describing the electron wave function in the z - direction.

4.4 Inter-band contributions

Let us finally discuss the fully inversion-symmetric limit of the model, $\lambda_+ = \lambda_-$ and $V_+ = V_-$. We notice that in this case the limit of Eq.(4.2.41) does not exist, because both e_1 and e_3 vanish (the spin splitting is identically zero!) while the value of Eq.(4.2.41) depends on the order in which e_1 and e_3 tend to zero, in particular on whether they tend to zero simultaneously, or e_1 tend to zero before e_3 , as in the “quasi-symmetric” case above. The origin of this apparently unphysical non-analytic behavior can be traced back to the singular character of the vertex Eq.(4.2.37) for vanishing spin splitting. Under these circumstances, the Dyakonov-Perel spin relaxation time Eq.(4.2.38) diverges, apparently implying spin conservation. However, even in the inversion-symmetric limit, inter-band effects provide spin relaxation processes which regularize the vertex. Such effects are typically negligible away from the inversion-symmetric limit, since they are proportional to the

square of the wave-function overlap between different bands and therefore scale as $(d_{\pm}/d)^2$. However, in the inversion-symmetric limit they cannot be neglected.

A full analysis of inter-band effects is still under investigation at the moment of writing this thesis. Let us consider a simplified case to explain how the inter-band contributions regularize Eq.(4.2.37). We will consider the case of only one band occupied ($n = 1$) and we will only take into account the contribution of the nearest band ($n = 2$). The vertex equation for $\Gamma_{ss'}^{11}(\mathbf{k})$ is

$$\begin{aligned} \Gamma_{ss'}^{11}(\mathbf{k}) &= \gamma_{ss'}^{11}(\mathbf{k}) + \frac{1}{2\pi N_0\tau} \sum_{\mathbf{k}'s_1s_2} \langle 1\mathbf{k}s | 1\mathbf{k}'s_1 \rangle \Gamma_{s_1s_2}^{11}(\mathbf{k}') \langle 1\mathbf{k}'s_2 | 1\mathbf{k}s' \rangle G_{1\mathbf{k}'s_1}^R G_{1\mathbf{k}'s_2}^A \\ &+ \frac{1}{2\pi N_0\tau} \sum_{\mathbf{k}'s_1s_2} \langle 1\mathbf{k}s | 1\mathbf{k}'s_1 \rangle \Gamma_{s_1s_2}^{12}(\mathbf{k}') \langle 2\mathbf{k}'s_2 | 1\mathbf{k}s' \rangle G_{1\mathbf{k}'s_1}^R G_{2\mathbf{k}'s_2}^A \\ &+ \frac{1}{2\pi N_0\tau} \sum_{\mathbf{k}'s_1s_2} \langle 1\mathbf{k}s | 2\mathbf{k}'s_1 \rangle \Gamma_{s_1s_2}^{21}(\mathbf{k}') \langle 2\mathbf{k}'s_1 | 1\mathbf{k}s' \rangle G_{2\mathbf{k}'s_1}^R G_{1\mathbf{k}'s_2}^A. \end{aligned} \quad (4.4.57)$$

The vertex equation for $\Gamma_{ss'}^{12}(\mathbf{k})$ is

$$\begin{aligned} \Gamma_{ss'}^{12}(\mathbf{k}) &= \gamma_{ss'}^{12}(\mathbf{k}) + \frac{1}{2\pi N_0\tau} \sum_{\mathbf{k}'s_1s_2} \langle 1\mathbf{k}s | 1\mathbf{k}'s_1 \rangle \Gamma_{s_1s_2}^{11}(\mathbf{k}') \langle 1\mathbf{k}'s_2 | 2\mathbf{k}s' \rangle G_{1\mathbf{k}'s_1}^R G_{1\mathbf{k}'s_2}^A \\ &+ \frac{1}{2\pi N_0\tau} \sum_{\mathbf{k}'s_1s_2} \langle 1\mathbf{k}s | 1\mathbf{k}'s_1 \rangle \Gamma_{s_1s_2}^{12}(\mathbf{k}') \langle 2\mathbf{k}'s_2 | 2\mathbf{k}s' \rangle G_{1\mathbf{k}'s_1}^R G_{2\mathbf{k}'s_2}^A. \end{aligned} \quad (4.4.58)$$

In contrast to the equation for Γ^{11} there is no Γ^{21} does not appear because it implies a $G_2^R G_2^A$ term whose integral will be almost zero. The integral is negligible because the most important contribution to the integrals of the Green functions comes from its poles. In the integrals concerning $G_2^R G_2^A$ terms there is no pole so we are allowed to neglect them. As we can see in Appendix B, the third term of Eq.(4.4.58) will be of order $|\langle f_{1\mathbf{k}s} | f_{2\mathbf{k}s'} \rangle|^2 / (1 +$

$\tau^2 E_G^2 \Gamma^{12}$ so we can neglect it and Eq.(4.4.58) becomes

$$\Gamma_{ss'}^{12}(\mathbf{k}) = \gamma_{ss'}^{12}(\mathbf{k}) + \frac{1}{2\pi N_0 \tau} \sum_{\mathbf{k}'s_1s_2} \langle 1\mathbf{k}s | 1\mathbf{k}'s_1 \rangle \Gamma_{s_1s_2}^{11}(\mathbf{k}') \langle 1\mathbf{k}'s_2 | 2\mathbf{k}s' \rangle G_{1\mathbf{k}'s_1}^R G_{1\mathbf{k}'s_2}^A.$$

We can then define $\rho_{IB} = \tau/\tau_{IB}$, that plays the role of the inter-band relaxation rate, as

$$\rho_{IB} = \frac{1}{2\pi N_0 \tau} \sum_{\mathbf{k}'s_1s_2} \langle 1\mathbf{k}s | 1\mathbf{k}'s_1 \rangle \langle 1\mathbf{k}'s_2 | 2\mathbf{k}s' \rangle G_{1\mathbf{k}'s_1}^R G_{1\mathbf{k}'s_2}^A \sim |\langle f_{1\mathbf{k}s} | f_{2\mathbf{k}s'} \rangle|^2 \frac{1}{1 + \tau^2 E_G^2}, \quad (4.4.59)$$

with $E_G = (4 - 1)E_0$. If we don't take into account the contribution of γ^{12} (we should remember that we want to see how inter-band contributions renormalize the vertex equation, but at this moment we do not have a full analysis of the the inter-band contributions to the SHC), the equation for Γ^{11} becomes

$$\Gamma^{11} = \gamma^{11} + (1 - \rho_{DP} - \rho_{IB})\Gamma^{11}, \quad (4.4.60)$$

with $\rho_{DP} = \tau/\tau_{DP}$. Hence

$$\Gamma^{11} \sim \frac{\gamma^{11}}{\rho_{DP} + \rho_{IB}} \quad (4.4.61)$$

Now if we are in the fully inversion-symmetric limit of the model, $\lambda_+ = \lambda_-$, $V_+ = V_-$ the vertex Γ^{11} does not diverge anymore. Its contribution to the SHC tends to zero when we substitute $e_3 = \rho_{DP} = 0$. This is not the exact result of the ‘‘ultra-symmetric’’ model. The value of both contributions, intra and inter-band, in this configuration, is one of the extensions to be developed in the near future. This preliminary calculation only shows how inter-band contributions cannot be neglected anymore if we are treating with a fully inversion-symmetric model. In this cases the inter-band mechanisms are the

4.5. The connection between the spin Hall and Edelstein effects 80

responsible of the non-conservation of the spin and τ_{IB} represents the spin relaxation time. The contribution of inter-band effects to the SHC, which is crucial in the inversion-symmetric case, is still under investigation at this moment.

4.5 The connection between the spin Hall and Edelstein effects

In Chapter 3 we showed that the Edelstein and the spin Hall conductivities are deeply connected in the 2DEG Rashba model. In this Section we will firstly derive this connection in the 2DEG Rashba model. To this end we will use the so-called $SU(2)$ quasiclassical approach to prove it. For more details we refer the interested reader to the Appendix C. Then we will ask ourselves if there is such a relation inside each subband of the insulator-metal-insulator model described in this Chapter.

It is convenient to describe spin-orbit coupling in terms of a non-Abelian gauge field $\mathcal{A} = \mathcal{A}^a \sigma^a / 2$, with $\mathcal{A}_y^x = 2m\alpha$ and $\mathcal{A}_x^y = -2m\alpha$. [83, 107, 108] If not otherwise specified, superscripts indicate spin components, while subscripts stand for spatial components. The first consequence of resorting to this language is the appearance of an $SU(2)$ magnetic field $\mathcal{B}_z^z = -(2m\alpha)^2$, which arises from the non-commuting components of the Bychkov-Rashba vector potential. Such a spin-magnetic field couples the charge current driven by an electric field, say along x , to the z -polarized spin current flowing along y . This is very much similar to the standard Hall effect, where two *charge* currents flowing perpendicular to each other are coupled by a magnetic field.

4.5. The connection between the spin Hall and Edelstein effects 81

The drift component of the spin current can thus be described by a Hall-like term

$$[J_y^z]_{drift} = \sigma_{drift}^{SHE} E_x. \quad (4.5.62)$$

It is however important to appreciate that this is not yet the full spin Hall current, i.e. σ_{drift}^{SHE} is not the full SHC. In the diffusive regime σ_{drift}^{SHE} is given by the classic formula $\sigma_{drift}^{SHE} = (\omega_c \tau) \sigma_D / e$, where $\omega_c = \mathcal{B}/m$ is the ‘‘cyclotron frequency’’ associated with the $SU(2)$ magnetic field, τ is the elastic momentum scattering time, and σ_D is the Drude conductivity. For a more general formula see Eq. (4.5.66) below.

In addition to the drift current, there is also a ‘‘diffusion current’’ due to spin precession around the Bychkov-Rashba effective spin-orbit field. Within the $SU(2)$ formalism this current arises from the replacement of the ordinary derivative with the $SU(2)$ covariant derivative in the expression for the diffusion current. The $SU(2)$ covariant derivative, due to the gauge field, is

$$\nabla_j \mathcal{O} = \partial_j \mathcal{O} + i [\mathcal{A}_j, \mathcal{O}], \quad (4.5.63)$$

with \mathcal{O} a given quantity being acted upon. The normal derivative, ∂_j , along a given axis j is shifted by the commutator with the gauge field component along that same axis. As a result of the replacement $\partial \rightarrow \nabla$ diffusion-like terms, normally proportional to spin density gradients, arise even in uniform conditions and the diffusion contribution to the spin current turns out to be

$$[J_y^z]_{diff} = 2m\alpha D s^y, \quad (4.5.64)$$

where $D = v_F^2 \tau / 2$ is the diffusion coefficient, v_F being the Fermi velocity. In the diffusive regime the full spin current J_y^z can thus be expressed in the

4.5. The connection between the spin Hall and Edelstein effects 82

suggestive form

$$J_y^z = \frac{D}{L_{so}} s^y + \sigma_{drift}^{SHE} E_x, \quad (4.5.65)$$

where $L_{so} = (2m\alpha)^{-1}$ plays the role of an ‘‘orientational spin diffusion length’’, related to the different Fermi momenta in the two spin-orbit split bands. For a detailed justification of Eq.(4.5.65) we refer the reader to Refs. [43, 107] and to Appendix C. The factor in front of the spin density in the first term of Eq.(4.5.65) can also be written in terms of the Dyakonov-Perel spin relaxation time, i.e. the ‘‘orientational spin diffusion time’’ given by $\tau_s = L_{so}^2/D$. In terms of τ and τ_s one has

$$\sigma_{drift}^{SHE} = \frac{e}{8\pi} \frac{2\tau}{\tau_s}, \quad (4.5.66)$$

which is indeed equivalent to the classical surmise given after Eq.(4.5.62). If we introduce the total SHC and the Edelstein Conductivity (EC) defined by

$$J_y^z = \sigma^{SHE} E_x, \quad s^y = \sigma^{EE} E_x \quad (4.5.67)$$

we may rewrite Eq.(4.5.65) as

$$\sigma^{EE} = \frac{\tau_s}{L_{so}} (\sigma^{SHE} - \sigma_{drift}^{SHE}). \quad (4.5.68)$$

In the standard Bychkov-Rashba model a general constraint from the equation of motion dictates that under steady and uniform conditions $J_y^z = 0$. Therefore the EC reads

$$\sigma^{EE} = -\frac{\tau_s}{L_{so}} \sigma_{drift}^{SHE} = -e \frac{m}{2\pi} \alpha \tau = -e N_0 \alpha \tau, \quad (4.5.69)$$

which is easily obtained by using the expressions given above and the single particle density of states in two dimensions, $N_0 = m/2\pi$ and equivalent to the value obtained in Chapter 3 through the Kubo formula.

4.5. The connection between the spin Hall and Edelstein effects **83**

We would like to know if there is a relation between both conductivities is present in each subband in the insulator-metal-insulator model. Unfortunately an equation as (4.5.68) is not valid in this model. The z -dependence of the non-Abelian spin-orbit coupling gauge field terms, $\mathcal{A} \rightarrow \mathcal{A}(z)$, implies more complicated kinetic effective equations.

The complete derivation of this kinetic, Boltzmann or Eilenberger, equations in the presence of non constant non-Abelian spin-orbit coupling gauge field terms, is one of the future perspectives that will be developed in the future.

Chapter 5

Thermospin effects: the spin Nernst effect

In this Chapter we will describe the connection between the spin-heat and spin-charge response in an electron/hole disordered Fermi gas with different types of spin-orbit coupling. We will calculate the so-called spin Nernst conductivity, and we will show that there is a relation between this value and the spin Hall conductivity value. This calculations will allow us to conclude that a metallic system could prove much more efficient as a heat-to-spin than as a heat-to-charge converter. We will work in natural units $\hbar = c = k_B = 1$

These results have been published in Phys. Rev. B 87, 085309, 2013 [109].

5.1 The heat and spin dialogue

The moving carriers in a metallic system, electrons or holes, transport both electric charge and heat. This gives rise to a number of thermoelectric effects

as well as a deep connection between thermal and electrical conductivities. A well known example is the Wiedemann-Franz law, which states that the ratio of the thermal to the electrical conductivity is the temperature times a universal number, the Lorenz number \mathcal{L}

$$\frac{\kappa}{\sigma} = \frac{\pi^2}{3} \left(\frac{1}{e}\right)^2 T = \mathcal{L}T \quad (5.1.1)$$

where e is the unit charge. Additionally, a magnetic field affects both thermal and electrical transport yielding both galvanomagnetic and thermomagnetic effects [110]. The above situation gets even more complicated when a third quantity transported by the carriers – the spin – is connected to the previous two by spin-orbit coupling. On the bright side, such a connection also opens up a plethora of new possibilities related to the manipulation of the additional spin degrees of freedom. This is testified by the recent rapid development of spintronics [2, 3] and spin caloritronics [70].

An important goal of spin caloritronics is the manipulation of the spin degrees of freedom via thermal gradients [67, 69, 71, 72, 111], particularly relevant when energy efficiency issues are considered [70].

We will focus in thermo-spin transport due to the charge carriers' dynamics [67, 71], considering disordered Fermi gases with spin-orbit coupling. We will discuss the particular case of the thermo-spin Hall effect – the generation of a spin current transverse to a thermal gradient, also called the spin Nernst effect. In so doing we will show that a simple relation connects the spin thermopower – the ratio between the spin response to a thermal gradient and that to an electric field – to the standard electric thermopower, and that the former can be strongly enhanced by the interplay between different SOC mechanisms.

Let us start with some basic phenomenological considerations along the lines of Refs. [112,113], and consider the bare-bones situation of an inversion symmetric, homogeneous and non-ferromagnetic material in the absence of magnetic fields. A particle current j_x can be driven either by an electric field or by a temperature gradient, and within the standard semiclassical approach one writes [59]

$$j_x = L_{11}E_x + L_{12}(-\nabla_x T) = \sigma E_x - e\mathcal{L}T\sigma'(-\nabla_x T). \quad (5.1.2)$$

Here $\sigma = -2eN_0D$ is the Drude conductivity up to a charge $-e$, with N_0 the density of states at the Fermi energy and D the diffusion constant, and $\sigma' = \partial_\mu\sigma$, μ being the chemical potential. Then the electric thermopower reads

$$S \equiv \frac{L_{12}}{L_{11}} = -e\mathcal{L}T\frac{\sigma'}{\sigma}. \quad (5.1.3)$$

This is the Mott's formula, which, as the Wiedemann-Franz law, is valid when we are dealing with transport phenomena in metals [114].

In the present simple case the connection between spin and particle currents due to spin-orbit coupling reads [112]

$$j_y^z = -\gamma j_x = L_{11}^s E_x + L_{12}^s (-\nabla_x T). \quad (5.1.4)$$

Here j_y^z is the z -polarized spin current flowing in the y direction arising in response to the particle current j_x , and $\gamma \ll 1$ is a dimensionless spin-orbit coupling constant. As an immediate consequence of Eqs.(5.1.2) and (5.1.4), the spin thermopower $S_s \equiv L_{12}^s/L_{11}^s$ is equal to S , since the SOC constant γ does not depend on the sources of a given particle current. Eq.(5.1.4) breaks down in the absence of inversion symmetry, and in order to see how the above

simple result is modified in a general situation, and to study its dependence on competing SOC mechanisms, we will move on to a microscopic treatment.

5.2 The spin equivalent of Mott's formula

Although our treatment is independent of dimensions (2D or 3D), in order to fix things we consider a disordered 2D Fermi gas in the x - y plane described by the Hamiltonian

$$H = \frac{k^2}{2m} + U(\mathbf{x}) + H_{\text{so}}, \quad (5.2.5)$$

with \mathbf{k} the 2D momentum and $U(\mathbf{x})$ the impurity potential. For the latter we assume the standard white noise disorder model and evaluate the impurity average in the Born approximation, $\langle U(\mathbf{x})U(\mathbf{x}') \rangle = (2\pi N_0 \tau)^{-1} \delta(\mathbf{x} - \mathbf{x}')$, with $N_0 = m/(2\pi)$ and τ the elastic scattering time, as we did in Chapter 3. The SOC term H_{so} will have different forms in the various cases considered below. Out of ease we recall the Rashba case

$$H_{\text{so}} = \alpha \boldsymbol{\sigma} \cdot \mathbf{k} \times \hat{\mathbf{e}}_z. \quad (5.2.6)$$

We assume the metallic regime and weak SO coupling conditions, $\epsilon_F \gg 1/\tau, \Delta_{\text{so}}$. Here ϵ_F is the Fermi energy in the absence of disorder and spin-orbit interaction and Δ_{so} is the spin splitting energy due to H_{so} . The a -polarized spin current flowing in the k -direction due to a generic thermal gradient is

$$j_i^a = \sum_l [\text{N}_{\text{sh}}]_{il}^a (-\partial_l T), \quad (5.2.7)$$

where N_{sh} is the spin-heat response tensor. Following Ref. [115] the latter is given in terms of the imaginary spin current-heat current kernel

$$[\text{N}_{\text{sh}}]_{il}^a T = \lim_{\Omega \rightarrow 0} \left\{ \frac{[Q_{\text{sh}}(i\Omega_\nu)]_{il}^a}{\Omega_\nu} \right\}_{i\Omega_\nu \rightarrow \Omega^R, \Omega^R = \Omega + i0^+}. \quad (5.2.8)$$

The spin current operator is given by the standard definition $j_i^a = (1/2)\{v_i, s^a\}$, v_i and s^a being the velocity and spin operators. Notice that the particle (charge) current operator is $(-e)j_i = (-e)v_i$. The heat current in the Matsubara representation reads [115]

$$j_i^h(\mathbf{k}, \epsilon_n, \epsilon_n + \Omega_\nu) = i\epsilon_{n+\nu/2} j_i, \quad (5.2.9)$$

with $\epsilon_n = \pi T(2n + 1)$, $\Omega_\nu = 2\pi T\nu$, and $\epsilon_{n+\nu/2} = \epsilon_n + \Omega_\nu/2$. The specific form of v_i depends on the choice of the SOC Hamiltonian. For instance in the Rashba case, Eq.(5.2.6), we have $v_{x,y} = k_{x,y}/m \mp \alpha\sigma^{y,x}$. By using the Kubo formula the response kernel is given by

$$[Q_{\text{sh}}]_{il}^a(i\Omega_\nu) = T \sum_{\epsilon_n, \mathbf{k}} i\epsilon_{n+\nu/2} \text{Tr} [j_i^a \mathcal{G}_n j_l \mathcal{G}_{n+\nu}], \quad (5.2.10)$$

where in this case the trace means the trace over the 2×2 matrices. The Matsubara Green functions $\mathcal{G}_n = \mathcal{G}(\mathbf{k}, \epsilon_n)$, $\mathcal{G}_{n+\nu} = \mathcal{G}(\mathbf{k}, \epsilon_n + \Omega_\nu)$ are matrices in spin space $\mathcal{G}_n = \mathcal{G}_n^0 + \sum_a \mathcal{G}_n^a \sigma^a$. Analogously, the spin-charge response kernel can be written as

$$[Q_{\text{sc}}]_{il}^a(i\Omega_\nu) = -eT \sum_{\epsilon_n, \mathbf{k}} \text{Tr} [j_i^a \mathcal{G}_n j_l \mathcal{G}_{n+\nu}], \quad (5.2.11)$$

leading to the spin-charge (particle) conductivity

$$[\sigma_{\text{sc}}]_{il}^a = \lim_{\Omega \rightarrow 0} \left\{ \frac{[Q_{\text{sc}}(i\Omega_\nu)]_{il}^a}{\Omega_\nu} \right\}_{i\Omega_\nu \rightarrow \Omega^R, \Omega^R = \Omega + i0^+}. \quad (5.2.12)$$

Although our treatment is general, to illustrate the procedure we take the Rashba case as an example. The average over disorder is evaluated in the Born approximation and leads to a self-energy

$$\Sigma(\epsilon_n) = \frac{1}{2\pi N_0 \tau} \sum_{\mathbf{k}} \mathcal{G}_n = -\frac{i}{2\tau} \text{sgn}(\epsilon_n), \quad (5.2.13)$$

which is diagonal in spin space. As we showed in Chapter 3, the off-diagonal terms in spin space of the Green function are odd in the momentum dependence and vanish upon integration. This remains valid also for other spin-orbit interaction terms as long as the Hamiltonian is time-reversal invariant.

To compute the thermo-spin Hall effect. i.e. the z -polarized spin current flowing along y generated by a thermal gradient along x , we need the response kernel $[Q_{\text{sh}}]_{yx}^z \equiv Q^{SHE}$, which reads

$$Q^{SHE}(i\Omega_\nu) = T \sum_{\epsilon_n} \sum_{\mathbf{k}} i\epsilon_{n+\nu/2} \text{Tr} [j_y^z \mathcal{G}_n j_x \mathcal{G}_{n+\nu}], \quad (5.2.14)$$

with

$$\mathcal{G}_n^0 = \frac{1}{2}(\mathcal{G}_{n,+} + \mathcal{G}_{n,-}) \quad (5.2.15)$$

$$\mathcal{G}_n^a = \frac{1}{2}(\hat{\mathbf{k}} \times \hat{\mathbf{e}}_z)^a (\mathcal{G}_{n,+} - \mathcal{G}_{n,-}) \quad (5.2.16)$$

$$\mathcal{G}_{n,\pm} = \left[i\epsilon_n + \mu - \frac{k^2}{2m} \mp \alpha k + \frac{i}{2\tau} \text{sgn}(\epsilon_n) \right]^{-1}, \quad (5.2.17)$$

μ being the chemical potential.

Notice that the analytic properties of the Green functions are determined by the sign of the imaginary frequency, therefore when performing the momentum integral in Eq.(5.2.14) one obtains a non-zero result only if the frequencies $\epsilon_n + \Omega_\nu$ and ϵ_n have opposite signs, which means that ϵ_n is restricted to the range $-\Omega_\nu < \epsilon_n < 0$. Exploiting that the external frequency is going to zero (cf. Eq.(5.2.12)) one thus has

$$\sum_{\mathbf{k}} \text{Tr} [j_i^a \mathcal{G}_n j_l \mathcal{G}_{n+\nu}] = -\frac{2\pi}{e} [\sigma_{\text{sc}}]_{il}^a (\mu + i\epsilon_n). \quad (5.2.18)$$

Eq.(5.2.14) only takes into account the so-called bare bubble. Vertex corrections [97, 116] will be considered later. According to Eq.(5.2.18) we now have

$$\sum_{\mathbf{k}} \text{Tr} [j_y^z \mathcal{G}_n j_x \mathcal{G}_{n+\nu}] = -\frac{2\pi}{e} \sigma^{SHE}(\mu + i\epsilon_n), \quad (5.2.19)$$

with $\sigma^{SHE}(\mu)$ the static spin-Hall conductivity calculated in Chapter 3. The thermo-spin Hall conductivity therefore reads

$$N^{SHE}T = -\lim_{\Omega \rightarrow 0} \left[\frac{2\pi T}{e\Omega_\nu} \sum_{n=-\nu}^{-1} i\epsilon_{n+\nu/2} \sigma^{SHE}(\mu + i\epsilon_n) \right]_{i\Omega_\nu \rightarrow \Omega^R}. \quad (5.2.20)$$

Before we continue we will show some technical details that will be important to solve 5.2.20.

Firstly we define

$$F(i\epsilon_n, i\Omega_\nu) = \sum_{\mathbf{k}} \text{Tr} [j_i^a \mathcal{G}_n j_l \mathcal{G}_{n+\nu}], \quad (5.2.21)$$

which allows us write the spin-heat and spin-charge responses as

$$\sigma_{sc} = \lim_{\Omega \rightarrow 0} \left\{ \frac{(-e)T}{\Omega_\nu} \sum_{\epsilon_n} F(i\epsilon_n, i\Omega_\nu) \right\}_{i\Omega_\nu \rightarrow \Omega^R}, \quad (5.2.22)$$

$$N_{sh} = \lim_{\Omega \rightarrow 0} \left\{ \frac{1}{\Omega_\nu} \sum_{\epsilon_n} i\epsilon_{n+\nu/2} F(i\epsilon_n, i\Omega_\nu) \right\}_{i\Omega_\nu \rightarrow \Omega^R}. \quad (5.2.23)$$

As mentioned before, the momentum integral yields a non-zero result only if the frequencies $\epsilon_n + \Omega_\nu$ and ϵ_n have opposite signs, which means that ϵ_n is restricted to the range $-\Omega_\nu < \epsilon_n < 0$. Since the external frequency is going to zero, so will $i\epsilon_n$, enabling one to expand F in powers of $i\epsilon_n$

$$F(i\epsilon_n, i\Omega_\nu) = F(0, i\Omega_\nu) + i\epsilon_n \frac{\partial F}{\partial i\epsilon_n}(0, i\Omega_\nu) + \dots \quad (5.2.24)$$

Replacing this expansion in Eq.(5.2.22) we have:

$$\sigma_{\text{sc}} = \lim_{\Omega \rightarrow 0} \left\{ \frac{eT}{\Omega_\nu} \sum_{n=-\nu}^{-1} F(0, i\Omega_\nu) + i\epsilon_n \frac{\partial F}{\partial i\epsilon_n}(0, i\Omega_\nu) + \dots \right\}_{i\Omega_\nu \rightarrow \Omega^R} \quad (5.2.25)$$

The first term of the sum is linear in Ω_ν , so when divided by Ω_ν in the zero-frequency limit it yields a non-zero contribution. The other terms of the sum, being at least quadratic in Ω_ν , clearly do not contribute. There follows

$$\sigma_{\text{sc}} = -\frac{e}{2\pi} F(0, 0). \quad (5.2.26)$$

This is enough to prove Eq.(5.2.18). To solve Eq.(5.2.20), we expand Eq.(5.2.23) in $i\epsilon_n$ and note that the zero order term of the sum vanishes since

$$\sum_{-\Omega_\nu < \epsilon_n < 0} \left(i\epsilon_n + \frac{i\Omega_\nu}{2} \right) = 0. \quad (5.2.27)$$

By noticing that

$$\sum_{-\Omega_\nu < \epsilon_n < 0} \left(i\epsilon_n + \frac{i\Omega_\nu}{2} \right) i\epsilon_n = \frac{\pi^2 T^2}{3} \nu (1 - \nu^2), \quad (5.2.28)$$

the only term contributing linearly in Ω_ν is the first order one. This leads to

$$N_{\text{sh}} = -e\mathcal{L}TF'(0, 0), \quad (5.2.29)$$

with \mathcal{L} the Lorenz number and $F' = \frac{\partial F}{\partial i\epsilon_n}$. The last step to solve Eq.(5.2.20) is the observation that the function F of Eq.(5.2.21) depends on ϵ_n through the combination $i\epsilon_n + \mu$, as it is evident from the expression of the Green functions in the restricted frequency range $-\Omega_\nu < \epsilon_n < 0$

$$\mathcal{G}_n = \left[i\epsilon_n + \mu - \frac{k^2}{2m} - \frac{i}{2\tau} - H_{SO} \right]^{-1} \quad (5.2.30)$$

$$\mathcal{G}_{n+\nu} = \left[i(\epsilon_n + \Omega_\nu) + \mu - \frac{k^2}{2m} + \frac{i}{2\tau} - H_{SO} \right]^{-1}, \quad (5.2.31)$$

where we have left unspecified the spin-orbit Hamiltonian for the sake of generality.

So we have obtained one of the most important results

$$N^{SHE} = -e\mathcal{L}T \frac{\partial(\sigma^{SHE})}{\partial\mu}, \quad (5.2.32)$$

with

$$\sigma^{SHE} = \frac{e}{8\pi} \frac{2\tau}{\tau_{DP}} = \frac{e}{8\pi} 2\tau D 4\alpha^2 m^2 = \frac{e}{8\pi} 8\tau^2 \alpha^2 \mu m, \quad (5.2.33)$$

which gives us the following result

$$N^{SHE}|_{\text{bare}} = -\frac{\pi^2 T}{3} \frac{m\alpha^2 \tau^2}{\pi}. \quad (5.2.34)$$

To connect this result with that of Ref. [71], in which $N^{SHE}T$ is computed in the clean limit, $\tau \rightarrow \infty$ we have to pay attention where τ appears. As we can see, τ only appears in the Matsubara matrix green functions. Taking the clean limit the original $\mathcal{G}_{n,\pm}$ becomes

$$\mathcal{G}_{n,\pm} = \left(\mu - \frac{k^2}{2m} \mp \alpha k - i\text{sgn}(\epsilon_n) (\pi T + |\epsilon'_n|) \right)^{-1}, \quad (5.2.35)$$

with $\epsilon'_n = \epsilon_n - 1$. The differences between this new Matsubara matrix green function with the previous one are that we have sent $1/2\tau \rightarrow \pi T$ and $\epsilon_n \rightarrow \epsilon'_n$. But as $|\epsilon'_n| \ll \pi T$ we can proceed as we did in the dirty case making the correspondent substitutions. Let us see that in our concrete example sending $\epsilon_n \rightarrow \epsilon'_n$ doesn't affect the Matsubara sum. The first Matsubara sum was

$$\sum_{-\Omega_\nu < \epsilon_n < 0} \left(i\epsilon_n + \frac{i\Omega_\nu}{2} \right) = 0. \quad (5.2.36)$$

That is equal to

$$\sum_{n=1}^{\nu} (i\pi T)^2 (-2n + 1 + \nu) (-2n + 1), \quad (5.2.37)$$

But as

$$\sum_{n=1}^{\nu} (i\pi T)^2 (-2n + 1 + \nu) = 0, \quad (5.2.38)$$

we can easily deduce that when we make the substitution $\epsilon_n \rightarrow \epsilon'_n$ in $\sigma^{SHE}(\mu + i\epsilon_n)$ both sums remains exactly the same. With this result we can also affirm that

$$\sum_{\epsilon_n = -\Omega_\nu}^0 i^2 \left(\epsilon_n + \frac{\Omega_\nu}{2} \right) \epsilon_n = \sum_{\epsilon_n = -\Omega_\nu}^0 i^2 \left(\epsilon_n + \frac{\Omega_\nu}{2} \right) (\epsilon_n + \Omega_\nu). \quad (5.2.39)$$

This is a necessary result because all our work was made making the $i\epsilon_n$ Taylor's expansion of $\sigma^{SHE}(\mu + i\epsilon_n)$ around μ , but it can also be made making the $i\epsilon_n + i\Omega_\nu$ Taylor's expansion of $\sigma^{SHE}(\mu + i\epsilon_n + i\Omega_\nu)$ around μ , what we have just proved that produces the same result.

Thus the effective replacement $1/2\tau \rightarrow \pi T$ in Eq.(5.2.34) yields the clean limit result

$$N^{SHE}|_{\text{clean}} = -\frac{m\alpha^2}{12\pi T}, \quad (5.2.40)$$

in agreement with Ref. [71].

Let us now discuss the vertex corrections. Taking them into account corresponds to sending $j_y^z \rightarrow J_y^z$, $j_x \rightarrow J_x$ and $j_x^h \rightarrow J_x^h$. At the level of the Born approximation either vertex could be renormalized: the bubble with J_y^z and j_x^h or that with j_y^z and J_x^h are equivalent. Moreover, since we neglect inelastic processes, $J_x^h = i\epsilon_{n+\nu/2} J_x$. For the Rashba case it is known that $J_x = 0$, i.e. $\sigma^{SHE} = 0$, and thus we immediately obtain

$$N^{SHE}|_{\text{dressed}} = 0. \quad (5.2.41)$$

However, notice that Eq.(5.2.20) holds for any form of the spin-orbit interaction term H_{so} , no matter whether of intrinsic or extrinsic nature. Therefore, once the spin-Hall conductivity σ^{SHE} of a given system is known, its

thermo-spin Hall conductivity N^{SHE} will follow at once. Even more generally, from the Matsubara formulation, Eqs. (5.2.8)-(5.2.18), we conclude that the spin-heat response of a disordered, spin-orbit coupled Fermi gas in the metallic regime is completely determined by its spin-charge response. This result holds in 2D and 3D, in the presence of arbitrary elastic scattering processes, possibly spin-dependent, and beyond the Born approximation, i.e. it has the same range of applicability of the Wiedemann-Franz law discussed in Ref. [115]. This is the first main result of this Chapter, which, after a Sommerfeld expansion, can be written in the very simple form

$$N_{sh} = -e\mathcal{L}T\sigma'_{sc}(\mu). \quad (5.2.42)$$

In other words Mott's formula for the electric thermopower $S = -e\mathcal{L}T\sigma'/\sigma$ has its symmetric spin equivalent

$$S_s = -e\mathcal{L}T\sigma'_{sc}/\sigma_{sc}. \quad (5.2.43)$$

Whether a direct relation between S_s and S exists is however not obvious and will be one of our next concerns.

5.3 Spin Nernst effect and spin thermopower in electron and hole gases

Specializing our treatment to some specific systems, we now have a two-fold aim: (i) to look for the possibility of efficient heat-to-spin conversion, $S_s \gg 1$; (ii) to establish a relation, if any, between S_s and S .

With this in mind, let us now take H_{so} due to extrinsic and Rashba SOC. This allows one to easily draw a set of more specific conclusions concerning

the thermo-spin response of the 2D Fermi gas, in particular regarding the interplay between different SOC and scattering mechanisms. To be explicit we take once more the disordered Rashba model as the initial example, and consider the presence of extrinsic SOC mechanisms, as we did in Chapter 3, and include (white noise) magnetic impurities. That is, we add to the Hamiltonian, Eq.(5.2.5), the terms

$$H_{\text{extr}} = -\frac{\lambda_e^2}{4} \boldsymbol{\sigma} \times \nabla V(\mathbf{x}) \cdot \mathbf{k}, \quad (5.3.44)$$

with λ_e an effective Compton wavelength, and

$$V_m(\mathbf{x}) = \sum_{\mathbf{i}} \mathbf{B} \cdot \boldsymbol{\sigma} \delta(\mathbf{x} - \mathbf{R}_i), \quad (5.3.45)$$

where \mathbf{B} is a random (white noise) magnetic field. The latter is handled in the Born approximation, $\langle V_m(\mathbf{x}) V_m(\mathbf{x}') \rangle = [3(2\pi N_0 \tau_{\text{sf}})]^{-1} \delta(\mathbf{x} - \mathbf{x}')$, with τ_{sf} the spin-flip time [37, 43]. Magnetic impurities change the extrinsic spin time $1/\tau_{so} \rightarrow 1/\tau_s \equiv 4/3\tau_{\text{sf}} + 1/\tau_{EY}$, with $1/\tau_{EY} = (1/\tau) (\lambda_e k_F/2)^4$ defined in Eq.(3.4.84). In a homogeneous bulk in steady state, following Eq.(3.4.91), the spin-Hall conductivity is easily computed following

$$\sigma^{SHE} = \left(\frac{1}{1 + \zeta} \right) \gamma \sigma, \quad (5.3.46)$$

where

$$\zeta = \frac{\tau_s}{\tau_{DP}} \quad (5.3.47)$$

$$\gamma = \gamma_{\text{intr}} + \gamma_{\text{sj}} + \gamma_{\text{ss}}, \quad (5.3.48)$$

with

$$\gamma_{\text{intr}} = -m\alpha^2\tau \quad \gamma_{\text{sj}} = \frac{\lambda_e^2 m}{4\tau} \quad \gamma_{\text{ss}} = \frac{\lambda_e^2 k_F^2}{16} 2\pi N_0 v_0, \quad (5.3.49)$$

and $\tau_{DP}^{-1} = (2m\alpha)^2 D$, the Dyakonov-Perel spin-relaxation rate. Via Eq.(5.2.42) one concludes

$$\sigma'^{SHE} = \left[\frac{\sigma'}{\sigma} + \frac{\gamma'}{\gamma} - \frac{\zeta'}{1+\zeta} \right] \sigma^{SHE}, \quad (5.3.50)$$

$$S_s = -e\mathcal{L}T \left[\frac{\sigma'}{\sigma} + \frac{\gamma'}{\gamma} - \frac{\zeta'}{1+\zeta} \right], \quad (5.3.51)$$

with the spin Hall thermopower $S_s = N^{SHE}/\sigma^{SHE}$. In the above, primed quantities are derivatives with respect to the chemical potential μ . Notice that the simple phenomenological argument of the introduction overlooks the μ -dependency of γ : the conclusion $S_s = S$ holds only for an energy-independent γ , and also an energy-independent ζ . Both σ^{SHE} and N^{SHE} depend on the ratio between τ_{DP} and τ_s and are in principle tunable, either by varying the doping, which affects τ_s , or by modulating α by varying the gate potential.

Let us consider some interesting cases using Eq.(5.3.50) and Eq.(5.3.51). When only Rashba SOC and magnetic impurities are present, we have $\tau_s = 3\tau_{sf}/4$ and $\gamma = \gamma_{int}$. By evaluating the various derivatives we obtain $\gamma' = 0$, $\zeta' = \zeta/\mu$, $\sigma' = \sigma/\mu$, which gives us the spin thermopower

$$S_s = -e\mathcal{L}T \frac{\sigma'}{\sigma} \frac{1}{1+\zeta}. \quad (5.3.52)$$

When SOC from impurities is present, too, the terms γ'/γ , ζ'/ζ in Eq.(5.3.50) are modified, leading to

$$S_s = -e\mathcal{L}T \frac{\sigma'}{\sigma} \left[1 + \frac{\gamma_{ss}}{\gamma} - \frac{\zeta}{1+\zeta} \left(1 - \frac{2\tau_s}{\tau_{EY}} \right) \right]. \quad (5.3.53)$$

The results so far obtained can be generalized to include the effects of the linear-in-momentum Dresselhaus SOC term described by the Hamiltonian

$$H_{so} = \beta (k_x \sigma^x - k_y \sigma^y). \quad (5.3.54)$$

It suffices to replace in the above $\gamma_{\text{intr}} = -m\tau(\alpha^2 - \beta^2)$, $1/\tau_{DP} = (2m)^2(\alpha^2 + \beta^2)D \equiv 1/\tau_{DP}^R + 1/\tau_{DP}^D$ and

$$\zeta = \frac{\tau_s}{\tau_{DP}} - 4 \frac{\tau_s^2 / (\tau_{DP}^R \tau_{DP}^D)}{\tau_s / \tau_{DP} + 1}. \quad (5.3.55)$$

Derivatives are trivial, but yield expressions too cumbersome to be conveniently written down. The results are thus plotted in Fig.5.1, and show the sensitivity of the spin thermopower to the various physical parameters in play. A modest modulation of the Rashba coupling constant could substantially modify S_s , either enhancing or decreasing it depending on the systems characteristics – we considered ratios α/β well within current experimental capabilities [117]. We will come back to this point in a moment.

Let us now consider our final example, a 2D hole gas as analyzed in Ref. [118]. The SOC interaction is cubic in momentum

$$H_{so} = \alpha_H \sigma_x [k_y (3k_x^2 - k_y^2)] + \alpha_H \sigma_y [k_x (3k_y^2 - k_x^2)], \quad (5.3.56)$$

and the spin Hall conductivity reads [118]

$$\sigma_H^{SHE} = -\frac{3\eta^2 (4\eta^2 - 1)}{(4\eta^2 + 1)^2} \frac{1}{\mu\tau} \sigma, \quad (5.3.57)$$

with $\eta = \alpha_H k_F^3 \tau$ ¹. Proceeding as before one gets

$$S_s = -e\mathcal{L}T \frac{\sigma'}{\sigma} \left[\frac{3(12\eta^2 - 1)}{(4\eta^2 + 1)(4\eta^2 - 1)} \right]. \quad (5.3.58)$$

All previous result can be cast in the simple form

$$S_s = SR_s, \quad (5.3.59)$$

¹The parameter η corresponds to what the authors of Ref. [118] call ζ .

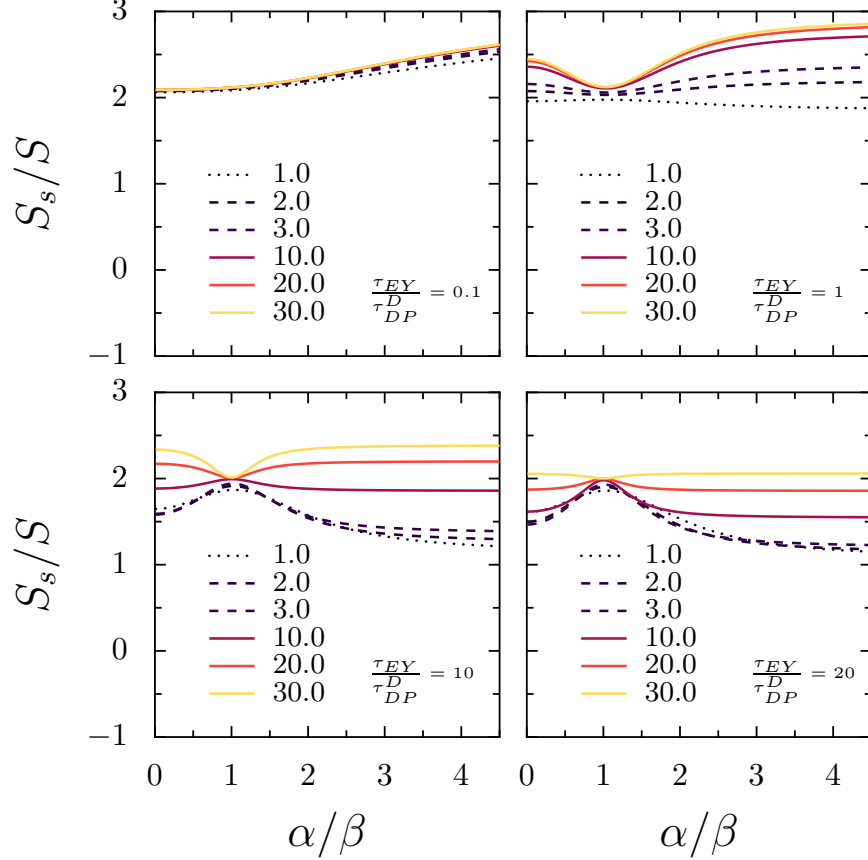


Figure 5.1: The spin thermopower S_s of a disordered 2D-electron gas with numerous competing SO mechanisms. Typical values for GaAs quantum wells are: mobility $\mu = 10^4 \text{cm}^2/\text{Vs}$, density $n = 10^{12} \text{cm}^{-2}$, effective extrinsic wavelength $\lambda_e = 4.7 \times 10^{-8} \text{cm}$, Dresselhaus coupling constant $\hbar\beta = 10^{-12} \text{eVm}$. There follows $\gamma_{ss} \gg \gamma_{intr}, \gamma_{sj}$, $\tau_{EY} \gg \tau_{DP}^D$. The Rashba coupling constant can be modulated by the gate potential [117]. Each panel shows the ratio S_s/S as a function of the ratio α/β for a given Elliot-Yafet scattering strength, strong to weak from top left to bottom right – panel 3 corresponds to standard GaAs. Magnetic scattering is strongest for the dotted curve, $\tau_{sf}/\tau_{DP}^D = 1$, and strong (weak) for the dashed (solid) curves, $\tau_{sf}/\tau_{DP}^D = 2, 3$ (10, 20, 30).

with R_s a number which depends on the various competing SOC mechanisms. Eq.(5.3.59) looks physically quite reasonable: in a metallic system in which electrons (or holes) are the sole carriers of charge, spin and heat, the heat-to-spin and heat-to-charge (particle) conversions are expected to be closely related. The examples considered show however that $R_s > 1$ could be easily achieved: in standard GaAs samples with Rashba and extrinsic SOC mechanisms one may estimate $R_{so} \sim 3$ [44], and the same value is obtained in a two-dimensional hole gas with purely cubic Rashba SOC in the diffusive regime ($\eta \ll 1$). If Dresselhaus SOC is also taken into account, similar values could be achieved, as shown in Fig.5.1. This suggests that metallic systems, typically characterized by low thermoelectric efficiencies, could be much more efficient in heat-to-spin conversion and therefore play a front role in spin caloritronics. Of course, whether substantially higher R_s values can be reached in different systems, e.g. in transition metals which already show a giant spin Hall response [119], or more exotic ones such as *p*-doped graphene [120] or topological insulators like HgTe [121], is an open and relevant question. Indeed, it would be interesting to establish whether it is always possible, within the regime in which the general expression (5.2.42) holds, to find such a simple connection between S_s and S . We therefore believe it desirable to experimentally test Eq.(5.3.59). This could be done rather straightforwardly in a setup like the one employed to first observe the spin Hall effect [122]: at low temperatures, the spin accumulation at the side edges of a two-dimensional Fermi gas could be optically measured first in response to a longitudinally applied bias, and then to a small temperature gradient along the same direction. All-electrical measurement schemes based

on H-bar geometries, exchanging again the applied bias with a temperature difference, would also be interesting though probably more delicate: in this case a temperature gradient along the side leg of the H-bar should be avoided or its effects compensated. Finally, it is well known that Mott's formula can be heavily affected by inelastic processes. Though the latter are beyond the scope of the present work, it would be interesting to study their effects on S_s and see whether any similarities between electric and spin thermopower exist also in their presence or not.

Chapter 6

Conclusions

Understanding spin-charge coupled dynamics in metal and semiconductor systems is of paramount importance to one of the main goals of spintronics: the manipulation of the spin degrees of freedom of carriers by purely electrical means. Within this context spin-orbit coupling gives rise to several interesting transport phenomena standing out for their technological importance, the spin Hall and the Edelstein effects.

To this end, in Chapter 4, we have developed a simple model for describing spin transport effects and spin-charge conversion in heterostructures consisting of a metallic film sandwiched between two different insulators. All the effects we have considered depend crucially on the three-dimensional nature of the system – in particular, the fact that the transverse wave functions depend on the in-plane momentum – and on the lack of inversion symmetry caused by the different properties of the top and bottom metal-insulator interfaces, each characterized by a different barrier height (gap) and spin-orbit coupling strength. After a careful consideration of vertex corrections we find

that the model supports a non-zero intrinsic SHC, in sharp contrast to the 2DEG Rashba case. Strikingly, in a “quasi-symmetric” junction the SHC reaches a maximal and universal value. We have also calculated the Edelstein effect for the same model and found that the induced spin polarization is the sum of two different contributions. The first one is analogous to the term found in the 2DEG Rashba case, whereas the second “anomalous” one has a completely different nature. Namely, it is inversely proportional to the scattering time, indicating that it is caused by the combined action of multiple electron-impurity scattering and spin-orbit coupling. We have also discussed the general connection between the non-vanishing SHC and the anomalous term in the EC. Furthermore, by Onsager’s reciprocity relations, our results are immediately relevant to the inverse Edelstein effect [123–125], in which a non-equilibrium spin density induces a charge current. Technical applications of this idea could lead to a new class of spin-orbit-coupling-based devices.

Thermoelectric studies are crucial if we are interested in describing all the transport properties of any physical system. In the same way, knowing the coupling between the energy and the spin will be crucial if we want to describe the transport properties of any spintronic device.

In Chapter 5 we have studied coupled spin and thermal transport in a disordered and spin-orbit coupled Fermi gas, calculating a general derivation of the spin Nernst effect. We have shown the existence of a general expression for the spin thermopower S_s with the same structure and an identical range of validity of Mott’s formula for the electric thermopower S . Finally, we have derived a simple and physically transparent relation connecting the two

quantities which suggests that metallic systems could be much more efficient in heat-to-spin than in heat-to-charge conversion.

There are a lot of open questions in the field of spintronics. Here we propose several topics that we would like to develop in the near future, some of which were mentioned at various points through the previous Chapters.

1. In Chapter 4 we have demonstrated the relation between the spin Hall and Edelstein conductivities in the insulator-metal-insulator junction. A general derivation of this relation in not-strictly two-dimensional Rashba coupled systems has not been done yet.
2. Inter-band effects are crucial when inversion symmetry is present. A complete description of inter-band effects in the insulator-metal-insulator junction will help us to understand how spin Hall effect arises in inversion symmetry materials. A lot of work has been done in centro-symmetric materials, mostly on Platinum [47], but some questions are still open
3. The results presented in Chapter 4 do not include the effects of extrinsic SOC. Which role do extrinsic SOC plays in this not-strictly two-dimensional Rashba coupled systems is still an open question.
4. The results presented in Chapters 4 and 5 correspond to theoretical models. Experiments which test these models are of central importance.
5. We have presented the spin Nernst effect in a two-dimensional Fermi gas with different spin-orbit coupling. The extension of this calculation to other systems with spin-orbit coupling, such as the insulator-metal-insulator junction presented in Chapter 4 or centro-symmetric materials

as Platinum, could present higher values of R_s .

6. A complete description of the effects of interactions, phonons and magnons in electrical and thermal spin transport effects has not been done at the moment.

The first two points have been the subject of recent work, which is, however, still in progress.

Appendix A

Effective Hamiltonians

Some details about the derivation of the effective Hamiltonians in Section 2.2 of Chapter 2 are discussed here. For an exhaustive and complete description of the problem we refer to the literature references given in the text.

A.1 The k.p method

First of all we will describe the eigenfunctions of Eq.(2.2.11) ket notation

$$\langle \mathbf{x} | \psi_{\nu \mathbf{k}} \rangle = \psi_{\nu \mathbf{k}}(\mathbf{x})$$

$$|\psi_{\nu \mathbf{k}}\rangle = \sum_{\nu'} e^{i\mathbf{k}\cdot\mathbf{x}} c_{\nu\nu'\mathbf{k}} |u_{\nu'0}\rangle \quad (\text{A.1.1})$$

Substituting this in the Schrödinger equation and projecting over the states $\langle u_{\nu 0} |$ we obtain

$$\begin{aligned} \langle u_{\nu 0} | \left[\left(\frac{p^2}{2m} + U + \frac{1}{4m_0^2} \boldsymbol{\sigma} \times \nabla U \cdot \mathbf{p} \right) + \frac{\mathbf{k}}{m_0} \cdot \left(\mathbf{p} + \frac{1}{4m_0} \boldsymbol{\sigma} \times \nabla V \right) \right. \\ \left. - \left(\epsilon_{\nu \mathbf{k}} - \frac{k^2}{2m_0} \right) \right] | \psi_{\nu \mathbf{k}}(\mathbf{r}) \rangle = \\ e^{i\mathbf{k}\cdot\mathbf{x}} \sum_{\nu'} \langle u_{\nu 0} | \left[\epsilon_{\nu 0} + \frac{\mathbf{k}}{m_0} \cdot \left(\mathbf{p} + \frac{1}{4m_0} \boldsymbol{\sigma} \times \nabla U \right) + \right. \\ \left. - \left(\epsilon_{\nu \mathbf{k}} - \frac{k^2}{2m_0} \right) \right] | u_{\nu' 0} \rangle c_{\nu \nu' \mathbf{k}} = \\ e^{i\mathbf{k}\cdot\mathbf{x}} \sum_{\nu'} \left[\left(\epsilon_{\nu 0} - \epsilon_{\nu \mathbf{k}} + \frac{k^2}{2m_0} \right) \delta_{\nu \nu'} + \frac{1}{m_0} \mathbf{k} \cdot \boldsymbol{\pi}_{\nu \nu'} \right] c_{\nu \nu' \mathbf{k}} = 0, \end{aligned}$$

as we know

$$\left[\frac{(-i\nabla)^2}{2m_0} + U + \frac{1}{4m_0^2} \nabla U \times (-i\nabla) \cdot \boldsymbol{\sigma} \right] | u_{\nu 0} \rangle = \epsilon_{\nu 0} | u_{\nu 0} \rangle, \quad (\text{A.1.2})$$

that is

$$\left[\frac{p^2}{2m_0} + U + \frac{1}{4m_0^2} \nabla U \times \mathbf{p} \cdot \boldsymbol{\sigma} \right] | u_{\nu 0} \rangle = \epsilon_{\nu 0} | u_{\nu 0} \rangle, \quad (\text{A.1.3})$$

and

$$\boldsymbol{\pi}_{\nu \nu'} = \langle u_{\nu 0} | \mathbf{p} + \frac{1}{4m_0^2} \nabla U \times \boldsymbol{\sigma} | u_{\nu' 0} \rangle. \quad (\text{A.1.4})$$

We intend each matrix element as an integral over the unit cell

$$\langle u_{\nu 0} | \hat{O} | u_{\nu' 0} \rangle = \int_{\text{cell}} d\mathbf{x} u_{\nu 0}^*(\mathbf{x}) O u_{\nu' 0}(\mathbf{x}), \quad (\text{A.1.5})$$

with \hat{O} a given hermitian operator and $\epsilon_{\nu 0}$ is the energy offset of the ν -th band at $\mathbf{k} = 0$. It is important to notice that Eq.(A.1.5) is valid when \hat{O} depends on position or momentum only and things get simplified.

We can easily see that \mathbf{p} represents the atomic momentum associated with the rapid oscillations of the lattice function $u_{\nu 0}$, whereas \mathbf{k} represents

the slow crystal momentum of the electrons at the bottom of the band. These allow us to approximate

$$\boldsymbol{\pi}_{\nu\nu'} \approx \langle u_{\nu 0} | \mathbf{p} | u_{\nu' 0} \rangle \quad (\text{A.1.6})$$

For this reason we will neglect terms like

$$\frac{1}{4m_0^2} \mathbf{k} \cdot \nabla U \times \boldsymbol{\sigma} \sim kp \quad (\text{A.1.7})$$

as compared to the diagonal one

$$\frac{1}{4m_0^2} \mathbf{p} \cdot \nabla U \times \boldsymbol{\sigma} \sim p^2 \quad (\text{A.1.8})$$

For the same reason in the presence of a non-crystalline potential $V(x)$ only the diagonal terms as the one of Eq.(A.1.8) will be taken into account.

A.2 Symmetries and the Kane model

The form of the Kane Hamiltonians are determined by the symmetries of the system . We will find some linear combinations \tilde{u}_i of the different $u_{\nu 0}$ as a basis so that these new basis share some particular symmetries with the Hamiltonian H , for example the total angular momentum $\mathbf{J} = \mathbf{L} + \mathbf{S}$ This \tilde{u}_i transforms according to a irreducible representation of the symmetry group of H , Γ_i .

If we chose as a basis $|J, m_j\rangle$ as our basis (see table A.1) the 8×8 Kane Hamiltonian reads

$$H_{8 \times 8} = \begin{pmatrix} H_{c,2 \times 2} & H_{cv,2 \times 6} \\ H_{cv,6 \times 2}^\dagger & H_{v,6 \times 6} \end{pmatrix} \quad (\text{A.2.9})$$

with

\tilde{u}_i	Γ	$ J, m_J\rangle$	u_{J, m_J}
\tilde{u}_1	Γ_6	$ \frac{1}{2}, +\frac{1}{2}\rangle$	$i S\rangle +\frac{1}{2}\rangle$
\tilde{u}_2	Γ_6	$ \frac{1}{2}, -\frac{1}{2}\rangle$	$i S\rangle -\frac{1}{2}\rangle$
\tilde{u}_3	Γ_8	$ \frac{3}{2}, +\frac{3}{2}\rangle$	$-\frac{1}{\sqrt{2}}(X\rangle + i Y\rangle) +\frac{1}{2}\rangle$
\tilde{u}_4	Γ_8	$ \frac{3}{2}, +\frac{1}{2}\rangle$	$-\frac{1}{\sqrt{6}}(X\rangle + i Y\rangle) -\frac{1}{2}\rangle + \sqrt{\frac{2}{3}} Z\rangle +\frac{1}{2}\rangle$
\tilde{u}_5	Γ_8	$ \frac{3}{2}, -\frac{1}{2}\rangle$	$+\frac{1}{\sqrt{6}}(X\rangle - i Y\rangle) +\frac{1}{2}\rangle + \sqrt{\frac{2}{3}} Z\rangle -\frac{1}{2}\rangle$
\tilde{u}_6	Γ_8	$ \frac{3}{2}, -\frac{3}{2}\rangle$	$+\frac{1}{\sqrt{2}}(X\rangle - i Y\rangle) -\frac{1}{2}\rangle$
\tilde{u}_7	Γ_7	$ \frac{1}{2}, +\frac{1}{2}\rangle$	$-\frac{1}{\sqrt{3}}(X\rangle + i Y\rangle) -\frac{1}{2}\rangle - \frac{1}{\sqrt{3}} Z\rangle +\frac{1}{2}\rangle$
\tilde{u}_8	Γ_7	$ \frac{1}{2}, -\frac{1}{2}\rangle$	$-\frac{1}{\sqrt{3}}(X\rangle - i Y\rangle) +\frac{1}{2}\rangle + \frac{1}{\sqrt{3}} Z\rangle -\frac{1}{2}\rangle$

Table A.1: Basis of the 8×8 Kane model. $|S\rangle$ denotes the s -like orbital and $|X\rangle, |Y\rangle, |Z\rangle$ the three p -like ones. $|\pm\frac{1}{2}\rangle$ is the spinor corresponding the spin up/down along the axis of quantization. Γ is the irreducible representation of the symmetry group of the zincblende crystal according to which each basis function transforms.

$$\begin{aligned}
H_{c,2 \times 2} &= \begin{pmatrix} V & 0 \\ 0 & V \end{pmatrix}, \\
H_{cv,2 \times 6} &= \begin{pmatrix} \frac{-1}{\sqrt{2}}Pk_+ & \sqrt{\frac{2}{3}}Pk_z & \frac{1}{\sqrt{6}}Pk_- & 0 & \frac{-1}{\sqrt{3}}Pk_z & \frac{-1}{\sqrt{2}}Pk_- \\ 0 & \frac{-1}{\sqrt{6}}Pk_+ & \sqrt{\frac{2}{3}}Pk_z & \frac{1}{\sqrt{2}}Pk_- & \frac{-1}{\sqrt{3}}Pk_+ & \frac{1}{\sqrt{3}}Pk_z \end{pmatrix}, \\
H_{v,6 \times 6} &= \begin{pmatrix} [V - E_g]\hat{I}_{4 \times 4} & \hat{O}_{4 \times 2} \\ \hat{O}_{2 \times 4} & [V - E_g - \Delta]\hat{I}_{2 \times 2} \end{pmatrix},
\end{aligned}$$

where

$$P = -i\frac{1}{m_0}\langle S|p_x|X\rangle = i\frac{1}{m_0}\langle S|p_y|Y\rangle = i\frac{1}{m_0}\langle S|p_z|Z\rangle, \quad (\text{A.2.10})$$

$$\begin{aligned} \Delta &= \frac{3}{4m_0^2}\langle X|\partial_y U\partial_x - \partial_x U\partial_y|Y\rangle \\ &= \frac{3}{4m_0^2} \times \langle \text{any cyclic permutations} \rangle \end{aligned} \quad (\text{A.2.11})$$

with $k_{\pm} = k_x \pm ik_y$, and taking the zero energy at the conduction band minimum, $\epsilon_{c0} = 0$. We should remember that U is the crystal potential and V the external one. With these matrixes we obtain the parameters shown in Chapter 2.

Appendix B

Integral of the Green functions

Some details about the integrals of the Green functions which appear in Chapters 3 and 4 will be explained here.

B.1 The intra-band integrals

Here we will explain how to calculate the different integrals concerning the Green functions within the same n-band

$$\begin{aligned}
 \sum_{\mathbf{k}} G_{n\mathbf{k}s}^R G_{n\mathbf{k}s}^A f(\mathbf{k}) &= N_0 \int \frac{d\xi}{-\xi - \epsilon_{n\mathbf{k}s} + \frac{i}{2\tau}} \frac{f(k)}{-\xi - \epsilon_{n\mathbf{k}s} - \frac{i}{2\tau}} \\
 &= N_0 \int \frac{d\rho}{-\rho + \frac{i}{2\tau} - \rho - \frac{i}{2\tau}} \frac{1}{1 + \nabla_{\xi} \epsilon_{n\mathbf{k}s}} \frac{f(k)}{1 + \nabla_{\xi} \epsilon_{n\mathbf{k}s}} = 2\pi N_{ns} \tau f(k_{Fns}),
 \end{aligned}
 \tag{B.1.1}$$

where $f(\mathbf{k})$ is assumed to be regular, N_{ns} is the density of states in the n -subband, k_{Fns} is the corresponding momentum, $\rho = \xi + \epsilon_{n\mathbf{k}s}$, and we have made the substitution $\sum_{\mathbf{k}}(\dots) \rightarrow N_0 \int_{-\infty}^{+\infty} d\xi(\dots)$, with $\xi = k^2/2m - \mu$ as we

did in Chapter 3. The densities of states at the Fermi level in each subband N_{ns} are evaluated from the formula

$$\frac{N_{ns}}{N_0} = \frac{k_{ns}}{|\nabla_k E_{nks}|_{k_{ns}}}, \quad (\text{B.1.2})$$

where k_{ns} is the solution of the equation $E_{nks} = E_F$.

The following integral also appears in Chapters 3 and 4

$$\begin{aligned} \sum_{\mathbf{k}} G_{n\mathbf{k}-}^R G_{n\mathbf{k}+}^A f(\mathbf{k}) &= N_0 \int \frac{d\xi}{-\xi - \epsilon_{nk-} + \frac{i}{2\tau}} \frac{f(k)}{-\xi - \epsilon_{nk+} - \frac{i}{2\tau}} \\ &\simeq N_0 \frac{2\pi N_0 \tau}{1 - i2\tau \Delta E_{nk_{F_n}}} f(k_{F_n}), \end{aligned} \quad (\text{B.1.3})$$

where $\Delta E_{nk_{F_n}} = (\epsilon_{nk+} - \epsilon_{nk-})/2 = E_0 n^2 (e_1 k_{F_n} + e_3 k_{F_n}^3)$, defined in Chapter 4.

The wave vectors k_{F_n+} and k_{F_n-} are determined by the equations

$$\begin{aligned} k_{F_n+}^2 + k_{F_n-}^2 &= 2k_F^2 \\ E_{nk_{F_n++}} &= E_{nk_{F_n--}} \end{aligned} \quad (\text{B.1.4})$$

with E_{nks} defined in Eqs.(4.1.7) and (4.1.10). Solving Eqs.(B.1.2), (B.1.2), (B.1.2), N_{ns} and $k_{F_{ns}}$ read

$$\begin{aligned} k_{F_{ns}} &= k_{F_n} + E_0 n^2 \left(s \frac{e_1}{2} - \frac{e_1^2}{8k_{F_n}} - s \left(\frac{e_1 e_2}{2} - \frac{e_3 k_{F_n}^2}{2} \right) \right) \\ N_{ns} &= N_0 \left(1 + E_0 n^2 \left(s \frac{e_1}{2k_{F_n}} - e_2 + s \left(\frac{e_1 e_2}{k_{F_n}} - \frac{3e_3 k_{F_n}}{2} - \frac{e_1^3}{16k_{F_n}^3} \right) \right) \right). \end{aligned} \quad (\text{B.1.5})$$

Hence, for instance,

$$\sum_{\mathbf{k}s} s G_{n\mathbf{k}s}^R G_{n\mathbf{k}s}^A k = 2\pi\tau \sum_s s k_{F_{ns}} N_{ns} = 4\pi N_0 \tau E_0 n^2 (e_1 + 2e_3 k_{F_n}^2). \quad (\text{B.1.6})$$

If we are dealing with the simple Rashba case the procedure is totally equivalent but we will not have the n -dependence in our integrals, and $E_0 e_1 \rightarrow -\alpha$ and $e_3 \rightarrow 0$.

B.2 The inter-band integrals

In the case of dealing with inter-band problems ($n = n'$), the new integrals have the following form

$$\sum_{\mathbf{k}} G_{n\mathbf{k}s}^R G_{n'\mathbf{k}s'}^A f(\mathbf{k}) = N_0 \int \frac{d\xi}{-\xi - \epsilon_{n\mathbf{k}s} + \frac{i}{2\tau}} \frac{f(k)}{-\xi - \epsilon_{n'\mathbf{k}s'} - \frac{i}{2\tau}}$$

$$\simeq N_0 \frac{2\pi N_0 \tau}{1 - i2\tau E_G} f(k_{F_n}), \quad (\text{B.2.7})$$

$$(\text{B.2.8})$$

which has the same form as Eq.(B.2.8), sending $\Delta E_{nk_{F_n}} \rightarrow E_G$, with $E_G = E_{n'\mathbf{k}s'} - E_{n\mathbf{k}s} \simeq (n'^2 - n^2)E_0$. As we can see the spin-dependence in this integrals is negligible.

Appendix C

Kinetic equations: a quasiclassical approach

Transport problems are treated classically via the Boltzmann equation. The Keldysh formalism [126], allows us to treat this problems at a quantum level [127]. When we are dealing with spin-based systems, $SU(2)$ becomes the symmetry group [13, 27, 43, 83, 107]. Here we will recall the kinetic equations for spin transport phenomena.

C.1 The $SU(2)$ formalism

The relation between the Edelstein and the spin Hall conductivities was cited in Chapters 3 and 4, specially in Eqs.(3.3.71),(4.5.65). Here we will briefly recall the quasiclassical approach in the $SU(2)$ formalism and derive this relation.

Let us start with the Hamiltonian,

$$H = \frac{k^2}{2m} + \mathbf{b} \cdot \boldsymbol{\sigma}, \quad (\text{C.1.1})$$

where \mathbf{b} is the internal magnetic field due to spin-orbit coupling, in the case of the 2DEG Rashba SOC model $\mathbf{b} = \alpha \mathbf{k} \times \mathbf{e}_z$. The Dyson equation reads

$$-i [G_0^{-1}(1, 1') \otimes \check{G}(1', 2)] = -i [\check{\Sigma}(1, 1') \otimes \check{G}(1', 2)], \quad (\text{C.1.2})$$

where the symbol \otimes indicates convolution/matrix multiplication over the internal variables, and $\check{G}, \check{\Sigma}$ are Keldysh 2×2 matrices

$$\check{G} = \begin{pmatrix} G^R & G^K \\ 0 & G^A \end{pmatrix} \quad \check{\Sigma} = \begin{pmatrix} \Sigma^R & \Sigma^K \\ 0 & \Sigma^A \end{pmatrix}, \quad (\text{C.1.3})$$

with $\check{\Sigma}$ is the self-energy matrix in the Born approximation and

$$G_0^{-1}(1, 1') = (i\partial_t - H) \delta(1 - 1'). \quad (\text{C.1.4})$$

Now we perform a gradient expansion to the Dyson equation, Eq(C.1.2), so the equation of motion for the Green's function \check{G} reads

$$\partial_t \check{G} + \frac{1}{2} \left\{ \frac{\mathbf{k}}{m} + \frac{\partial}{\partial \mathbf{k}} (\mathbf{b} \cdot \boldsymbol{\sigma}), \frac{\partial}{\partial \mathbf{x}} \check{G} \right\} + i [\mathbf{b} \cdot \boldsymbol{\sigma}, \check{G}] = -i [\check{\Sigma}, \check{G}]. \quad (\text{C.1.5})$$

Now we will define the Eilenberger Green function as

$$\check{g} = \frac{i}{\pi} \int d\xi \check{G}, \quad \xi = k^2/2m - \mu \quad (\text{C.1.6})$$

If we integrate Eq.(C.1.5) respect to ξ , retaining terms to first order in $|\mathbf{b}|/\epsilon_F$, where ϵ_F is the well know Fermi energy, we obtain

$$\sum_{s=\pm} \left(\partial_t \check{g}_s + \frac{1}{2} \left\{ \frac{\mathbf{k}_s}{m} + \frac{\partial}{\partial \mathbf{k}} (\mathbf{b}_s \cdot \boldsymbol{\sigma}), \frac{\partial}{\partial \mathbf{x}} \check{g}_s + i [\mathbf{b}_s \cdot \boldsymbol{\sigma}, \check{g}_s] \right\} \right) = -i [\check{\Sigma}, \check{g}]. \quad (\text{C.1.7})$$

The retarded component g^R (and similarly the advanced one g^A) is written as a sum of the contributions associated to the two spin-split Fermi surfaces $g_{\pm}^R = (1 \mp \partial_{\xi} b) \left(\frac{1}{2} \pm \frac{1}{2} \hat{\mathbf{b}} \cdot \boldsymbol{\sigma} \right)$. The electrical field is normally included in the quasiclassical equations of motion by substituting $\partial_{\mathbf{x}} \rightarrow \partial_{\mathbf{x}} - |e| \mathbf{E} \partial_{\epsilon}$. In the absence of the field the equilibrium Keldysh component is $g^K = 2 \tanh\left(\frac{\xi}{2T}\right) g^R$. By representing the matrices in the eigenstates basis [37], the Keldysh component of Eq.(C.1.7) reads

$$\begin{aligned} \hat{k}_x E \left(v_F + \sigma_z \frac{k_+ N_+ - k_- N_-}{2N_0 m} \right) + (\sigma_z \hat{k}_x - \sigma_y \hat{k}_y) \alpha E \\ + i\alpha k [\sigma_z, \tilde{g}] = -\frac{1}{\tau} (\tilde{g} - \langle \tilde{g} \rangle), \end{aligned} \quad (\text{C.1.8})$$

where \tilde{g} has still a structure in spin space $\tilde{g} = \tilde{g}_0 \sigma_0 + \sum_i \tilde{g}_i \sigma_i$ and the original and physical Keldysh g -components can be written as a function of the new ones

$$\begin{aligned} g_0 &= \tilde{g}_0 \\ g_x &= \hat{k}_y \tilde{g}_z + \hat{k}_x \tilde{g}_y \\ g_y &= -\hat{k}_x \tilde{g}_z + \hat{k}_y \tilde{g}_y \\ g_z &= -\tilde{g}_x. \end{aligned} \quad (\text{C.1.9})$$

In this basis the spin current, j_y^z , and the spin polarization, s^y , are expressed as

$$j_y^z = -\frac{N_0}{4} \int d\epsilon \langle v_y g_z \rangle = \frac{N_0}{4} \int d\epsilon \langle v_y \tilde{g}_x \rangle \quad (\text{C.1.10})$$

$$s^y = -\frac{N_0}{4} \int d\epsilon \langle g_y \rangle = -\frac{N_0}{4} \int d\epsilon (\langle \hat{k}_y \tilde{g}_y \rangle - \langle \hat{k}_x \tilde{g}_z \rangle). \quad (\text{C.1.11})$$

After projecting Eq.(C.1.8) on the Pauli matrix components and solving the

equations one finds

$$\langle \hat{k}_y \tilde{g}_x \rangle = -\frac{E}{4b_0} \left(2\alpha + \frac{k_+ N_+ - k_- N_-}{2N_0 m} \right) \quad (\text{C.1.12})$$

$$\langle \hat{k}_y \tilde{g}_y \rangle = \frac{1}{2b_0 \tau} \langle \hat{k}_y \tilde{g}_x \rangle \quad (\text{C.1.13})$$

$$\begin{aligned} \langle \hat{k}_x \tilde{g}_z \rangle &= -E\tau \left(\alpha + \frac{k_+ N_+ - k_- N_-}{2N_0 m} \right) \\ &\quad - \frac{1}{2b_0 \tau} \langle \hat{k}_y \tilde{g}_x \rangle. \end{aligned} \quad (\text{C.1.14})$$

At this point it is easy to see how Eqs.(3.3.71),(4.5.65) appear, just substituting the results of Eqs.(C.1.12-C.1.14) in Eq.(C.1.11)

Bibliography

- [1] S. A. Wolf, D. D. Awschalom, R. A. Buhrman, J. M. Daughton, S. Von Molnár, M. L. Roukers, A. Y. Chtchelkanova, and D. M. Treger, “Spintronics: A spin-based electronics vision for the future,” *Science*, vol. 294, p. 1488, 2001.
- [2] I. Žutić, J. Fabian, and S. Das Sarma, “Spintronics: Fundamentals and applications,” *Rev. Mod. Phys.*, vol. 76, p. 323, 2004.
- [3] D. D. Awschalom and M. E. Flatté, “Challenges for semiconductor spintronics,” *Nature Physics*, vol. 3, p. 153, 2007.
- [4] G. A. Prinz, “Magnetoelectronics,” *Science*, vol. 282, p. 1660, 1998.
- [5] M. N. Baibich, J. M. Broto, A. Fert, F. N. Van Dau, F. Petroff, P. Etienne, G. Creuzet, A. Friederich, and J. Chazelas, “Giant magnetoresistance of (001)fe/(001)cr magnetic superlattices,” *Phys. Rev. Lett.*, vol. 61, p. 2472, 1988.
- [6] G. Binasch, P. Grünberg, F. Saurenbach, and W. Zinn, “Enhanced magnetoresistance in layered magnetic structures with antiferromagnetic interlayer exchange,” *Phys. Rev. B*, vol. 39, p. 4828, 1989.

-
- [7] S. S. P. Parkin, C. Kaiser, A. Panchula, P. M. Rice, B. Hughes, M. Samant, and S. H. Yang, “Giant tunnelling magnetoresistance at room temperature with mgo (100) tunnel barriers,” *Nat. Mat.*, vol. 3, p. 862, 2004.
- [8] J. E. Hirsch, “Spin hall effect,” *Phys. Rev. Lett.*, vol. 83, p. 1834, 1999.
- [9] S. Zhang, “Spin hall effect in the presence of spin diffusion,” *Phys. Rev. Lett.*, vol. 85, p. 393, 2000.
- [10] S. Murakami, N. Nagaosa, and S.-C. Zhang, “Dissipationless quantum spin current at room temperature,” *Science*, vol. 301, p. 1348, 2003.
- [11] J. Sinova, D. Culcer, Q. Niu, N. A. Sinitsyn, T. Jungwirth, and A. H. MacDonald, “Universal intrinsic spin hall effect,” *Phys. Rev. Lett.*, vol. 92, p. 126603, 2004.
- [12] H.-A. Engel, E. I. Rashba, and B. I. Halperin in *Handbook of Magnetism and Advanced Magnetic Materials* (H. Kronmüller and S. Parkin, eds.), vol. V, pp. 2858–2877, Chichester, UK: Wiley, 2007.
- [13] R. Raimondi, C. Gorini, P. Schwab, and M. Dzierzawa, “Quasiclassical approach to the spin hall effect in the two-dimensional electron gas,” *Phys. Rev. B*, vol. 74, p. 035340, 2006.
- [14] D. Culcer and R. Winkler, “Steady states of spin distributions in the presence of spin-orbit interactions,” *Phys. Rev. B*, vol. 76, p. 245322, 2007.

-
- [15] D. Culcer and R. Winkler, "Generation of spin currents and spin densities in systems with reduced symmetry," *Phys. Rev. Lett.*, vol. 99, p. 226601, 2007.
- [16] D. Culcer, E. M. Hankiewicz, G. Vignale, and R. Winkler, "Side jumps in the spin hall effect: Construction of the boltzmann collision integral," *Phys. Rev. B*, vol. 81, p. 125332, 2010.
- [17] W.-K. Tse, J. Fabian, I. Žutić, and S. Das Sarma, "Spin accumulation in the extrinsic spin hall effect," *Phys. Rev. B*, vol. 72, p. 241303, 2005.
- [18] V. M. Galitski, A. A. Burkov, and S. Das Sarma, "Boundary conditions for spin diffusion in disordered systems," *Phys. Rev. B*, vol. 74, p. 115331, 2006.
- [19] T. Tanaka and H. Kontani, "Giant extrinsic spin hall effect due to rare-earth impurities," *New Journal of Physics*, vol. 11, p. 013023, 2009.
- [20] E. M. Hankiewicz and G. Vignale, "Spin-hall effect and spin-coulomb drag in doped semiconductors," *J. Phys. Cond. Matt.*, vol. 21, p. 235202, 2009.
- [21] G. Vignale, "Ten years of spin hall effect," *J. Supercond. Nov. Magn.*, vol. 23, p. 3, 2010.
- [22] Y. K. Kato, R. C. Myers, A. C. Gossard, and D. D. Awschalom, "Observation of the spin hall effect in semiconductors," *Science*, vol. 306, p. 1910, 2004.

- [23] V. Sih, R. C. Myers, Y. K. Kato, W. H. Lau, A. C. Gossard, and D. D. Awschalom, “Spatial imaging of the spin hall effect and current-induced polarization in two-dimensional electron gases,” *Nature Physics*, vol. 1, p. 31, 2005.
- [24] J. Wunderlich, B. Kaestner, J. Sinova, and T. Jungwirth, “Experimental observation of the spin-hall effect in a two-dimensional spin-orbit coupled semiconductor system,” *Phys. Rev. Lett.*, vol. 94, p. 047204, 2005.
- [25] N. P. Stern, S. Ghosh, G. Xiang, M. Zhu, N. Samarth, and D. D. Awschalom, “Current-induced polarization and the spin hall effect at room temperature,” *Phys. Rev. Lett.*, vol. 97, p. 126603, 2006.
- [26] N. P. Stern, D. W. Steuerman, S. Mack, A. C. Gossard, and D. D. Awschalom, “Time-resolved dynamics of the spin hall effect,” *Nature Physics*, vol. 4, p. 843, 2008.
- [27] C. Gorini, *Quasiclassical methods for spin-charge coupled dynamics in low-dimensional systems*. PhD thesis, Augsburg University, Augsburg, 2009.
- [28] M. I. Dyakonov and V. I. Perel, “Current-induced spin orientation of electrons in semiconductors,” *Phys. Lett. A*, vol. 35, p. 459, 1971.
- [29] N. F. Mott and H. S. W. Massey, *The Theory of Atomic Collisions*. Oxford University Press, 1964.

- [30] Y. A. Bychkov and E. I. Rashba, "Side jump contribution to spin-orbit mediated hall effects and berry curvature," *J. Phys. C*, vol. 17, p. 6039, 1984.
- [31] R. Raimondi and P. Schwab, "Spin-hall effect in a disordered two-dimensional electron system," *Phys. Rev. B*, vol. 71, p. 033311, 2005.
- [32] E. G. Mishchenko, A. V. Shytov, and B. I. Halperin, "Spin current and polarization in impure two-dimensional electron systems with spin-orbit coupling," *Phys. Rev. Lett.*, vol. 93, p. 226602, 2004.
- [33] A. Khaetskii, "Nonexistence of intrinsic spin currents," *Phys. Rev. Lett.*, vol. 96, p. 056602, 2006.
- [34] E. M. Hankiewicz and G. Vignale, "Coulomb corrections to the extrinsic spin-hall effect of a two-dimensional electron gas," *Phys. Rev. B*, vol. 73, p. 115339, 2006.
- [35] E. M. Hankiewicz, G. Vignale, and M. E. Flatté, "Spin-hall effect in a [110] gaas quantum well," *Phys. Rev. Lett.*, vol. 97, p. 266601, 2006.
- [36] T. Kimura, Y. Otani, T. Sato, S. Takahashi, and S. Maekawa, "Room-temperature reversible spin hall effect," *Phys. Rev. Lett.*, vol. 98, p. 156601, 2007.
- [37] C. Gorini, P. Schwab, M. Dzierzawa, and R. Raimondi, "Spin polarizations and spin hall currents in a two-dimensional electron gas with magnetic impurities," *Phys. Rev. B*, vol. 78, p. 125327, 2008.

- [38] W.-K. Tse and S. Das Sarma, “Intrinsic spin hall effect in the presence of extrinsic spin-orbit scattering,” *Phys. Rev. B*, vol. 74, p. 245309, 2006.
- [39] L. X. Hayden, R. Raimondi, M. E. Flatté, and G. Vignale, “Intrinsic spin hall effect at asymmetric oxide interfaces: Role of transverse wave functions,” *Phys. Rev. B*, vol. 88, p. 075405, 2013.
- [40] Y. Niimi, M. Morota, D. H. Wei, C. Deranlot, M. Basletic, A. Hamzic, A. Fert, and Y. Otani, “Extrinsic spin hall effect induced by iridium impurities in copper,” *Phys. Rev. Lett.*, vol. 106, p. 126601, 2011.
- [41] M. Gradhand, D. V. Fedorov, P. Zahn, and I. Mertig, “Extrinsic spin hall effect from first principles,” *Phys. Rev. Lett.*, vol. 104, p. 186403, 2010.
- [42] J. L. Cheng and M. W. Wu, “Kinetic investigation of the extrinsic spin hall effect induced by skew scattering,” *Journal of Physics: Condensed Matter*, vol. 20, p. 085209, 2008.
- [43] R. Raimondi, P. Schwab, C. Gorini, and G. Vignale, “Spin-orbit interaction in a two-dimensional electron gas: a $su(2)$ formulation,” *Ann. Phys. (Berlin)*, vol. 524, p. 153, 2012.
- [44] R. Raimondi and P. Schwab, “Tuning the spin hall effect in a two-dimensional electron gas,” *Europhys. Lett.*, vol. 87, p. 37008, 2009.
- [45] S. Valenzuela and M. Tinkham, “Direct electronic measurement of the spin hall effect,” *Nature*, vol. 442, p. 176, 2006.

- [46] S. O. Valenzuela and M. Tinkham, "Electrical detection of spin currents: The spin-current induced hall effect (invited)," *Journal of Applied Physics*, vol. 101, no. 9, 2007.
- [47] L. Vila, T. Kimura, and Y. Otani, "Evolution of the spin hall effect in pt nanowires: Size and temperature effects," *Phys. Rev. Lett.*, vol. 99, p. 226604, 2007.
- [48] T. Seki, Y. Hasegawa, S. Mitani, S. Takahashi, H. Imamura, S. Maekawa, J. Nitta, and K. Takanashi, "Giant spin hall effect in perpendicularly spin-polarized fept/au devices," *Nat Mater*, vol. 7, p. 125, 2008.
- [49] T. Tanaka, H. Kontani, M. Naito, T. Naito, D. S. Hirashima, K. Yamada, and J. Inoue, "Intrinsic spin hall effect and orbital hall effect in 4d and 5d transition metals," *Phys. Rev. B*, vol. 77, p. 165117, 2008.
- [50] K. Nomura, J. Wunderlich, J. Sinova, B. Kaestner, A. H. MacDonald, and T. Jungwirth, "Edge-spin accumulation in semiconductor two-dimensional hole gases," *Phys. Rev. B*, vol. 72, p. 245330, 2005.
- [51] Y. Lyanda-Geller and A. Aronov, "Nuclear electric resonance and orientation of carrier spins by an electric field," *JETP Lett.*, vol. 50, p. 431, 1989.
- [52] V. Edelstein, "Spin polarization of conduction electrons induced by electric current in two-dimensional asymmetric electron systems," *Solid State Communications*, vol. 73, no. 3, p. 233, 1990.

- [53] I. Mihai Miron, G. Gaudin, S. Auffret, B. Rodmacq, A. Schuhl, S. Pizzini, J. Vogel, and P. Gambardella, “Current-driven spin torque induced by the rashba effect in a ferromagnetic metal layer,” *Nature Materials*, vol. 9, no. 3, p. 230, 2010.
- [54] J.-i. Inoue, G. E. W. Bauer, and L. W. Molenkamp, “Diffuse transport and spin accumulation in a rashba two-dimensional electron gas,” *Phys. Rev. B*, vol. 67, p. 033104, 2003.
- [55] C. L. Yang, H. T. He, L. Ding, L. J. Cui, Y. P. Zeng, J. N. Wang, and W. K. Ge, “Spectral dependence of spin photocurrent and current-induced spin polarization in an InGaAs/InAlAs two-dimensional electron gas,” *Phys. Rev. Lett.*, vol. 96, p. 186605, 2006.
- [56] H. J. Chang, T. W. Chen, J. W. Chen, W. C. Hong, W. C. Tsai, Y. F. Chen, and G. Y. Guo, “Current and strain-induced spin polarization in InGaN/GaN superlattices,” *Phys. Rev. Lett.*, vol. 98, p. 136403, 2007.
- [57] W. F. Koehl, M. H. Wong, C. Poblenz, B. Swenson, U. K. Mishra, J. S. Speck, and D. D. Awschalom, “Current-induced spin polarization in gallium nitride,” *Appl. Phys. Lett.*, vol. 95, p. 072110, 2009.
- [58] S. Kuhlen, K. Schmalbuch, M. Hagedorn, P. Schlamme, M. Patt, M. Lepsa, G. Güntherodt, and B. Beschoten, “Electric field-driven coherent spin reorientation of optically generated electron spin packets in ingaas,” *Phys. Rev. Lett.*, vol. 109, p. 146603, 2012.
- [59] N. Ashcroft and N. Mermin, *Solid State Physics*. Philadelphia: Saunders College, 1976.

- [60] X. Wang, J. Xiao, A. Manchon, and S. Maekawa, “Spin-hall conductivity and electric polarization in metallic thin films,” *Phys. Rev. B*, vol. 87, p. 081407, 2013.
- [61] H. Adachi, K. ichi Uchida, E. Saitoh, and S. Maekawa, “Theory of the spin seebeck effect,” *Reports on Progress in Physics*, vol. 76, no. 3, p. 036501, 2013.
- [62] K. Uchida, S. Takahashi, K. Harii, J. Ieda, W. Koshibae, K. Ando, S. Maekawa, and E. Saitoh, “Observation of the spin seebeck effect,” *Nat. lett.*, vol. 455, p. 778, 2008.
- [63] K. Uchida, J. Xiao, H. Adachi, J. Ohe, S. Takahashi, J. Ieda, T. Ota, Y. Kajiwara, H. Umezawa, H. Kawai, G. E. W. Bauer, S. Maekawa, and E. Saitoh, “Spin seebeck insulator,” *Nat. Mat.*, vol. 9, p. 894, 2010.
- [64] K. Uchida, T. Ota, H. Adachi, J. Xiao, T. Nonaka, Y. Kajiwara, G. E. W. Bauer, S. Maekawa, and E. Saitoh, “Spin seebeck insulator,” *J. Appl. Phys.*, vol. 111, p. 103903, 2012.
- [65] C. M. Jaworski, J. Yang, S. Mack, D. D. Awschalom, R. C. Myers, and J. P. Heremans, “Observation of the spin-seebeck effect in a ferromagnetic semiconductor,” *Nat. Mat.*, vol. 9, p. 898, 2010.
- [66] C. M. Jaworski, J. Yang, S. Mack, D. D. Awschalom, R. C. Myers, and J. P. Heremans, “Spin-seebeck effect: A phonon driven spin distribution,” *Phys. Rev. Lett.*, vol. 106, p. 186601, 2011.
- [67] T. S. Nunner and F. von Oppen, “Quasilinear spin-voltage profiles in spin thermoelectrics,” *Phys. Rev. B*, vol. 84, p. 020405(R), 2011.

- [68] K. Tauber, M. Gradhand, D. V. Fedorov, and I. Mertig, “Extrinsic spin nernst effect from first principles,” *Phys. Rev. Lett.*, vol. 109, p. 026601, Jul 2012.
- [69] C. M. Wang and M. Q. Pang, “Thermally induced spin polarization and thermal conductivities in a spin-orbit coupled two-dimensional electron gas,” *Solid State Communications*, vol. 150, p. 1509, 2010.
- [70] G. E. W. Bauer, E. Saitoh, and B. J. van Wees, “Spin caloritronics,” *Nat. Mat.*, vol. 11, p. 391, 2012.
- [71] Z. Ma, “Spin hall effect generated by a temperature gradient and heat current in a two-dimensional electron gas,” *Solid State Communications*, vol. 150, pp. 510 – 513, 2010. Spin Caloritronics.
- [72] A. Slachter, F. L. Bakker, and B. J. van Wees, “Modeling of thermal spin transport and spin-orbit effects in ferromagnetic/nonmagnetic mesoscopic devices,” *Phys. Rev. B*, vol. 84, p. 174408, 2011.
- [73] S. Tölle, C. Gorini, and U. Eckern, “Room-temperature spin thermoelectrics in metallic films,” *Phys. Rev. B*, vol. 90, p. 235117, 2014.
- [74] M. I. Dyakonov, *Spin Physics in Semiconductors*. Springer, 2008.
- [75] J. M. Luttinger and W. Kohn, “Motion of electrons and holes in perturbed periodic fields,” *Phys. Rev.*, vol. 97, pp. 869–883, 1955.
- [76] R. Winkler, *Spin-orbit Coupling Effects in Two-dimensional Electron and Hole Systems*. Springer, Berlin, 2003.

- [77] R. Lassnig, “ $\mathbf{k} \cdot \mathbf{p}$ theory, effective-mass approach, and spin splitting for two-dimensional electrons in GaAs-GaAlAs heterostructures,” *Phys. Rev. B*, vol. 31, p. 8076, 1985.
- [78] R. S. Calsaverini, E. Bernardes, J. C. Egues, and D. Loss, “Intersubband-induced spin-orbit interaction in quantum wells,” *Phys. Rev. B*, vol. 78, p. 155313, 2008.
- [79] S. Datta, *Electronic transport in mesoscopic systems*. Cambridge University Press, 1995.
- [80] J. H. Davies., *The Physics of Low-dimensional Semiconductors*. Cambridge University Press, 2006.
- [81] G. Dresselhaus, “Spin-orbit coupling effects in zinc blende structures,” *Phys. Rev.*, vol. 100, pp. 580–586, 1955.
- [82] E. I. Rashba, “Spin currents in thermodynamic equilibrium: The challenge of discerning transport currents,” *Phys. Rev. B*, vol. 68, p. 241315(R), 2003.
- [83] I. V. Tokatly, “Equilibrium spin currents: Non-abelian gauge invariance and color diamagnetism in condensed matter,” *Phys. Rev. Lett*, vol. 101, p. 106601, 2008.
- [84] V. K. Dugaev, M. Inglot, E. Y. Sherman, and J. Barnaś, “Robust impurity-scattering spin hall effect in a two-dimensional electron gas,” *Phys. Rev. B*, vol. 82, p. 121310, 2010.
- [85] J. Rammer, *Quantum Transport Theory*. Reading: Westview, 2004.

-
- [86] J. Rammer, *Quantum field theory of Non-equilibrium States*. Cambridge: Cambridge University Press, 2007.
- [87] L. D. Landau and E. M. Lifshitz, *Course of Theoretical Physics, Vol. III*. Oxford: Butterworth-Heinemann, 1964.
- [88] G. D. Mahan, *Many Particle Physics, Third Edition*. New York: Plenum, 2000.
- [89] A. Abrikosov, L. Gorkov, and I. Dzyaloshinski, *Methods of quantum field theory in statistical physics*. New York, N.Y.: Dover, 1963.
- [90] H. B. Callen, *Thermodynamics*. New York, N.Y.: John Wiley & Sons, Inc., 1960.
- [91] A. L. Fetter and J. D. Walecka, *Quantum theory of many-particle systems*. International series in pure and applied physics, New York, NY: McGraw-Hill, 1971.
- [92] H. Bruus and K. Flensberg, *Many-body quantum theory in condensed matter physics - an introduction*. Oxford University Press, 2004.
- [93] R. Kubo, "Statistical-mechanical theory of irreversible processes. i. general theory and simple applications to magnetic and conduction problems," *Journal of the Physical Society of Japan*, vol. 12, no. 6, pp. 570–586, 1957.
- [94] R. Kubo, M. Yokota, and S. Nakajima, "Statistical-mechanical theory of irreversible processes. ii. response to thermal disturbance," *Journal of the Physical Society of Japan*, vol. 12, no. 11, pp. 1203–1211, 1957.

- [95] R. Kubo, M. Toda, and N. Hashitsume, *Statistical Physics*. Berlin, Germany: Springer, 1985.
- [96] S. Doniach and E. H. Sondheimer, *Green's Functions for Solid State Physicists*. Imperial College Press, 1998.
- [97] P. Schwab and R. Raimondi, "Magnetoelectronic transport of a two-dimensional metal in the presence of spin-orbit coupling," *Eur. Phys. J. B*, vol. 25, p. 483, 2002.
- [98] O. V. Dimitrova, "Spin-hall conductivity in a two-dimensional rashba electron gas," *Phys. Rev. B*, vol. 71, p. 245327, 2005.
- [99] W.-K. Tse and S. Das Sarma, "Spin hall effect in doped semiconductor structures," *Phys. Rev. Lett.*, vol. 96, p. 056601, 2006.
- [100] L. Berger, "Side-jump mechanism for the hall effect of ferromagnets," *Phys. Rev. B*, vol. 2, p. 4559, 1970.
- [101] J. Borge, C. Gorini, G. Vignale, and R. Raimondi, "Spin hall and edelstein effects in metallic films: From two to three dimensions," *Phys. Rev. B*, vol. 89, p. 245443, 2014.
- [102] Y. Niimi, Y. Kawanishi, D. H. Wei, C. Deranlot, H. X. Yang, M. Chshiev, T. Valet, A. Fert, and Y. Otani, "Giant spin hall effect induced by skew scattering from bismuth impurities inside thin film cubi alloys," *Phys. Rev. Lett.*, vol. 109, p. 156602, 2012.
- [103] A. G. Rybkin, A. M. Shikin, V. K. Adamchuk, D. Marchenko, C. Biswas, A. Varykhalov, and O. Rader, "Large spin-orbit splitting

- in light quantum films: Al/w(110),” *Phys. Rev. B*, vol. 82, p. 233403, 2010.
- [104] F. T. Vas’ko, “Spin splitting in the spectrum of two-dimensional electrons due to the surface potential,” *Pis’ma Zh. Eksp. Teor. Fiz.*, vol. 30, no. 9, pp. 574–577, 1979.
- [105] S. Mathias, A. Ruffing, F. Deicke, M. Wiesenmayer, I. Sakar, G. Bihlmayer, E. V. Chulkov, Y. M. Koroteev, P. M. Echenique, M. Bauer, and M. Aeschlimann, “Quantum-well-induced giant spin-orbit splitting,” *Phys. Rev. Lett.*, vol. 104, p. 066802, Feb 2010.
- [106] H. A. Engel, B. I. Halperin, and E. Rashba, “Theory of spin hall conductivity in n -doped gaas,” *Phys. Rev. Lett.*, vol. 95, p. 166605, 2005.
- [107] C. Gorini, P. Schwab, R. Raimondi, and A. L. Shelankov, “Non-abelian gauge fields in the gradient expansion: Generalized boltzmann and eilenberger equations,” *Phys. Rev. B*, vol. 82, p. 195316, 2010.
- [108] A. Takeuchi and N. Nagaosa, “Theory of electrical spin manipulation in spin-orbit coupling systems,” *arXiv:1309.4205*, 2013.
- [109] J. Borge, C. Gorini, and R. Raimondi, “Spin thermoelectrics in a disordered fermi gas,” *Phys. Rev. B*, vol. 87, p. 085309, 2013.
- [110] E. H. Sondheimer, “The theory of the galvanomagnetic and thermomagnetic effects in metals,” *Proc. R. Soc. Lond. A*, vol. 193, p. 484, 1948.

-
- [111] B. Scharf, A. Matos-Abiague, I. Žutić, and J. Fabian, “Theory of thermal spin-charge coupling in electronic systems,” *Phys. Rev. B*, vol. 85, p. 085208, 2012.
- [112] M. I. Dyakonov, “Magnetoresistance due to edge spin accumulation,” *Phys. Rev. Lett.*, vol. 99, p. 126601, 2007.
- [113] P. Schwab, R. Raimondi, and C. Gorini, “Inverse spin hall effect and anomalous hall effect in a two-dimensional electron gas,” *EPL (Europhysics Letters)*, vol. 90, p. 67004, 2010.
- [114] M. Jonson and G. D. Mahan, “Mott’s formula for the thermopower and the wiedemann-franz law,” *Phys. Rev. B*, vol. 21, p. 4223, 1980.
- [115] D. R. Niven and R. A. Smith, “Electron-electron interaction corrections to the thermal conductivity in disordered conductors,” *Phys. Rev. B*, vol. 71, p. 035106, 2005.
- [116] R. Raimondi, M. Leadbeater, P. Schwab, E. Caroti, and C. Castellani, “Spin-orbit induced anisotropy in the magnetoconductance of two-dimensional metals,” *Phys. Rev. B*, vol. 64, p. 235110, 2001.
- [117] S. Giglberger, L. E. Golub, V. V. Bel’kov, S. N. Danilov, D. Schuh, C. Gerl, F. Rohlfing, J. Stahl, W. Wegscheider, D. Weiss, W. Prettl, and S. D. Ganichev, “Rashba and dresselhaus spin splittings in semiconductor quantum wells measured by spin photocurrents,” *Phys. Rev. B*, vol. 75, p. 035327, 2007.

- [118] T. L. Hughes, Y. B. Bazaliy, and B. A. Bernevig, “Transport equations and spin-charge propagating mode in a strongly confined two-dimensional hole gas,” *Phys. Rev. B*, vol. 74, p. 193316, 2006.
- [119] H. Kontani, T. Tanaka, D. S. Hirashima, K. Yamada, and J. Inoue, “Giant orbital hall effect in transition metals: Origin of large spin and anomalous hall effects,” *Phys. Rev. Lett.*, vol. 102, p. 016601, 2009.
- [120] I. V. Tokatly, “Orbital momentum hall effect in p -doped graphane,” *Phys. Rev. B*, vol. 82, p. 161404, 2010.
- [121] M. König, S. Wiedmann, C. Brüne, A. Roth, H. Buhmann, L. W. Molenkamp, X. L. Qi, and S.-C. Zhang, “Quantum spin hall insulator state in $hgte$ quantum wells,” *Science*, vol. 318, p. 766, 2007.
- [122] Y. K. Kato, R. C. Myers, A. C. Gossard, and D. D. Awschalom, “Current-induced spin polarization in strained semiconductors,” *Phys. Rev. Lett.*, vol. 93, p. 176601, 2004.
- [123] K. Shen, G. Vignale, and R. Raimondi, “Inverse edelstein effect,” *Phys. Rev. Lett.*, vol. 112, p. 096601, 2014.
- [124] S. D. Ganichev, E. L. Ivchenko, V. V. Bel’kov, S. A. Tarasenko, M. Sollinger, D. W. an W. Wegscheider, and W. Prettl, “Spin-galvanic effect,” *Nature*, vol. 417, p. 153, 2002.
- [125] J. C. R. Sánchez, L. Vila, G. Desfonds, S. Gambarelli, J. P. Attané, J. M. D. Teresa, C. Magén, and A. Fert, “Spin-to-charge conversion using rashba coupling at the interface between non-magnetic materials,” *Nature Commun.*, vol. 4, p. 2944, 2013.

- [126] L. V. Keldysh, "Diagram technique for nonequilibrium processes," *JETP*, vol. 20, p. 1018, 1965.
- [127] J. Rammer and H. Smith, "Quantum field-theoretical methods in transport theory of metals," *Rev. Mod. Phys.*, vol. 58, p. 323, 1986.

Acknowledgements

I would really like to thank the city of Rome for this fantastic three years. I am very grateful to Prof. Roberto Raimondi for his continuous and enthusiastic support during this time. I am in debt with him for his help, suggestions and guidance. I would also like to mention Prof. Vignale and Dr. Gorini for stimulating and instructive discussions.